# HIDRAULICA

HYDRAULICS-PNEUMATICS-TRIBOLOGY-ECOLOGY-SENSORICS-MECHATRONICS

2023
December
No. 4

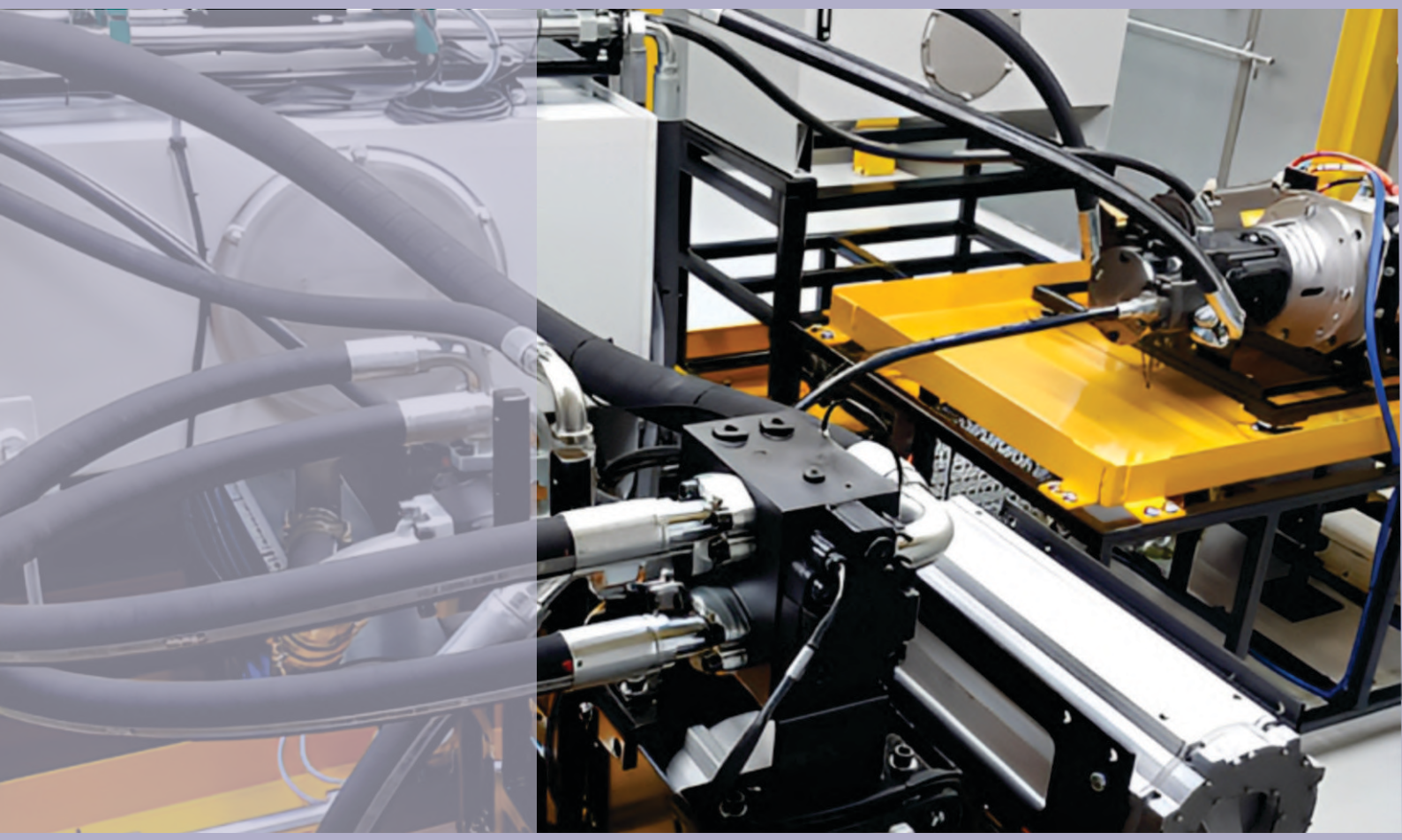

ISSN 1453 - 7303
ISSN-L 1453 - 7303

https://hidraulica.fluidas.ro

## CONTENTS

***Published by:***
***Hydraulics and Pneumatics Research Institute, Bucharest-Romania***
Address: 14 Cuţitul de Argint, district 4, Bucharest, 040558, Romania
Phone: +40 21 336 39 91; Fax: +40 21 337 30 40; e-Mail: ihp@fluidas.ro; Web: www.ihp.ro
***with support from:***
***National Professional Association of Hydraulics and Pneumatics in Romania - FLUIDAS***
e-Mail: fluidas@fluidas.ro; Web: www.fluidas.ro

**HIDRAULICA Magazine** is indexed by international databases

**ISSN 1453 – 7303; ISSN – L 1453 – 7303**

## EDITORIAL

### Cercetarea viitorului în România

Dr. Ing. Gabriela Matache
REDACTOR ȘEF

Cercetarea științifică și tehnologică reprezintă motorul inovației și progresului. În România, există o bogată tradiție în domenii precum matematică, fizică, chimie și inginerie, care a contribuit la realizări remarcabile de-a lungul istoriei. Cu toate acestea, pentru a asigura o dezvoltare sustenabilă, este esențial să consolidăm și să extindem aceste eforturi, abordând provocările actuale și viitoare.

Investițiile în cercetare și dezvoltare (R&D) sunt cruciale pentru a stimula inovația și creativitatea. Guvernul, sectorul privat și instituțiile academice trebuie să colaboreze strâns pentru a crea un mediu propice pentru cercetare. Este nevoie de finanțare adecvată, facilități de cercetare modernizate și programe de susținere a cercetătorilor. În plus, promovarea colaborării între sectorul public și cel privat poate contribui la transferul eficient de cunoștințe și tehnologii către industrie.

Un alt aspect crucial este educația. Dezvoltarea cercetării în România depinde în mare măsură de calitatea sistemului educațional. Este nevoie de investiții în pregătirea tinerilor în domeniile științifice și tehnologice. Programe de educație STEM (știință, tehnologie, inginerie și matematică) ar trebui să fie promovate încă din școli, pentru a stimula interesul și talentul în aceste domenii pentru viitorii tineri cercetători.

O altă provocare este atragerea și menținerea cercetătorilor talentați în țară. Este nevoie de politici și programe care să ofere stimulente pentru cercetători, inclusiv condiții de lucru atractive, oportunități de avansare și recunoaștere adecvată. Colaborările internaționale și schimburile de experiență ar trebui, de asemenea, încurajate pentru a menține conexiuni solide cu comunitățile științifice globale.

Totuși, provocările sunt multiple. Birocrația excesivă, lipsa de fonduri și concurența acerbă pentru resurse pot reprezenta piedici majore în calea progresului. Este important să se implementeze politici eficiente pentru eliminarea acestor obstacole și pentru a crea un mediu propice inovației.

În concluzie, cercetarea viitorului în România necesită eforturi concertate din partea tuturor actorilor implicați. Investiții susținute în R&D, îmbunătățirea sistemului educațional, atragerea și menținerea talentele și eliminarea obstacolelor birocratice vor contribui la construirea unei baze solide pentru viitorul țării noastre.

## EDITORIAL

### Research in Romania in Coming Years

Ph.D.Eng. Gabriela Matache
EDITOR-IN-CHIEF

Scientific and technological research is the engine of innovation and progress. In Romania, there is a rich tradition in fields such as mathematics, physics, chemistry and engineering, which has contributed to remarkable achievements throughout history. However, to ensure sustainable development, it is essential that we strengthen and expand these efforts, addressing current and future challenges.

Investments in research and development (R&D) are crucial to drive innovation and creativity. Government, the private sector and academic institutions must work closely together to create an enabling environment for research. Adequate funding, modernized research facilities and programmes to support researchers are needed. In addition, fostering collaboration between the public and private sectors can contribute to the efficient transfer of knowledge and technologies to industry.

Another crucial aspect is education. The development of research in Romania largely depends on the quality of the educational system. Investments are needed in the training of young people in scientific and technological fields. STEM (Science, Technology, Engineering and Mathematics) education programmes should be promoted from schools, to stimulate interest and talent in these fields for future young researchers.

Another challenge is attracting and keeping talented researchers in the country. Policies and programmes are needed to provide incentives for researchers, including attractive working conditions, opportunities for advancement and adequate recognition. International collaborations and exchanges of experience should also be encouraged to maintain strong connections with global scientific communities.

However, the challenges are many. Excessive bureaucracy, lack of funds and fierce competition for resources can be major obstacles to progress. It is important to implement effective policies to remove these obstacles and create an environment conducive to innovation.

In conclusion, research in coming years in Romania requires concerted efforts from all the actors involved. Sustained investment in R&D, improving the education system, attracting and retaining talent and removing bureaucratic obstacles will help build a solid foundation for our country's future.

# Experimental Research on the State of Stress and Deformations of Cylindrical Structures Subjected to Internal Pressure

Assist. Prof. PhD. Eng. **Gheorghe Cosmin CIOCOIU[1,*],** Assoc. Prof. PhD. Eng. **Ion DURBACĂ[1],**
Assoc. Prof. PhD. Eng. **Nicoleta SPOREA[1],** Professor Ph. D. Eng. **Alin DINIȚĂ[2]**,
Lecturer Ph. D. Eng. **Georgiana Luminiţa ENĂCHESCU[1]**,
Lecturer Ph. D. Eng. **Anca Mădălina DUMITRESCU[1]**

[1] POLITEHNICA University of Bucharest, Romania

[2] PETROLEUM-GAS University of Ploiești, Romania

* cgcosmin@gmail.com

***Abstract:*** *The paper presents the experimental results obtained from the tests carried out on a cylindrical body with variable geometry, subjected to an internal pressure in three steps. The present work discusses the case of a transition without fillet from a thickness of the wall to a smaller one of the cylindrical body, in which case the values of the normal strains and the corresponding stress are determined experimentally. In the present case, strain gauge method was used.*

***Keywords:*** *Normal strains, stress, tensometry*

## 1. Introduction

Pressured equipment is widely used in all industrial activities, as chemical plants, power plants, gas, fuel and utilities pipelines, etc. The intensive development of the economy requires intensive construction of new, and modernization of main pipelines, vertical and horizontal tanks, pressure vessels and apparatus, etc. Long time exploitation of pipelines and other cylindrical structures leads to their failure that can be accelerated by the internal and external conditions such as corrosion or erosion. The substances flowing or stored inside generally have chemical or erosive aggressiveness that is difficult to control, in association with high temperature and pressure parameters. This puts a challenge to engineers: to evaluate the progress of mechanical damage [1,2].

Damage processes may be initialized due to the accumulation of stress concentrators that may cause initiation and growth of surface cracks and finally may lead to failures. Structural failure in pipes occurs due to a diversity of causes. One of the causes is the formation of stress concentration zones in the pipe wall. These include surface defects [3-8] located inside or outside constructions, geometric discontinuities in static equipment: assemblies with flanges [9-21], jackets for heating/cooling [22-25], horizontal supports and/or vertical [24-30], dynamic - centrifugal equipment [33, 34] etc., but also shape deviations [35 - 37].

Industrial equipment for thermal and/or chemical processes are made with a particularly complex constructive configuration, characteristic for each practical case. Even if a single metal material or associations of different materials are used, it is often necessary to resort to a variable geometry of the walls (different thicknesses). The respective passages can be without, or with fillet, or progressively variable passage from one thickness to another. As a result, in the respective areas and in the neighboring portions, it is necessary to carefully analyze the stress state, to detect the maximum values and compare them with the minimum allowable strength, for the certification of the construction.

This article considers the determination of the stress manifested on the outer cylindrical surface of some areas with different geometries, using the strain gauge method.

Strain gauge method is an effective method for the practical verification of the state of mechanical stress in the situation of a technical system, which is difficult to analyze through analytical procedures, because it allows the measurement of normal strains in several directions and the application of analytical formulas corresponding to the theory of elasticity [38 - 40].

Strain gauge method is used in various fields, such as equipment engineering, the aerospace industry, the automotive industry and in materials research. This technique can be used to measure mechanical stress in materials such as metal, rubber, polymers, or composite materials.

## 2. Materials and methods

### 2.1. Description of the materials and methods used

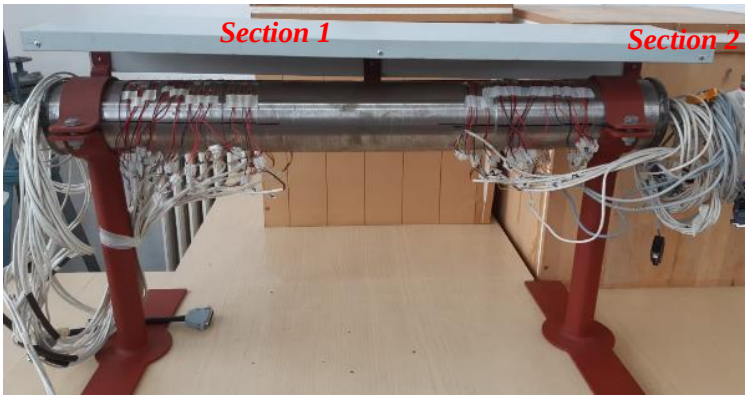


**Fig. 1.** Experimental model

For research purposes addressed in the present case, a model was created for carrying out the experiments. The design, manufacture, and assembly of the experimental model (fig. 1) were carried out in the laboratory of the Faculty of Mechanical and Mechatronic Engineering, Department of Industrial Process Equipment, within Politehnica University of Bucharest.
The construction material of the experimental model is P265GH, having the symbolization 1.4025, according to EN 10216 (yield stress $R_{0,2} = 388\ \mathrm{N/mm^2}$; ultimate tensile strength, $R_m = 542\ \mathrm{N/mm^2}$; elongation at break $A = 32\%$).
The other components and characteristics of the experimental model are as follows: pipe Ø 114.3 mm x 8 mm x 931 mm; cover Ø 114.3x10mm, 2 pcs.; pipe supports, 2 pcs.; equipment protection made of sheet metal with a thickness of 1mm; 2 connections 21/2"; supply valve 21/2"; Afriso manometer, $p_{max}$ = 4 MPa.


a)

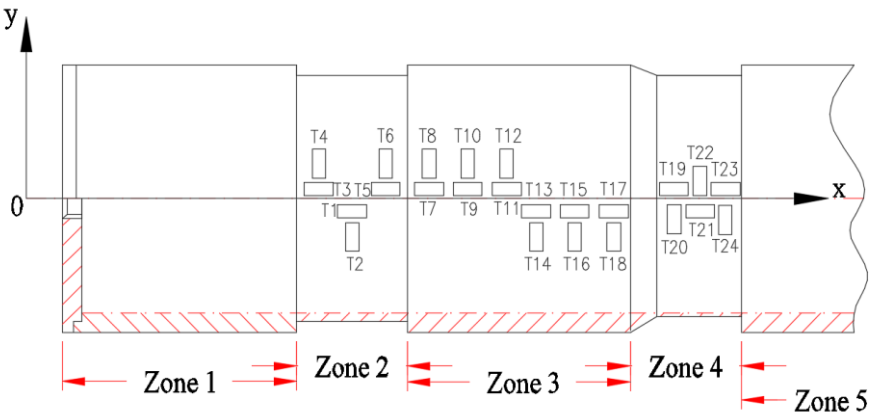


b)

**Fig. 2.** Experimental model - Section 1
a) Section 1; b) Sketch 1 – location of transducers 1, 2, 3 ... 24.

Transducers were placed on the experimental model according to figures 2 and 3. The model was divided into two sections: section 1 (left side – with pressure gauge) and section 2 (right side – with the power connection). The model was divided into 9 zones. Zones 1, 5 and 9 were zones of constant thickness, which no transducers were attached, and which, in the present work, were not considered for research. Zones 2, 3, 4, 6, 7 and 8 are zones of different thicknesses and different diameter variations, where transducers have been placed as follows:

- zone 2, with transducers $T_1 \ldots T_6$, on the length $L_1 = 50\ mm$, the outer diameter of the pipe $\phi 109\ mm$;
- zone 3, with transducers $T_7 \ldots T_{18}$, on the length $L_2 = 100\ mm$, the outer diameter of the pipe $\phi 113.5\ mm$;
- zone 4, with transducers $T_{19} \ldots T_{24}$, on the length $L_3 = 50\ mm$, the outer diameter of the pipe $\phi 109.5mm$;
- zone 6, with transducers $T_{25} \ldots T_{30}$, on the length $L_4 = 50\ mm$, the outer diameter of the pipe $\phi 108.5mm$;
- zone 7, with transducers $T_{31} \ldots T_{42}$, on the length $L_5 = 100\ mm$, the outer diameter of the pipe $\phi 113.5\ mm$;
- zone 8, with transducers $T_{43} \ldots T_{48}$, on the length $L_6 = 50\ mm$, the outer diameter of the pipe $\phi 108.5\ mm$.


a)

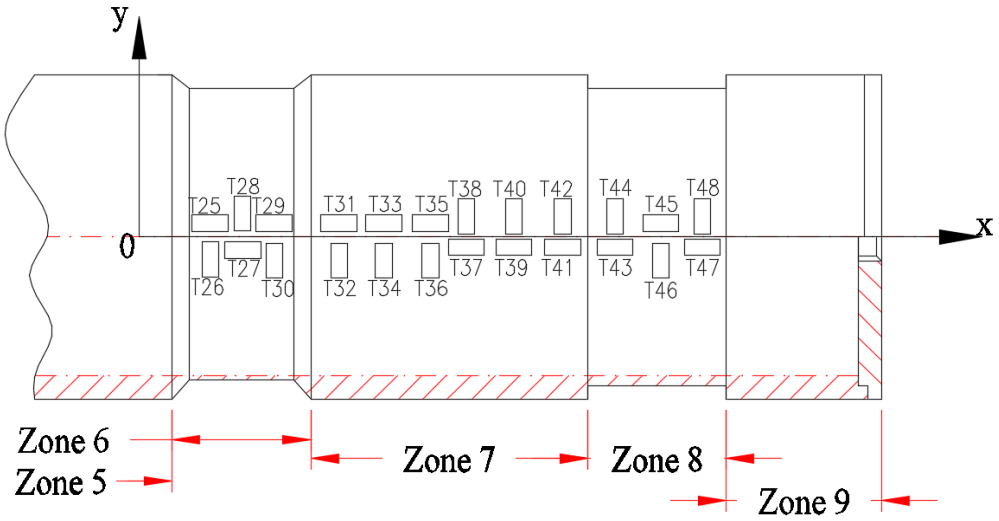


b)

**Fig. 3.** Experimental model - section 2
a) Section 2; b) Sketch 2 – location of transducers 25, 26, 27...48.

During the testing, the following cases were considered:
1. In case 1, an internal pressure was used in the equipment up to the value $p_1$ = 1 [MPa], after which it was discharged to the value 0 MPa.
2. In case 2, an internal pressure was used in the equipment up to the value $p_2$ = 2 [MPa], after which it was discharged to the value 0 MPa.
3. In case 3, an internal pressure in the equipment was raised to the value $p_3$ = 3 [MPa], after which it was discharged to the value 0 MPa.
With the help of the MGC plus tensometric bridges, specific linear deformations in the radial direction and in the circumferential direction, at the above-mentioned up/down pressures, were obtained.
The calculation of the stress on each area of the experimental model, depending on the internal pressure, was carried out with the formulas from [36 - 38]:

$$\sigma_{1j} = \frac{p \cdot R_{mj}}{2 \cdot \delta_j}, \quad \sigma_{2j} = \frac{p \cdot R_{mj}}{\delta_j}, \tag{1}$$

where $p$ is the internal pressure;

$$R_{mj} = \frac{R_{ej} + R_i}{2}, \tag{2}$$

where $R_{mj}$ - the average radius of the considered cylindrical part,
$R_{ej}$ - the outer radius of the section "$j$",
$R_i$ - the inner radius of the section "$j$".

and:

$$\delta_j = R_{ei} - R_i, \tag{3}$$

where $\delta_j$, the thickness of the zone where the strain gauges were placed.
According to the experimentally processed data, the specific linear deformations $\varepsilon_{1j}$ (μm/m) and $\varepsilon_{2j}$ (μm/m), respectively the values of the stress $\sigma_{1j}$ and $\sigma_{2j}$, using the relations [36 - 38] :

$$\sigma_{1j} = \frac{E}{1-\mu^2} \cdot \left( \varepsilon_{1j} + \mu \cdot \varepsilon_{2j} \right) \left[ N / mm^2 \right], \quad (4)$$

$$\sigma_{2j} = \frac{E}{1-\mu^2} \cdot \left( \varepsilon_{2j} + \mu \cdot \varepsilon_{1j} \right) \left[ N / mm^2 \right], \quad (5)$$

where E - the modulus of longitudinal elasticity (Young's modulus), in N/mm$^2$, $\mu$ - the transverse contraction coefficient (Poisson's ratio), $\varepsilon_{1j}$ ,$\varepsilon_{2j}$ - the normal specific linear strains in the radial and circumferential directions, determined on the length of the cylindrical section " $j$ ", in μm/m.
The equivalent von Mises stress, in each zone, were calculated with the formula [36 - 38]:

$$\sigma_{echj}^{IV} = \sqrt{\sigma_{1j}^{\ 2} + \sigma_{2j}^{\ 2} - \sigma_{1j} \cdot \sigma_{2j}} \ . \quad (6)$$

### 2. 2. Equipment used

The following equipment was used for the experiments:
1. Test stand (fig. 4);

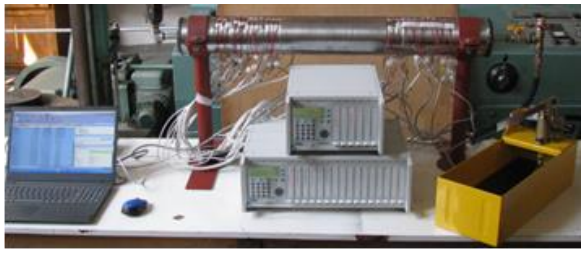

**Fig. 4**. Test stand

2. Pump with pressure gauge (fig.5);

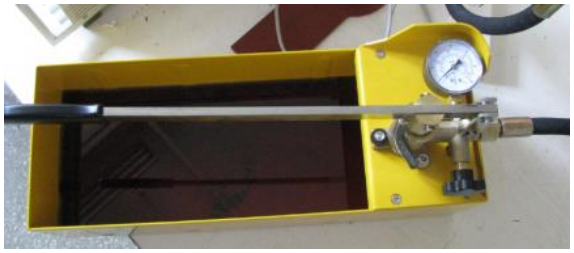

**Fig. 5.** Pump

3. MGCplus 1 and MGCplus 2 equipments (fig.6), necessary for data acquisition (MGCplus 1 acquired 40 measurement points, and MGCplus 2 acquired 8 measurement points).
4. Lenovo laptop (fig. 7) with Catman Easy software, necessary for the acquisition of experimental data.


**Fig. 6.** MGCplus 1 and MGCplus 2 equipment

**Fig. 7.** Lenovo laptop

## 3. Experimental results

The resulting theoretical equivalent stress, $\sigma_{ech\,t}$, calculated with formula (6), respectively relations (1), along the length of Section 1 (zones 2, 3 and 4) and along the length of Section 2 (zones 6, 7 and 8), are presented in Table 1:

**Table 1:** Equivalent stress calculated in the 6 zones

| Pressure [MPa] | Zone 2 | Zone 3 | Zone 4 | Zone 6 | Zone 7 | Zone 8 |
|---|---|---|---|---|---|---|
| | $\sigma_{ech\,t}$ [MPa] | | | | | |
| $p_1 = 1$ | 8.39 | 6.03 | 8.03 | 8.78 | 8.99 | 5.89 |
| $p_2 = 2$ | 16.78 | 12.07 | 16.07 | 17.56 | 17.98 | 11.78 |
| $p_3 = 3$ | 25.17 | 18.10 | 24.10 | 26.34 | 26.97 | 17.67 |

The theoretical equivalent stresses, calculated along the length of each section, without concentrations influenced by discontinuities, are used for comparison with the values of the experimental equivalent stresses in the different sections shown in Figures 8-13.
Figures 8-13 show only the calculations corresponding to each section, where the strain gauges have been glued.
Figures 8-13 show the experimental equivalent stress variations, calculated with formula (6), along the length of Section 1 (zones 2, 3 and 4) and along the length of Section 2 (zones 6, 7 and 8) – in sections with strain gauges.

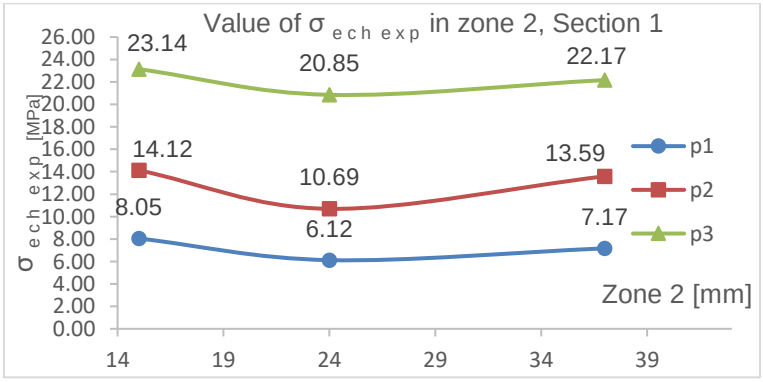


**Fig. 8.** The values of the experimental equivalent stress in zone 2, Section 1

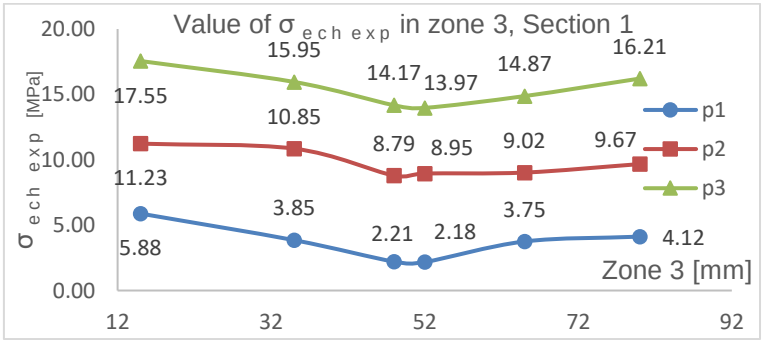


**Fig. 9.** The values of the experimental equivalent stress in zone 3, Section 1

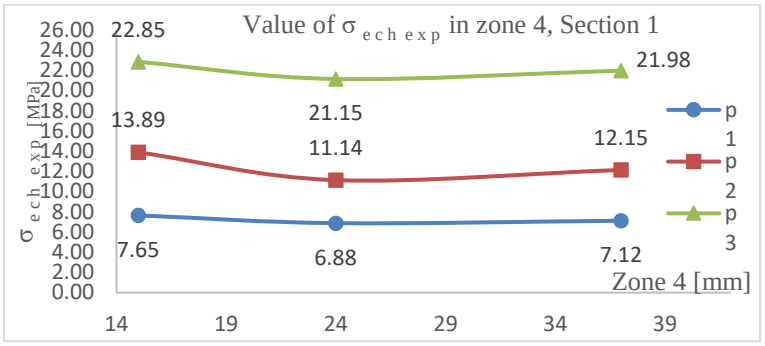


**Fig. 10.** The values of the experimental equivalent stress in zone 4, Section 1

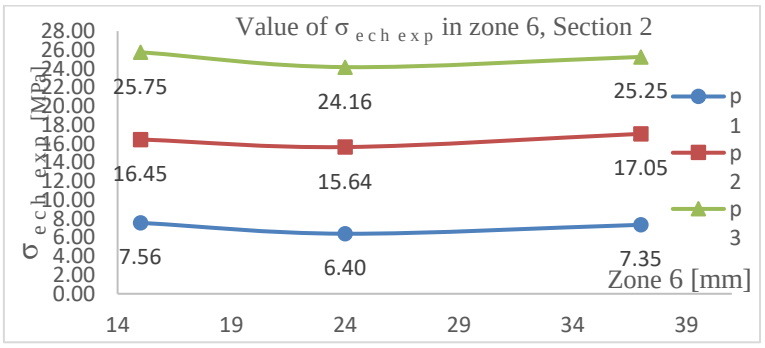


**Fig. 11.** The values of the experimental equivalent stress in zone 6, Section 2

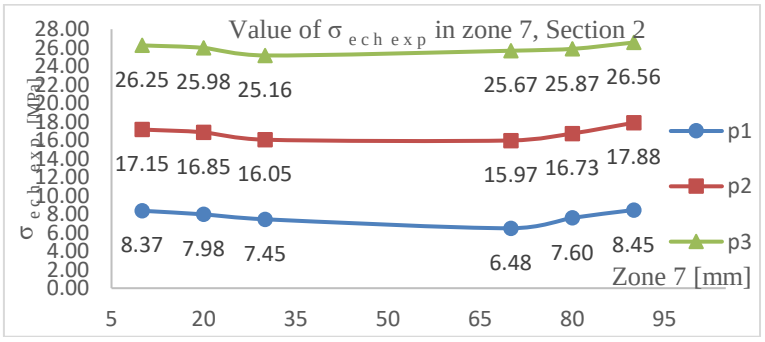


**Fig. 12.** The values of the experimental equivalent stress in zone 7, Section 2

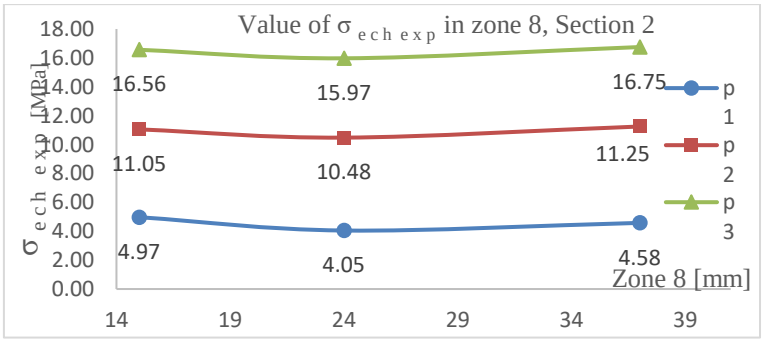


**Fig. 13.** The values of the experimental equivalent stress in zone 8, Section 2

The experimental results obtained in this work, showed that when the internal pressure increases, there is a gradual increase in the values of specific linear strains, meridional (axial) stress and annular (circumferential) stress; respectively the equivalent stress, established based on the fourth strength theory.

Finally, the maximum value of the equivalent stress, for given conditions, working pressure and temperature, can be compared with the resistance/allowable stress, characteristic of the material from which the cylindrical body is made.
It is observed that for all analyzed areas, the values of the measured equivalent stress are lower than the values of the theoretical equivalent stress. For example, in zone 7, for the pressure $p_2 = 2\,MPa$, the value $\sigma_{ech\,mas} = 15.97\,MPa \quad < \quad \sigma_{ech\,t} = 17.98\,MPa$.
The experiment was carried out under normal working conditions and at ambient temperature.

## 4. Conclusions

From the interpretation of the obtained results, it can be observed that with an increase in the internal pressure, the value of the stress in the radial and annular direction also increases.
The normal strains in the two directions, radial and annular, were automatically recorded with the help of MGC plus strain gauges. Based on the recorded values, the axial and annular stress, respectively the equivalent stress, were calculated. *It is noted that the experimental values of equivalent stress are lower, than the membrane equivalent stress.* The differences are insignificant, within the present experiment.
Considering the results obtained, the development of research in the field is encouraged, by further evaluating a methodology for the analytical study of specific linear strains and stress, considering progressive thickness transitions or appropriate fillets. In this sense, the method of finite elements can be used, respectively the method of short structural elements. The results obtained by means of the mentioned study variants can be compared in value, to establish the maximum safety in the operation of a cylindrical body-type pressurized equipment, during design or during operation. In this way, the actual duration of operation is evaluated, in each case.

### References

[1] Zhangabay, Nurlan, Ulanbator Suleimenov, Akmaral Utelbayeva, Svetlana Buganova, Akzhan Tolganbayev, Karshyga Galymzhan, Serik Dossybekov, Kanat Baibolov, Roman Fediuk, Mugahed Amran, Bolat Duissenbekov, and Aleksandr Kolesnikov. "Experimental research of the stress-strain state of prestressed cylindrical shells taking into account temperature effects." *Case Studies in Construction Materials* 18 (July 2023): e01776.
[2] Moustabchir, H., J. Arbaoui, Zitouni Azari, S. Hariri, and Catalin Iulian Pruncu. "Experimental / numerical investigation of mechanical behaviour of internally pressurized cylindrical shells with external longitudinal and circumferential semi-elliptical defects." *Alexandria Engineering Journal* 57, no. 3 (September 2018): 1339-1347.
[3] Ghavamian, Aidin, Faizal Mustapha, B.T Hang Tuah Baharudin, and Noorfaizal Yidris. "Detection, Localisation and Assessment of Defects in Pipes Using Guided Wave Techniques: A Review." *Sensors* 18, no. 12 (2018): 4470.
[4] Liu, C., J. Dobson, and P. Cawley. "Efficient generation of receiver operating characteristics for the evaluation of damage detection in practical structural health monitoring applications." *Proceedings of the Royal Society A: Mathematical, Physical and Engineering Sciences* 473 (March 2017): 20160736.
[5] Farhidzadeh, A., A. Ebrahimkhanlou, and S. Salamone. "Corrosion damage estimation in multi-wire steel strands using guided ultrasonic waves." Paper presented at the SPIE Smart Structures and Materials+ Nondestructive Evaluation and Health Monitoring Conference, San Diego, CA, USA, March 8–12, 2015.
[6] Kharrat, M. *Design and Development of a Torsional Guided-Waves Inspection System for the Detection and Sizing of Defects in Pipes*. Ph.D. Thesis. Ecole Centrale de Lyon, Écully, France, 2012.
[7] Ying, Y. *A Data-Driven Framework for Ultrasonic Structural Health Monitoring of Pipes*. Ph.D. Thesis. Carnegie Mellon University, Pittsburgh, PA, USA, 2012.
[8] Kirby, R., Z. Zlatev, and P. Mudge. "On the scattering of torsional elastic waves from axisymmetric defects in coated pipes." *Journal of Sound and Vibration* 331, no. 17 (August 2012): 3989–4004.
[9] Iatan, I.R. *Theoretical and experimental research on constructions with ribbed flanges* / *Cercetări teoretice şi experimentale privind construcţiile cu flanşe cu nervuri*. Ph.D. Thesis. Polytechnic Institute of Bucharest, 1979.
[10] Jinescu, V.V., and N. Teodorescu. "Method for calculation of flanged assemblies." / "Metodă pentru calculul asamblărilor cu flanșe." *Construcţia de Maşini* 52, no. 12 (2000): 1-8.

[11] The American Society of Mechanical Engineers (ASME). *Boiler and Pressure Vessel Code. Section VIII, Division 2, Rules for construction of pressure vessels*. July 01, 2010.
[12] ***. EN 1591. *Flanges and their joints - Design rules for gasketed circular flange connections - Part 1: Calculation*, 2014.
[13] Estrada, H. "Analysis of leakage in bolted flanged joints using contact finite element analysis." *Journal of Mechanics Engineering and Automation* 5, no. 3 (March 2015): 135-142.
[14] Kumar, V., P.V. Singh, S. Angra, and S. Rani. "Design and optimization of weld neck flange for pressure vessel." Paper presented at the Vth International Symposium on "Fusion of Science and Technology", New Delhi, India, January 18 – 22, 2016.
[15] Jinescu, V.V., G. Urse, and A. Chelu. "Evaluation and completion the design methods of pressure vessels flange joints." *Revista de Chimie* 69, no. 8 (2018): 1954-1961.
[16] Urse, G., I. Durbacă, and C.I. Panait. "Some research results on the tightness and strength of flange joints." *Journal of Enneering Sciences and Innovation* 3, no. 2 (2018): 107-130.
[17] ***. EN 1092 – 1: 2018. *Flanges and their joints – Circular flanges for pipes, valves, fittings and accessories, PN designated – Part 1: Steel flanges*. NSAI Standards, 2018.
[18] Ma, B., Y. Zhu, F. Jin, Q. Ding, and X. Guo. "A lightweight optimal design model for bolted flange joints without gaskets considering its sealing performance." *Proceedings of the Institution of Mechanical Engineers, Part E: Journal of Process Mechanical Engineering* 232, no. 2 (2018): 234-255.
[19] Roman (Urse), G. *Research on the Correlation between Stiffness, Strength and Leakage of Flat Annular Flange Assemblies of Pressure Vessels* / *Cercetări referitoare la corelaţia dintre rigiditatea, rezistenţa şi etanşeitatea asamblărilor cu flanşe plate inelare ale recipientelor sub presiune*. Ph.D. Thesis. Politehnica University of Bucharest, 2019.
[20] Roman (Urse), G. "Comparative analysis of current international standards for calculations flanges joint with gasket inside the circle location of the bolt holes." *Revista de Chimie* 71, no. 3 (2020): 1-8.
[21] Iatan, I.R., G. Roman (Urse), Gh. Tomescu, and A. Chelu. "Analytical study of thermomechanical strength of assemblies with optional plane flanges. The effect of the flange ring rotation around the median circumference." *Revista de Chimie* 71, no. 3 (2020): 79-89.
[22] The American Society of Mechanical Engineers (ASME). *PCC – 1 – 2019 – Guidelines for pressure boundary bolted flange joint assembly*. ASME, New York, USA.
[23] Iatan, I. R., and I.M. Prodea. "Stress conditions in the evacuation areas of working media from containers with heating/cooling jackets (I)." / "Stări de solicitare în zonele de evacuare a mediilor de lucru din recipientele cu mantale de încălzire/răcire (I)." *Tehnologia Inovativă – Revista "Construcţia de maşini"* 59, no. 1 (2007): 85-92.
[24] Romanian Standards Association / Asociația de Standardizare din România - ASRO. SR EN 13445-3. Nonflammable pressure vessels, Part 3: Design / Recipiente sub presiune nesupuse la flacără. Partea 3: Proiectare. Vol. 2/3. July 2004.
[25] Constantinescu, I., and T. Tacu. *Resistance calculations for technological machines* / *Calcule de rezistenţă pentru utilaje tehnologice*. Bucharest, Technical Publishing House, 1979.
[26] Moos, R.D. *Pressure Vessel. Design Manual*. Houston, Texas, Gulf Publishing Company, 1997.
[27] Romanian Standards Institute / Institutul Român de Standardizare. *Collection of commented standards. Containers and vessels under pressure* / *Culegere de standarde comentate. Recipiente şi vase sub presiune*. CSCM – Rvp. Bucharest, Documentary Information Office for the Machine Construction Industry Publishing House / Editura Oficiul de Informare Documentară pentru Industria Construcţiilor de Maşini, 1997.
[28] ASRO. STAS 5455 – 82. *Side supports for containers. Shapes and dimensions* / *Suporturi laterale pentru recipiente. Forme şi dimensiuni*.
[29] ***. AD 2000-Data sheet S 3/4 / AD 2000-Merkblatt S 3/4. General verification of stability for pressure vessels - Vessels with support brackets / Allgemeiner Standsicherheitsnachweis für Druckbehälter - Behälter mit Tragpratzen. Technical rules / Technische Regel, Oktober 1991.
[30] British Standard Institute (BSI). BS 5500- 88. British Standard Specification for Unfired Fusion Welded Pressure Vessels.
[31] The American Society of Mechanical Engineers (ASME). *Boiler and Pressure Vessel Code, Section VIII, "Pressure Vessels", Div.1*. ASME, New York, USA, 1987.
[32] Iatan, I.R., T. Sima, and N. Sporea. "Models regarding the calculation of lateral supports of pressure vessels." / "Modele privind calculul reazemelor laterale ale recipientelor sub presiune." *Revista de Chimie* 52, no. 10 (2001): 593-599.
[33] Iatan, I.R., E. Stoican, N. Botea, and C. Hristescu. "Calculation and construction of centrifuge drums. I. Non-rigid cylindrical drums, with flat bottoms and covers, for sedimentation." / "Calculul şi construcţia tamburelor centrifugelor. I. Tambure cilindrice nerigidizate, cu funduri şi capace plane, pentru sedimentare." *Revista de Chimie* 36, no. 12 (1985): 1138-1145.

[34] Iatan, I.R., M. Jugănaru, and M.-F. Ștefănescu. “Calculation and construction of centrifuge drums. II. States of deformations and stress in flat circular bottoms.“ / “Calculul şi construcţia tamburelor centrifugelor. II. Stări de deformaţii şi de tensiuni în fundurile circulare plane.” *Revista de Chimie* 41, no. 1 (1990): 67-74.

[35] Păunescu, M., I.R. Iatan, and C.D. Tacă. “Aspects regarding the lifetime of a pressure vessel, with deviations from the geometric shape.” / “Aspecte privind durata de viaţă a unui recipient sub presiune, cu abateri de la forma geometrică.” *Bulletin of the Polytechnic Institute of Bucharest* / *Buletinul Institutului Politehnic din Bucureşti* 49 (1987): 87-91.

[36] Iatan, I.R., M. Păunescu, and C.D. Tacă. “On the stress concentration in the joint area of two cylindrical ferrules with shape deviations.” / “Asupra concentrării de tensiuni în zona îmbinare a două virole cilindrice cu abateri de formă.” *Bulletin of the Polytechnic Institute of Bucharest, Mechanical Series* / *Buletinul Institutului Politehnic din Bucureşti, Seria Mecanică* 56 – 57 (1984 – 1985): 170-178.

[37] Zichil, V., I.R. Iatan, L. Bibire, P. Busuioceanu, and L. Şerban. “Thermomechanical loading in beveled area between two cylindrical shells with different thicknesses. Theoretical study – Conections loads.” *Journal of Engineering Studies and Research* 20, no. 1 (2014): 87-100.

[38] Buzdugan, Gheorghe. *Strength of materials* / *Rezistența materialelor*. Bucharest, Technical Publishing House, 1980.

[39] Pavel, Alecsandru. *Pipes. Piping. Tubular components. Tubular columns* / *Țevi. Tubulaturi. Componente tubulare. Coloane tubulare*. Bucharest, Ilex Publishing House, 2003.

[40] Tripa, Pavel. *Experimental methods for determining deformations and mechanical stress* / *Metode experimentale pentru determinarea deformaţiilor şi tensiunilor mecanice*. Timişoara, MIRTON Publishing House, 2010.

# Inertial and Video Methods – A Non-Invasive Approach to Measuring the Human 's Upper Limb Joints Biomechanical Parameters

PhD. Eng. **Cristian Radu BADEA[1],** PhD. Eng. **Paul-Nicolae ANCUȚA[1],**
PhD. Student Eng. **Sorin Ionuț BADEA[1],** Dipl. Eng. **Florentina BADEA[1]**

[1] The National Institute of Research and Development in Mechatronics and Measurement Technique (INCDMTM)

adresacontact@gmail.com; paul.ancuta@incdmtm.ro; sorin_ib@yahoo.com; mihaiflori@yahoo.com

***Abstract:*** *The correction of the biomechanics of human movements is an extremely important activity both for the civilian environment (in which we include: domestic, lucrative activities and those related to sports training) and for the military, as this allows the optimization of neuromuscular control and also the increase of the efficacy of physical and mental resources allocation, in humans. This fact leads to a reduction of the injury risks, to the correction of certain anatomical-functional deficiencies/limitations and last but not least, it allows the improvement of the individual's quality of life. The non-invasive character of certain biomechanical analyses gives them a privileged status because the degree of intrusion and discomfort endured by the human subject subjected to the analysis is minimal, a fact that allows a better interaction with him in terms of he's availability of physical and mental involvement. From the category of these non-invasive systems for biomechanical analysis of motion, as well as of posture, the most used (due to their facilities) are video and inertial ones. They allow qualitative/quantitative evaluations of posture (static determinations) and/or human motion (dynamic determinations).*

***Keywords:*** *Inertial motion analysis, video motion analysis, biomechanics, body landmarks, neuromuscular, human joints angles, joint's range of motion (ROM), upper limbs*

## 1. Introduction

The non-contact analysis of human movements using video systems and dedicated software applications involves locating in the video images some landmarks intrinsic to the anatomy of the human body, such as the wrists (shoulder, hip, thigh, knee, etc.). These anatomical landmarks allow the identification of body segments and subsequently, through software analysis, the necessary measurements and validations involved in postural analysis. One such video analysis system of human movements is the MediaPipe Pose Landmarker which uses machine learning (ML) models and provides body landmarks in image coordinates and 3D world coordinates [1].
In the field of human biomechanics analysis, inertial systems have stood out in particular due to the accurate representation of human joints, from the point of view of their degrees of freedom, through the possibility of recording the movements of body segments without the risk of obstruction (such as it is found in the case of video analyses) and last but not least by their level of portability. However, the quality of the results offered by the inertial systems is particularly influenced by the quality of their calibration, which is dependent on the accuracy of the estimation of the sizes of the various anatomical segments.
Motion analyses that can be carried out by non-invasive video or inertial methods can be classified into two categories, namely:

- analyses in which attention is directed at the quality of human movements. This category includes postural analysis, gait analysis [2], range of motion determination, etc.;
- analyses in which attention is directed at the amount of movement achieved. As an example, in this regard, we can mention the analyses that follow the realization of a certain number of movements made in total or in a certain unit of time.

## 2. Previous and related works

In the paper [3] an introduction is made in the field of inertial motion analysis, focusing its attention on the analysis that is carried out with the help of modern mechatronic inertial motion capture

systems, highlighting both the advantages and disadvantages of using such a system and highlighting the main constituent elements of these systems as well as the necessary steps that must be performed to be able to perform such an analysis.
In the paper [4] there are presented the most important aspects related to the occurrence of positioning errors that appeared during the motion analysis sessions carried out with the help of the Xsens MVN system, before and after the post-processing of the information captured by to the MEMS sensors of the system, located on the human body, and related to the scenario in which the action takes place at the floor level (considered as having an incompressible surface), this representing the only element of contact between the human subject under analysis and the environment.
In the paper [5] there are presented the most important elements that Xsens MVN inertial motion analysis system uses in order to be able to generate results that reflect as precisely as possible the real situation analysed. This article presents the results of the motion analyses that which aimed to highlight the facilities and limitations arising from the use of contact points between the subject under analysis and the environment (which are usually anatomical protrusions considered to have the potential to physically interact with the environment, for example: the heel, elbow, knee) and also the graphic elements used by the dedicated software - MVN Analyze, as landmarks for the inertial analyses carried out;

## 3. Material and method

The analyses carried out in this study were based on the following physical elements/systems: an inertial motion analysis system, a stereo vision type camera, a laptop, a digital protractor, an angle gauge, a roulette, a ruler, a fixed bars assembly and elements of props used as physical benchmarks for carrying out calibrations and respectively for ensuring the necessary framework for carrying out experiments under repeatability conditions.
From the software point of view, the analyses mentioned in this work were carried out using MediaPipe and OpenCV for video analysis and MVN Analyze for inertial analysis.

### 3.1 Hardware and software used in the video analysis

The hardware and software architectures used in this study contained the following distinct elements:

- From the hardware point of view:
  - Laptop DELL Vostro 15 3000 (two USB 2.0 ports, a USB 3.0 port, an Ethernet port, headphone/mic jack, DVD drive, VGA port, 15inch display 1366x768, core i5 8th Gen, 8 Mb RAM);
  - Intel RealSense D435 Web Camera, which is equipped with a pair of depth sensors, an RGB sensor and an infrared projector and is connected via USB 3.0 Type-C.
- From the software point of view:
  - UBUNTU operating system version 18.04.6 LTS;
  - OpenCV software package version 4.7.0;
  - The MediaPipe software package;
  - Python version 3.10.5.

### 3.2 Inertial motion analysis system

In regards to the Xsens MVN inertial motion analysis system, the carried-out tests were aimed on testing the advantages and disadvantages of such the system, as well as on the comparison between the this and a video analysis system. On the motion analyses field, Xsens MVN represents one of the best performing inertial systems [6][7]. Xsens MVN is based on a MEMS sensor network, each of which contains a combination of accelerometer, gyroscope and magnetic field sensors, whose signals are processed by a microcontroller, by means of advanced processing algorithms, in order to obtain information regarding the kinematics of the body segments of the

individual under analysis and its global positioning. The obtained data is being then transferred to a virtual biomechanical model, which reproduces, in real time, the movements of the person in question.

The hardware subassembly used in the study is called MVN Link and is a 3D kinematic analysis system, adapted to the human body, composed of a network of MEMS, interconnected by means of electrical cables, mounted/mountable, in predetermined positions, on a "Lycra" type of suit, the latter allowing the user to have maximum freedom of movement, but also having the role of reducing the time required for the positioning/repositioning of the MEMS. MVN Link can be used both indoors and outdoors, on rough terrain, in areas with low lighting. The results provided by MVN Link do not require post-processing, since the MEMS used do not suffer from the occlusion phenomenon, as in the case of optical markers. Also, the data provided by this system can easily be used by other software applications.

This system benefits from the presence of several extremely important elements, some of which are even innovations implemented for the first time by the manufacturer of this system, Xsens, namely:

- the lack of orientation constraints, applied to the virtually modelled segments, as well as angular constraints applied to the joints, since the modelling of the joints of the virtual mannequin is based on the human anatomical structures that allow 6 degrees of freedom [8]. The information obtained is not manipulated by the system, to create the appearance of natural movements, but reflects exactly the values measured by the system's MEMS [9] [10].
- the communication between the inertial system and the computer is wireless. The signal frequency is relatively low, around 100Hz, but this fact does not affect the quality of the analysis of movement due to the fact that the sampling frequency of the signal, by MEMS, is very high, of approx. 1000 Hz;
- the possibility of including the analysed type of movement, in one scenario at a time, depending on the characteristics of the floor (incompressible, respectively compressible-elastic floor), on the performing the movement on different levels (as in the case of the analysis of the stairs climbing /descending, vertical walls climbing, etc.), or on the absence of a clear contact with the ground (as is the case with the analysis of skating and/or skiing);

### 3.3 Types of biomechanical analyses performed and their specific requirements

For each of the systems used (video and inertial), the biomechanical analyses were structured in two sections, as follows:

- The static analysis section – dedicated to the calibration of the two analysis systems used. The focus on this section was put on the capacity of the two motion analysis systems to determine, in static conditions, the joint angles at the level of the elbows of the human subject (alternating biceps-triceps contractions, see Fig.1);

**Fig. 1.** Successive positions of the human subject carried out for the static determination of the flexion angle of the right elbow joint

- The dynamic analysis section – dedicated to the ability of the two motion analysis systems to determine, in dynamic conditions, the correct joint's range of motion for the elbow joint. Thus,

this section was composed of a set of five sessions intended for the analysis of the flexion/extension movements of the right and left elbow joint respectively, consisting of ten movements having different amplitudes.

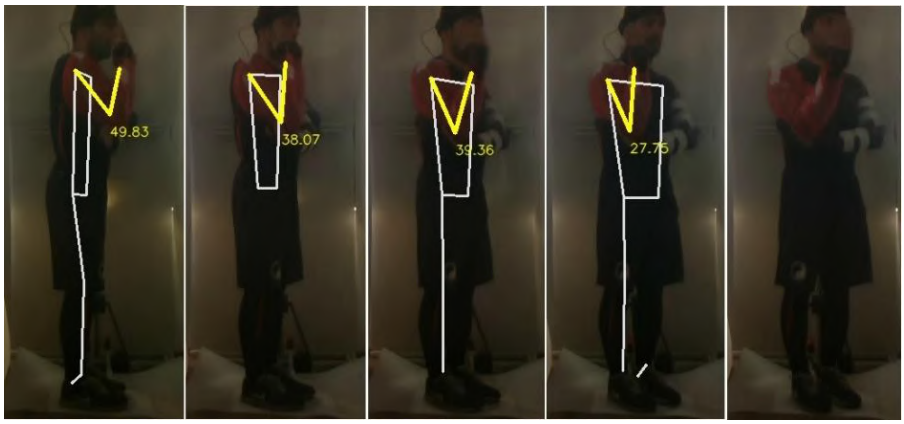


**Fig. 2.** Successive positions of the human subject for measuring the right elbow joint flexion angle

In order to fulfil the proposed objective, certain conditions were imposed and respected, as follows:
- to ensure that the human subject can obtain and maintain the joint angles as correctly as possible (necessary for the static analysis), a specially designed angle gauge was used so that it could be placed and maintained between the arm and forearm, having the angle of interest of 90°;
- an electronic protractor with a resolution of 0.1° was used and mounted at the level of the studied joint, distally, on its lateral face, in order to ensure a standardized measurement of the angles and the of joint's range of motion;
- during the motion analysis sessions, the human subject was equipped with the sensory suit of the Xsens MVN inertial motion analysis system;
- in regard to the elbow joint, the analysis sessions carried out also included experiments in which the corresponding upper limb was wrapped in a red cloth, to increase the accuracy of the determinations by obtaining a colour contrast in relation to the sensory suit;
- in order to ensure a proper procedure, the analysis sessions were carried out by reporting the positions of the human subject to fixed elements. Thus, a fixed bars assembly was used to ensure the necessary framework for performing motion analyses under repeatability conditions;
- in accordance with the previously mentioned objective, a set of five analysis sessions was created in which the entire body of the human subject was positioned angularly rotated in relation to the calibration landmark, by 0°, 15°, 30°, 45° and 60° (see Fig.1);
- in the case of video analyses, a software application was written in order to create twenty *.avi* files during the flexion-extension exercise of the right elbow for each position of the human subject's body using the video camera. These films were analysed frame by frame in order to identify the coordinates of the three points of interest (shoulder, elbow and wrist for the upper limb) necessary to calculate the joint angle. At the same time during the movement cycles, the sensors positioned on the special training suit sent the acquired data to the inertial motion analysis software, this software determining the joint angle in real time. Figures 1 and 2 (presented above) show the static and dynamic video analysis sessions of the elbow joint of the human subject.

## 4. Results

Both in the case of video analysis and in the case of the inertial one the numerical results obtained were analysed and represented in the form of graphs of variation of the measured size, namely of the angles of the joints of the elbows of the human subject under analysis. As mentioned before, the first section for each of the two types of motion analysis is dedicated to static conditions, and the second one to dynamic conditions.

### 4.1 Video monitoring - the right arm in a fixed position regarding the flexion angle of the elbow

The graphs in Fig.3 shows the measurement data of the 90° flexion angle of the right elbow joint depending on the processed video frame.

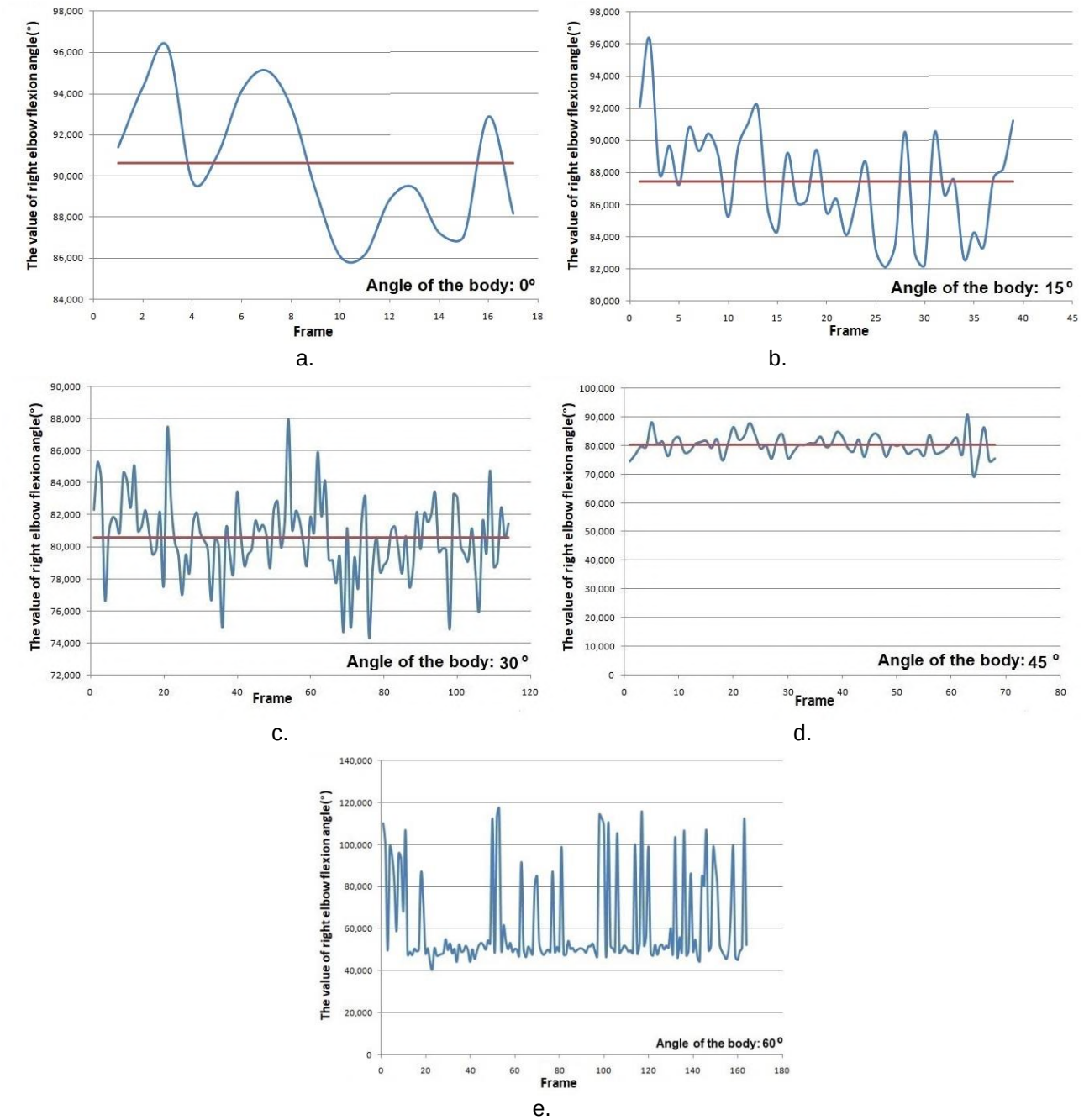


**Fig. 3.** The data extracted from the video frames regarding the angles of the right elbow joint, having the angle gauge mounted on its inner face - comparative results obtained after post-processing

In this analysis there were image frames in which human body landmarks could be detected by software and therefore the flexion angle was not represented on the graphs. Table 1 shows the data processing situation for the angular position in static conditions of the right elbow joint, as it was monitored by the video application.

**Table 1:** The data acquired and processed by the video application for the static flexion position of the right elbow joint

| The position of the body relative to the fixed reference on the floor | Number of frames having detected Landmarks | Average value of flexion angle (°) |
|---|---|---|
| Rotation: 0° | 17 | 90,61 |
| Rotation: 15° | 39 | 87,43 |
| Rotation: 30° | 114 | 80,56 |
| Rotation: 45° | 68 | 80,17 |
| Rotation: 60° | 164 | N/A |

### 4.2 Video monitoring - the right elbow flexion/extension

The graphs in Fig.4 shows the variation of the flexion/extension angles value of the right elbow as it is extracted from the processed frames.

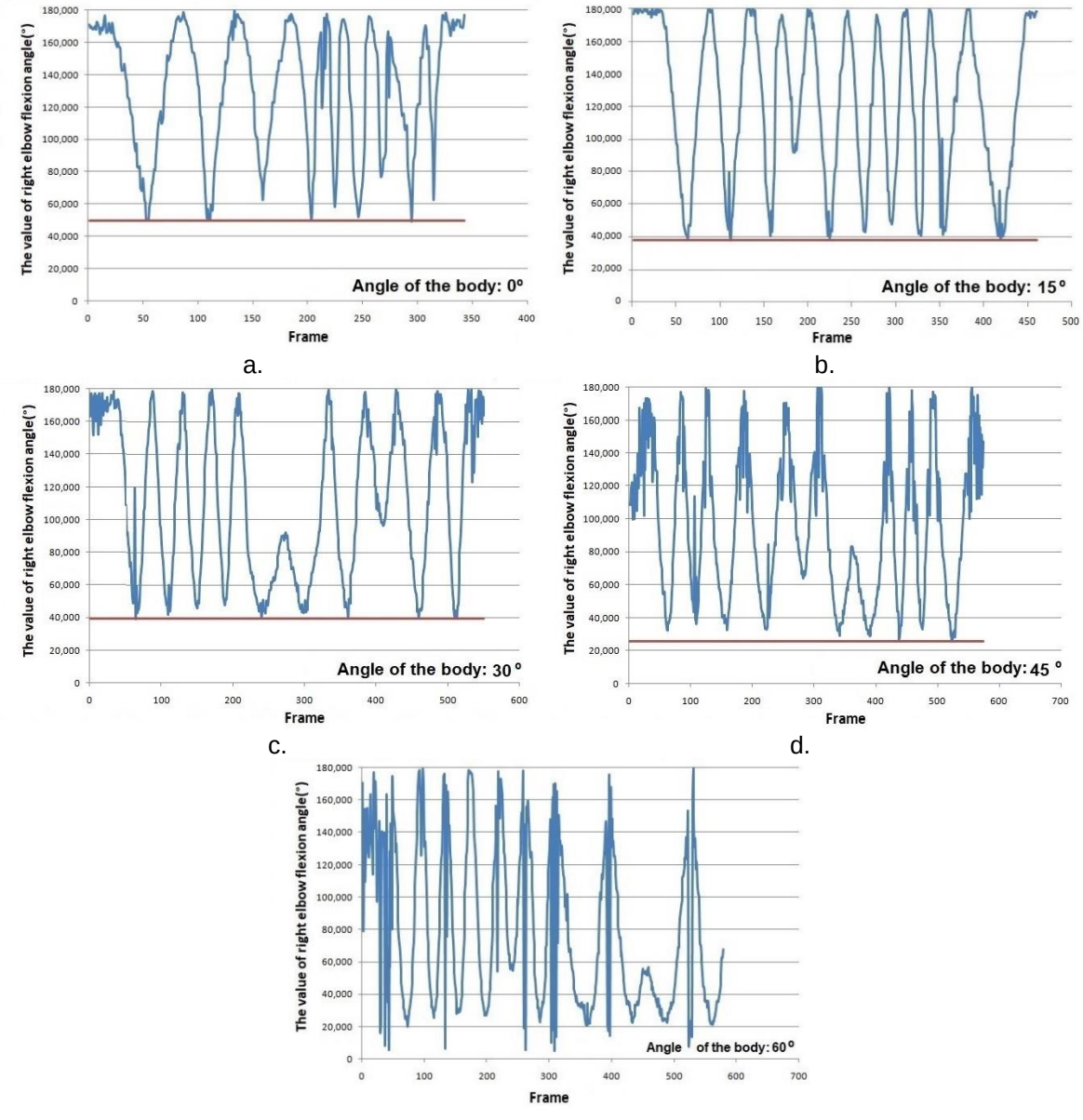


**Fig. 4.** The results obtained after processing the video frames of flexion/extension movements at the level of the right elbow joint

As in the previous case, in this analysis sessions there were image frames in which human body landmarks could be detected by software and therefore the flexion/extension angle was not represented on the graphs. This was the case of the set of frames associated with the rotation position of the human body at 60°, where the dispersion of the data did not allow the quick detection, using software successive comparisons, of the minimum value of the flexion/extension angle. Table 2 shows the data processing situation for the flexion movement of the right arm, as it was monitored by the video application.

**Table 2:** The data acquired and processed by the video application for the movement of the right elbow

| The position of the body relative to the fixed reference | Total number of frames | Number of frames having detected Landmarks | Minimum flexion angle (°) |
|---|---|---|---|
| Rotation: 0° | 672 | 342 | 49,83 |
| Rotation: 15° | 536 | 461 | 38,07 |
| Rotation: 30° | 601 | 551 | 39,36 |
| Rotation: 45° | 588 | 574 | 25,75 |
| Rotation: 60° | 615 | 614 | Not detected |

### 4.3 Inertial motion analysis using *Xsens MVN* system - static section

In order to create a static scenario within these analyses the human subject had to maintain, with or without external help, certain positions corresponding to certain joint angles (at the level of the elbow joint) determined with the help of the electronic protractor and/or the 90° angle gauge.
For the purpose of determining the correctness of the estimation of joint angles and of joint's range of motion, with the help of the Xsens MVN inertial motion analysis system, the values provided by the system in question were compared with those recorded on the digital protractor, as well as with the angle determined by positioning the angle gauge inside the joints in question. A digital protractor was chosen because it is commonly used in anthropometric measurements, being known as a goniometer. So, this analysis sessions were focused both on the determination of a relationship of proportionality between the values indicated on the digital protractor and those provided by the Xsens MVN inertial system, as well as on the verification of the accuracy of the latter. Fig.5 shows the results obtained in the case of the previously mentioned analysis. For this analysis, the human subject had to keep his forearm in three consecutive different positions, corresponding to the following flexion/extension angles indicated on the digital protractor: -8.8°, 65.2° and 98° respectively.

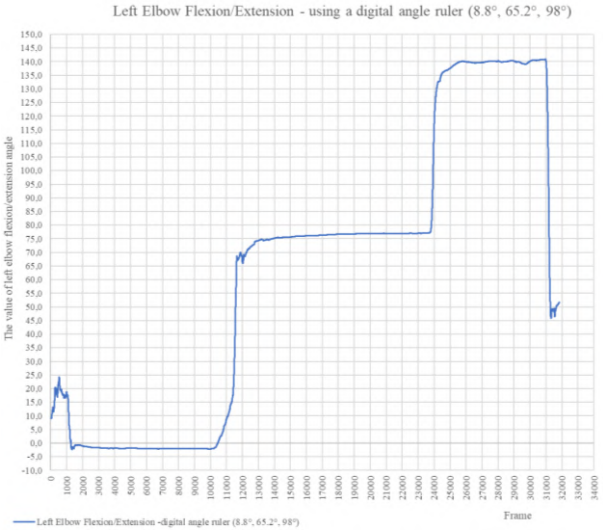


**Fig. 5.** The results obtained using Xsens MVN inertial analysis system, in the case of maintaining the flexion/extension angles at the level of the left elbow joint, for three different angular positions

In the graph represented in Fig.5, one can see the three levels corresponding to the previously mentioned flexion/extension angles. Following an elementary calculation, it can be established that

the angle of -8.8° indicated on the digital protractor corresponds to an extension angle of -1.98° in the inertial system. If there was a proportionality between these two measurements, it would mean that for the flexion angle of 65.2° indicated on the electronic protractor, the inertial system should indicate an angle of approximately 14.67°, respectively for the flexion angle of 98° indicated on the electronic protractor, the inertial system should indicate an angle of approximately 22.05°. However, the graph shows an angle of approximately 76.64° and 139.94°, respectively. The situation is repeated if the other two angles indicated by the digital protractor are taken as a reference. It thus emerges the fact that a proportionality between the two measurements cannot be determined, this fact could be due to one of the following phenomena: the occurrence of a gross error of the inertial system, or the change in the position of the digital protractor in relation to the initial position.

Considering the fact that the digital protractor was placed and fixed on the external face of the arm and the forearm respectively, the conducted experiments highlighted the following aspects:

- in regard to the joint's range of motion recorded with the help of the digital protractor the maximum and minimum values differed not only from one session to another (each session presupposing a repositioning of the digital protractor on the arm of the human subject under analysis), but also from one movement to another. The differences were created, as expected, by the location of the joint of the digital protractor in relation to the studied joint, by the muscular reaction at the stroke ends of the movement, a phenomenon that produced the displacement of the measuring instrument used, in relation to his initial position. More precisely, this change in the position of the digital protractor during movement was due to the impossibility of fixing in place the measuring instrument in question, directly on the bone surfaces (which has the advantage of not changing its three-dimensional shape in relation to the joint angle) and the lack of fixed physical landmarks having a well-defined shape, which allows precise and repeatable successive repositioning;
- a displacement of the digital protractors positions still occurred in relation to its initial position, even if the forearm was kept in supination throughout the execution of the flexion/extension movements at the elbow joint. As expected, another thing happened in this situation, namely the decrease of the maximum amplitude of the studied joint, by decrementing the value of the upper limit of the flexion angle, due to the biceps muscle contraction necessary to maintain the supination of the forearm.

The phenomenon described above was also observed in the case of the analyses performed with the angle gauge positioned on the inner face of the elbow joint. In the case of these analyses, the attention was focused on the ability of the inertial system to provide values that indicate that the movement at the level of the elbow joint it is blocked, due to the placement of the mentioned instrument inside the elbow joint and to its fastening on the arm and forearm. The graph in Fig.6, clearly shows that Xsens MVN inertial system correctly indicates the fact that the flexion angle at the level of the right elbow joint is properly maintained within certain limits.


**Fig. 6. The graphical representation of** the amplitude of the variation of the flexion/extension angle at the level of the right elbow joint, blocked due to the positioning of the angle gauge inside it

The graph in fig.6 shows that the variation of the flexion angle it is relatively small (approximately 0.4°) and is most likely due to the attempt of the human subject under analysis to maintain the imposed angular position. Thus, it can be observed that, even in the case of physical blocking of the joint movement, there is still an angular variation due to the modification of the shape of the muscles with which the angle gauge is in contact, this amplitude being able to decrease once the biceps muscle gets in a relaxed state. It should be mentioned, in the case of this analysis, the fact that the digital protractor did not register changes in the angle value. This clearly denotes the fact that this last-mentioned instrument cannot be mounted so well as to be able to record even the smallest possible variations and also clearly highlights the involvement of the bicep's contraction in the angular variations that occur, as well as a compression of the soft body segments in contact with the angle gauge. An extremely important element in this analysis is that the value of the flexion angle is different from the value of the angle gauge, due to the fact that the latter is in contact with the muscles and not with the bones, the joint angles being determined according to the specialized literature by reference to bone structures. It should be mentioned that the flexion/extension angle within the Xsens MVN it is represented by the angle between the forearm in the "0" position of the calibration of the system in question and the position of the forearm at a certain moment in time. More precisely, the flexion angle does not represent the angle between the arm and the forearm. Xsens MVN thus assigns positive angle values to the flexion movement and negative values to the extension movement, regardless of whether it is the upper or lower limb.
A new analysis was carried out, in order to confirm or deny this assumption, that contained five sessions, which assumed the repetition of the restriction of the elbow joint movement. In this case, the human subject has had the task of maintaining the same muscle tension in the analysed joint, on the inner side of which the angle gauge was placed. Analysing the data provided by the Xsens MVN inertial system, it can be seen that it correctly indicates the blockage at the level of the elbow joint (see Fig.7), in all five dedicated sessions.

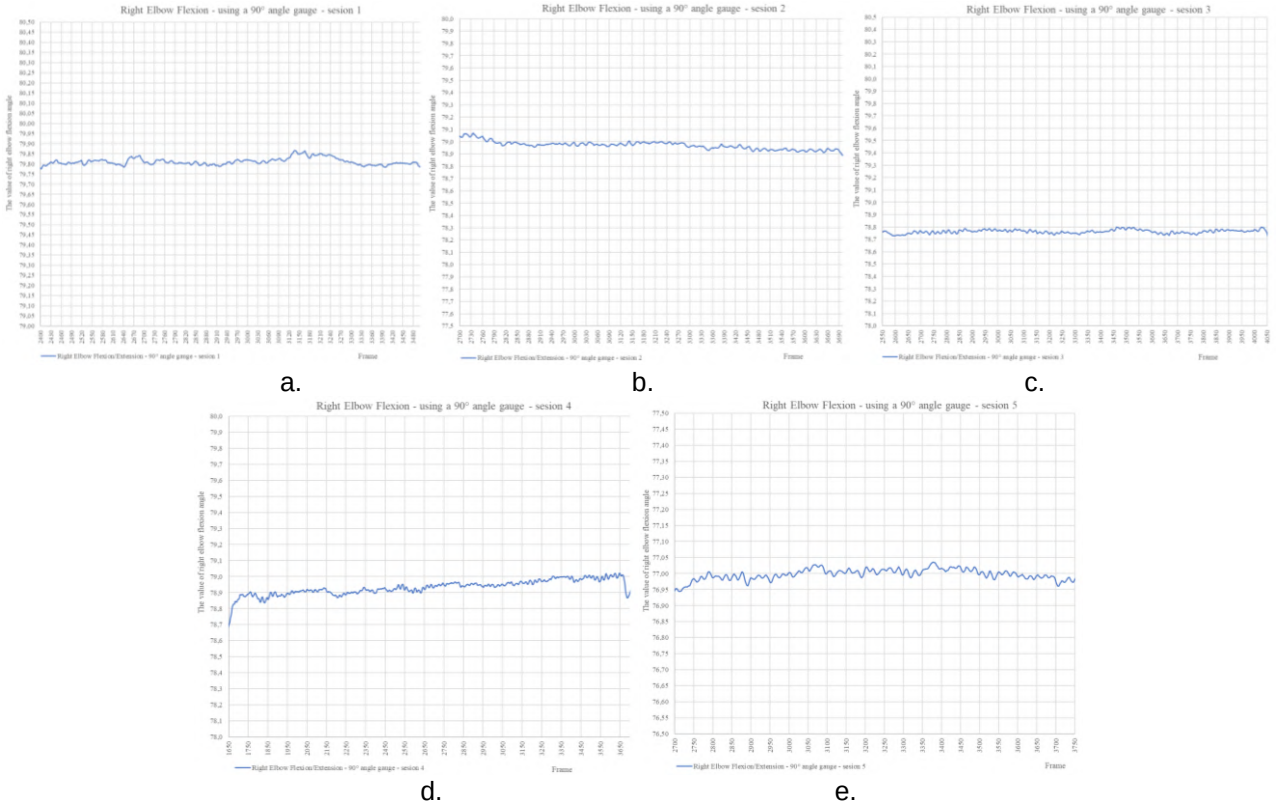


**Fig. 7.** The results obtained in the five motion analysis sessions carried out using Xsens MVN, regarding the amplitude of the variation of the flexion/extension angle at the level of the right elbow joint, blocked due to the positioning of the angle gauge inside it

The amplitude of variation of the flexion angle (in the case of the elbow joint) is the same in all five sessions (approximately 0.4° - see Fig.7), differing only in the average value of the angle in

question. The observed variation is clearly due to a combination of factors, namely: the different muscle tension from one session to another, the impossibility of identical placement of the angle gauge from one session to another and the compressibility of soft anatomical elements (skin and muscles).
Consequently, it can be said that the hypothesis of the appearance of an angular variation due to the human subject's attempt to maintain the position even in the case of a physical blockage applied to the joint in question, in contact with the angle gauge, is confirmed.

### 4.4 Inertial motion analysis using *Xsens MVN* system - dynamic section

During these motion analyses, the human subject had to perform ten flexions/extensions at the level of the elbow joint, the movements being limited or not in a certain direction with the help of props whose shape and position in space cannot be modified. In these analyses the purpose was to determine the ability of the Xsens MVN inertial system to properly determine the flexion/extension angle and respectively the joint’s range of motion. In this situation, the role of the prop was to ensure the necessary framework for the execution of joint movements with a predetermined range of motion, limited by the contact at the end of the stroke between the moving body segments and it.

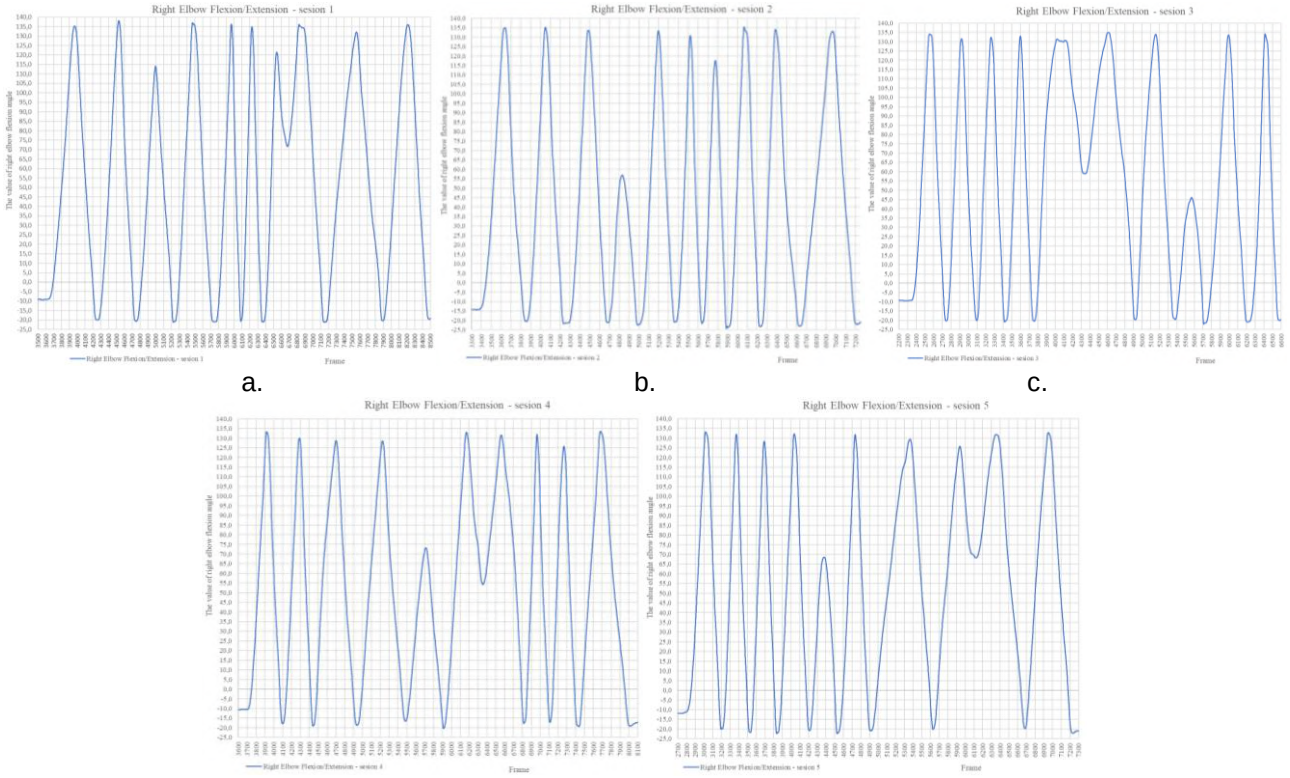


**Fig. 8.** The data obtained in the five motion analysis sessions carried out with the help of Xsens MVN, regarding the range of motion at the level of the right elbow joint

The movements in the case of the elbow joint were mechanically limited by the contact with the outer face of the chin of the human subject undergoing analysis (having his head previously fixed in an immutable position) for the entire duration of an analysis session. Intermediate flexion/extension movements were also performed, in order to clearly demonstrate the ability of the Xsens MVN inertial system to properly determine the flexion angle. As can be seen in Fig.8, the amplitude differences between the ten flexion/extension movements performed in each analysis session are clearly highlighted. It can also be observed that the average value of the range of motion is approximately the same in the five sessions, the small differences of tenths of a degree being most likely generated by the compression of the soft body segments, following the contact with the limiting elements.

### 4.5 Video analysis method versus inertial method – a comparative approach

The results generated by the inertial motion analysis system and data obtained by processing successive video frames were processed to obtain the flexion-extension angles. The graphs have local minima and maxima, which correspond to incomplete flexion-extension movements. The flexion-extension movements performed faster or slower are highlighted on the graph by the numerical value of the ascending and descending slopes associated with each movement. As expected, for all the graphs obtained with the help of the inertial system, the maximum and minimum values of the measured angles (for the full flexion movement) are not affected by the positioning of the human subject's body in relation to the video camera image plane. Instead, the minimum values of the angles measured with the help of the video application, corresponding to full flexion, are different, depending on the rotation angle of the human body compared to the fixed reference on the floor. In order to allow a comparative analysis of the quality of the graphic representations, the values of the angle supplements obtained through video analysis were represented in the graph in Fig.9.b.

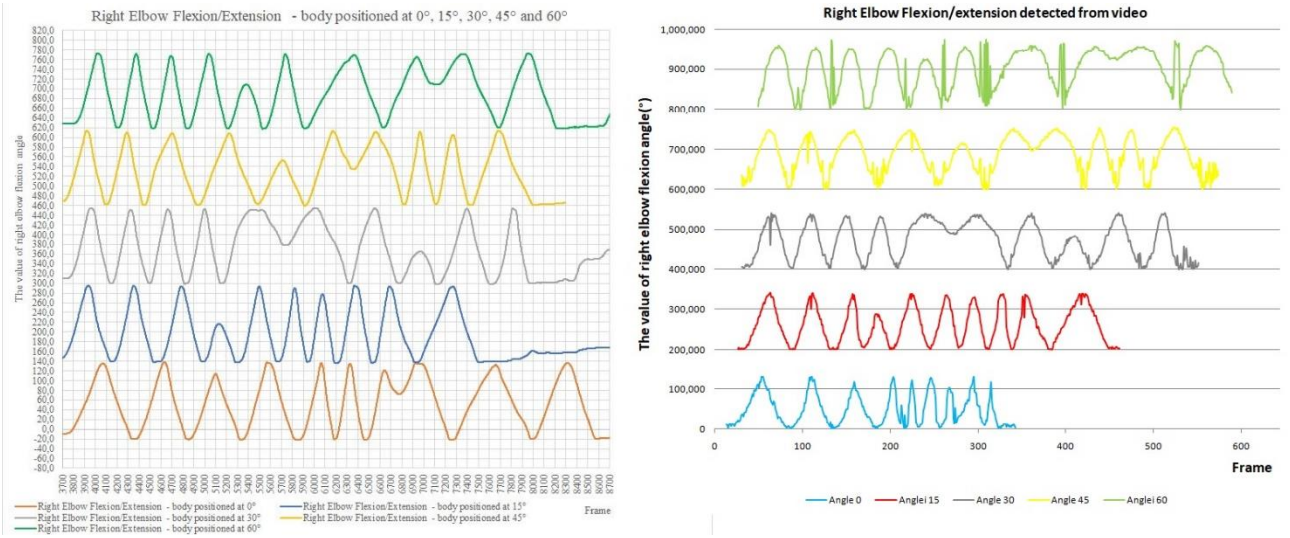


a. b.

**Fig. 9.** The comparative results of flexion/extension movements at the right elbow joint level, obtained with: a) Xsens MVN inertial system; b) video analysis

Analysing the graph in fig.9, one can clearly see that the data extracted using video analysis has a different number of points because body landmarks could not be extracted from some video frames. In some successive video frames from the film associated with the positioning of the human body at 60° from the camera plane, incorrect positions for the shoulder, elbow and wrist were detected, for the shoulder the calculated angle values are not acceptable. The synoptic analysis of the two graphs indicates that the allure of these graphs is the very similar.

### 5. Conclusions

Using MediaPipe software for video analysis of moving images of the human body is an affordable method of calculation and quantitative evaluation of the movements made by human subjects during sports training. The carried-out sessions revealed the fact that the relative position of the human subject to the room plane influences the calculated value of the flexion-extension angle. Because both the T-shirt and the pants of the sports suit, used by the human subject, are black, some image frames could not be processed. So, the optimum solution was to create a colour contrast between the moving arm and the rest of the body. Taking into account the previously mentioned facts, we can assert that, if the video analysis includes an initial stage of adequate calibration, this method will also allow a qualitative evaluation of the movements of human subjects. Future research will address the following aspects: augmenting the video analysis method with data delivered by acceleration, rotation, magnetic sensors and measuring the distance

of the human body from the video camera plane, as well as increasing the speed of real-time detection of body landmarks, by writing software applications in the C++ language.
Using Xsens MVN inertial system provides a precise method of motion analysis when the quality of the information provided by it is evaluated from a biomechanical point of view. More precisely, for the cases presented in the present paper, this means that the precision of measuring the joints angles and the joint's range of motion must be correlated with the phenomena that occur in the case of the human joint motion and not through the prism of a hinge-type mechanical joint, in which the joint elements are non-deformable. Thus, in a biomechanical analysis, the biological component can significantly modify the result of the analysis, mainly due to the high deformability of the anatomical elements involved both in making the movement and in limiting it, as well as due to the precision of making the movements, or more exactly the level of neuromuscular control of the human subject under analysis. Although the digital protractor is used in the anthropometric measurements (goniometer), it was found during the tests described in this article, that it cannot represent a standard for the evaluation of the two analysis systems (inertial and video), mainly due to the impossibility of achieving a precise, stable and repeatable positioning of the measuring instrument, on the segments of the human body joints.

**Acknowledgments**

This work was carried out through the NUCLEU Program, conducted with the support of MCID (Ministry of Research, Innovation and Digitization), project number: PN 23 43 03 01 -17N/2023. This scientific paper provides the opportunities for the creating international collaborations through the project "Support Center for International RDI projects in the field of Mechatronics and Cyber-MixMechatronics", Grant agreement no. 323/340002/23.09.2020, SMIS 108119.

**References**

[1] MediaPipe. "Pose landmark detection guide." Accessed October 2, 2023 https://developers.google.com/mediapipe/solutions/vision/pose_landmarker/.
[2] Constantin, Anghel, and Gheorghe I. Gheorghe. "CMOS transducer with linear response using negative capacity that can be used in mechatronic systems for force measurement in human walking analysis and in the future in MEMS and NEMS applications." Paper presented at the CONTROLO 2016 - 12th Portuguese Conference on Automatic Control, Guimarães, Portugal, September 14-16, 2016. *CONTROLO 2016. Lecture Notes in Electrical Engineering* 402 (2017): 483–494.
[3] Badea, Cristian Radu. "Researches on inertial mechatronic motion analysis systems, based on mems." *The Scientific Bulletin of VALAHIA University, Section –MATERIALS and MECHANICS* 16, no. 15 (2018): 44-50.
[4] Badea, Cristian Radu, and Sorin Ionuț Badea. "The positioning errors generated by Xsens MVN inertial system during the analysis of Push-ups exercise, using the Single Level scenario, before and after the calling of REPROCESS function." *International Journal of Mechatronics and Applied Mechanics*, no. 4 (2018): 120-133.
[5] Badea, Cristian Radu. ''Study on the influence of contact points, scenarios and graphical reference elements on the motion analysis process, carried out using the inertial mechatronic system MVN Analyze.'' *International Journal of Mechatronics and Applied Mechanics* 2, no. 6 (2019): 74-81.
[6] Schepers, Martin, Matteo Giuberti, and Giovanni Bellusci. ''Xsens MVN: Consistent Tracking of Human Motion Using Inertial Sensing.'' XSENS TECHNOLOGIES B.V., Technical Report, March 2018.
[7] Guo, Liangjie, and Shuping Xiong. ''Accuracy of Base of Support Using an Inertial Sensor Based Motion Capture System.'' *Sensors* 17, no. 9 (September 2017): 2091.
[8] Roetenberg, Daniel, Henk Luinge, and Per Slycke. ''Xsens MVN: Full 6DOF human motion tracking using miniature inertial sensors.'' XSENS TECHNOLOGIES B.V., April 2013.
[9] Zhang, Jun-Tian, Alison C. Novak, Brenda Brouwer, and Qingguo Li. ''Concurrent validation of Xsens MVN measurement of lower limb joint angular kinematics.'' *Physiological Measurement* 34, no. 8 (August 2013): 63-69.
[10] Wouda, Frank J., Matteo Giuberti, Giovanni Bellusci, and Peter H. Veltink. ''Estimation of Full-Body Poses Using Only Five Inertial Sensors: An Eager or Lazy Learning Approach?'' *Sensors* 16, no. 12 (December 2016): 2138.

# Double Gumbel Function Optimization through PSO and Maximum Likelihood for Data Analysis Using AI

Dr. **Maritza ARGANIS**[1,*], M.Eng. **Margarita PRECIADO**[2,*]

[1] Universidad Nacional Autónoma de México. Instituto de Ingeniería. Facultad de Ingeniería, México

[2] Instituto Mexicano de Tecnología del Agua, Jiutepec, Mor.

* MArganisJ@iingen.unam.mx; preciado@tlaloc.imta.mx

***Abstract:*** *Maximum annual hydrological frequency analysis data series requires techniques use to estimate distribution functions parameters; in case of univariate distribution functions that have more than two parameters, traditional methods complexity, such as the moment's method, increases. In this research, the five double Gumbel distribution parameters of a function were estimated to approximate maximum annual daily measured rainfall data from a climatological station located at state of Jalisco, Mexico. To achieve this objective, Bing AI tool was used to develop a program in Python language that uses PSO particle cluster optimization algorithm from evolutionary computing using as an objective function the likelihood maximization function. Bing AI was oriented by giving a search interval taken from result reported by a program that uses traditional least squares technique and with this, it was possible to eliminate errors in the AI program that finally gave adjustments with a standard error of 13.858 acceptable for data estimation with return periods between 5 and 30 years standard fitting error.*

***Keywords:*** *Bing IA, evolutionary computation, frequency analysis, objective function, annual maximum dairy precipitation*

## 1. Introduction

Functions optimization is a fundamental aspect in data analysis, as it allows finding the optimal values that maximize or minimize a certain metric. In particular, the double Gumbel function is widely used in various fields, such as statistics and engineering, to model extreme distributions, specifically in hydrological analysis this distribution function is typical of precipitation data or runoff in coastal sites subject to the presence of hurricanes at certain year times and also in sites where winter rains known as "equipatas" occur [1, 2]. In this paper, we will explore how the combination of PSO (Particle Swarm Optimization) optimization technique and maximum likelihood approach can improve efficiency and accuracy in optimizing double Gumbel function for data analysis. Furthermore, we will leverage machine learning power of (AI) to further enhance this process.

## 2. Methodology

### 2.1 Double Gumbel function

Double Gumbel function [1,3] is a probability distribution that is used to model extreme events in a data set. The distribution function and density function take the form of equations 1 and 2. It is observed that it has 5 parameters p, $\alpha_1$, $\beta_1$, $\alpha_1$ and $\beta_2$, so the use of traditional parameter estimation techniques, for example moments are elaborate since it must be considered up to the fifth population and sample moment.

$$F(x) = p\left(e^{-e^{-y_1}}\right) + (1-p)\, e^{-e^{-y_2}} \tag{1}$$

$$f(x) = p\,\alpha_1\, e^{-e^{-y_1}} + (1-p)\,\alpha_2\, e^{-e^{-y_2}} \tag{2}$$

### 2.2 Optimization by Maximum Likelihood and PSO

Optimizing a function involves finding parameters that best fit the observed data. In frequency analysis, a classic optimization technique is maximum likelihood method, which consists of finding density function parameters f(x) of a variable x that maximize likelihood function L given by density function product valued at each known value xi; this means that objective function in this paper takes equation 3 form.

$$OF = máx(\prod_{i=1}^{n} f(xi, p, \alpha_1, \beta_1, \alpha_2, \beta_2) \quad (3)$$

Some tools for t frequency analysis maximum annual data series use least squares regression technique to solve problem, usually aided with logarithmic transformations use.

In this paper, it is proposed to use Particle Swarm Optimization tool, from evolutionary computing.

By combining PSO with maximum likelihood approach to double Gumbel function optimize, we can obtain more accurate and reliable results and, therefore, obtain a better double Gumbel function estimation

### 2.3 Particle Swarm Optimization (PSO)

It is a random algorithm with great potential and a simple form that makes an analogy of social behavior that species such as fish and birds naturally follow; it was proposed in 1995 [4]. Algorithm randomly generates a population of candidate solutions, called a particle swarm, in each iteration each particle has a position in solution search problem space, each particle has a velocity vector with which it moves in solution search space; particles interact and learn from each other; each particle has a memory of its best personal position and all particle swarm have a best global position. In each iteration, position and each particle velocity are obtained; for this, a vector is defined that goes from position in one iteration x_i (t) to best personal position p_i (t) and another vector that connects position in one iteration with best global position g(t); each particle moves parallel to its velocity vector, to vector that associates it with its best personal position and parallel to best global position obtaining each particle position in next iteration; vector that connects position in previous iteration with position in next iteration is particle velocity at next iteration. Mathematically, this is expressed as indicated in equations 4 and 5.

$$v_i(t+1) = wv_i(t) + c_1\big(p_i(t) - x_i(t)\big) + c_2(g(t) - x_i(t)) \quad (4)$$

$$x_i(t+1) = x_i(t) + v_i(t+1) \quad (5)$$

The equation to update the velocity in terms of its components at the next instant $v_{ij}(t+1)$ is (equation 6):

$$v_{ij}(t+1) = wv_{ij}(t) + r_1c_1\left(p_{ij}(t) - x_{ij}(t)\right) + r_2c_2(g_i(t) - x_{ij}(t)) \quad (6)$$

And to update the position in terms of its components, we have (equation 7)

$$x_{ij}(t+1) = x_{ij}(t) + v_{ij}(t+1) \quad (7)$$

In equation 6, first term is called inertia term and coefficient w is inertia coefficient. Coefficients c1 and c2 are called acceleration coefficients, second term is known as cognitive component and the last term is known as social component. $r_1$ and $r_2$ are random numbers with a uniform distribution [0,1].

### 2.4 Bing AI

With advances in machine learning, field of we can now leverage AI power to enhance optimization process by grouping evolutionary computation use to perform likelihood function maximization.

By using AI in this process, we can take machine learning capabilities advantage to further improve optimization. For example, we can use supervised machine learning algorithms to train a model that can predict the optimal double Gumbel function parameters from previously observed data. This would allow us to speed up optimization process and obtain more accurate results in real time.

In this case, different instructions were given to Bing AI chat [5] to build a program in Python language that could be run on the Anaconda© Jupiter notebook platform [6] Input data to the problem, methods desired to solve it, and desired output were specified in detail. First program generated by Bing AI chat marked various errors associated with the dimensioning of the vector containing the search variables. Additionally, Bing AI chat had to be told in more detail that density function f(x) would be used for optimization and the distribution function F(x) and a transformed variable z for drawing the behavior of the information. After about five trials, program was successfully executed for randomly generated x data; subsequently, specific data from an analyzed site were added to perform the parameter retrieval procedure. Initial program code that worked is shown in Figure 1.

```
import numpy as np
import matplotlib.pyplot as plt
import pyswarms as ps
# Definition of the x vector with the data
nd = 32
x =
np.array([56.8,40,81.8,43,100,36.2,60,52.5,65,108.5,42.6,42.1,118.5,40.2,30.5,30.5,35,52.6,70,40,30,60,40,45,60,65,65,65,50,45,80,65
])
# Definition of the objective function
def f(params):
    p, alpha1, alpha2, beta1, beta2 = params
    y1 = alpha1 * (x - beta1)
    y2 = alpha2 * (x - beta2)
    return p * np.exp(-np.exp(-y1)) + (1 - p) * np.exp(-np.exp(-y2))
# Definition of the cumulative distribution function F(x)
def F(params):
    return np.cumsum(f(params))
# Definition of the likelihood function
def likelihood(swarm):
    n_particles = swarm.shape[0]
    return np.array([-np.sum(np.log(f(swarm[i]))) for i in range(n_particles)])
# Configuration of the optimizer
options = {'c1': 0.5, 'c2': 0.3, 'w':0.9}
optimizer = ps.single.GlobalBestPSO(n_particles=10,dimensions=5,options=options)
# Execution of the optimizer and storage of the likelihood function at each iteration
iters = 20
likelihood_values = []
for i in range(iters):
    cost,pos = optimizer.optimize(likelihood,iters=1)
    likelihood_values.append(cost)
# Graphing the results
plt.plot(range(iters), likelihood_values,'-')  # Calculated data with lines
plt.xlabel('Iteration number')  # Label for the horizontal axis
plt.ylabel('Likelihood')  # Label for the vertical axis
plt.show()
# Print the optimal parameters
print("The optimal parameters found with maximum likelihood are:")
print(f"p: {pos[0]}, alpha1: {pos[1]}, alpha2: {pos[2]}, beta1: {pos[3]}, beta2: {pos[4]}")
# Calculate and print the value of the function f(x) with optimized values
fx_opt = f(pos)
print(f"The value of the function f(x) calculated with these optimized values is: {fx_opt}")
# Calculate and print the value of the likelihood function with optimized values
likelihood_opt = likelihood(np.array([pos]))
print("The value of the likelihood function calculated with these optimized values is: {likelihood_opt}")
```

**Fig. 1.** Maximum likelihood code optimization program using PSO generated by Bing AI Chat

## 2.5 Input data

Thirty two historical record maximum daily precipitation data from climatological station 14064 from Clicom database, located in the state of Jalisco in Mexico [7], were considered (Figure 2).

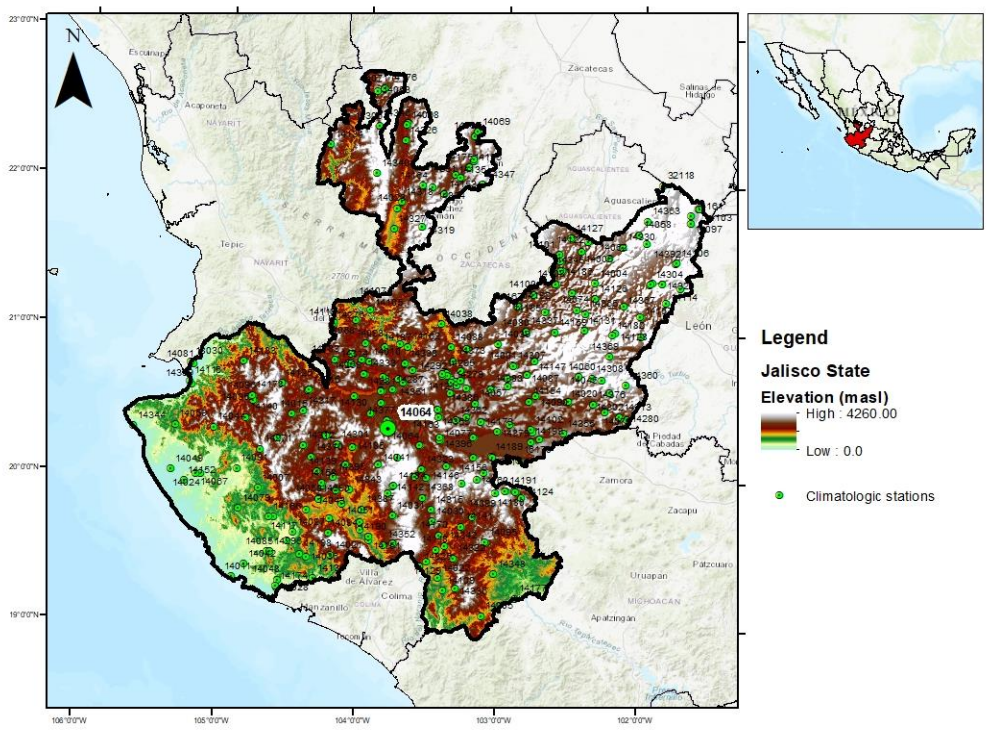


**Fig. 2.** Climatological station location used in our analysis, Jal. Mexico. Source: Own elaboration

## 3. Results

Final program made by Bing AI chat, feeding it with annual maximum daily rainfall data from station 14064, program resulted in Figure 3, which reports objective function value for each iteration. It is worth noting that program uses a method that originally minimizes, and for this reason, result of likelihood function value appears with opposite sign to indicate that a maximum value was obtained.

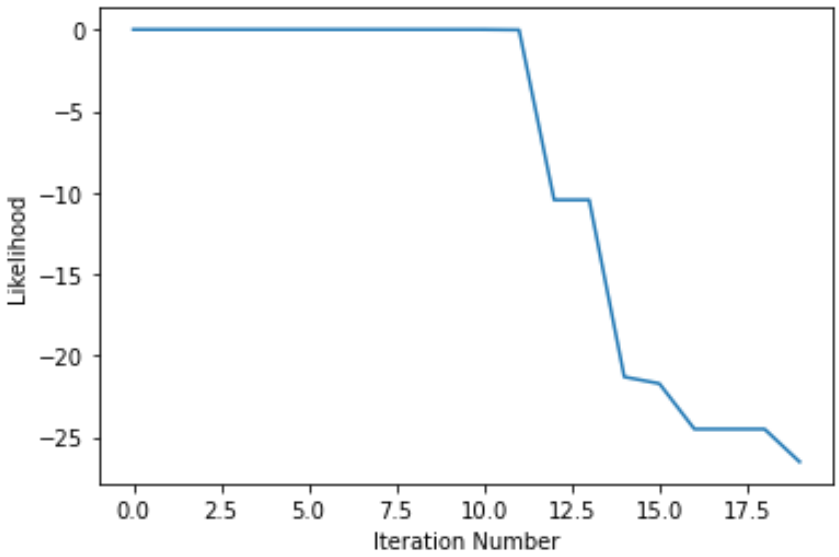


**Fig. 3.** Iteration number Graph vs optimized likelihood function value. Source: PSO program and maximum likelihood in Python from Bing AI chat. In Jupiter notebook. Anaconda

Program also reports information in Figure 4.

Optimal parameters found with maximum likelihood are: p: 2.290741286980267, alpha1: 0.5105690232088207, alpha2: -0.1679911851544585, beta1: -0.2712261197011611, beta2: 2.4006206416271803 The value of the function f(x) calculated with these optimized values is: [2.29074129 2.29074128 2.29074129 2.29074129 2.29074129 2.29074127 2.29074129 2.29074129 2.29074129 2.29074129 2.29074129 2.29074129 2.29074128 2.29074094 2.29074094 2.29074125 2.29074129 2.29074129 2.29074128 2.29074084 2.29074129 2.29074128 2.29074129 2.29074129 2.29074129 2.29074129 2.29074129 2.29074129 2.29074129 2.29074129 2.29074129]. The value of the likelihood function calculated with these optimized values is: [-26.52401456]

**Fig. 4.** Results reported by the PSO program and maximum likelihood in Python from Bing AI chat. In Jupiter notebook. Anaconda

From Figure 4, we have that parameters obtained by PSO algorithm are: p: 2.2907, α1: 0.5106, β1: -0.2712, α2: -0.1680, β2: 2.4006.

Additionally, program reports density function value f(x) evaluated at each x value, as well as objective function value of -26.5240

Upon reviewing previous results, it was observed that p value obtained by program is outside values that probabilistically define such parameters (p can only take values between 0 and 1), but this information was not included in algorithm so it was necessary to make modifications, asking Bing AI chat to add instructions to add such restrictions. Final modified program appears in Figure 5.

```
import numpy as np
import matplotlib.pyplot as plt
import pyswarms as ps
# Definition of the x vector with the data
nd = 32
x=
np.array([56.8,40,81.8,43,100,36.2,60,52.5,65,108.5,42.6,42.1,118.5,40.2,30.5,30.5,35,52.6,70,40,30,60,40,45,60,65,65,65,50,45,80,65
])
# Definition of the objective function
def f(params):
    p, alpha1, alpha2, beta1, beta2 = params
    y1 = alpha1 * (x - beta1)
    y2 = alpha2 * (x - beta2)
    return p * np.exp(-np.exp(-y1)) + (1 - p) * np.exp(-np.exp(-y2))
# Definition of the cumulative distribution function F(x)
def F(params):
    return np.cumsum(f(params))
# Definition of the likelihood function
def likelihood(swarm):
    n_particles = swarm.shape[0]
    return np.array([-np.sum(np.log(f(swarm[i]))) for i in range(n_particles)])
# Optimizer configuration
options = {'c1': 0.5, 'c2': 0.3, 'w':0.9}
# Definition of particle boundaries
bounds = (np.array([0,-1000,-1000,-1000,-1000]), np.array([1,1000,1000,1000,1000]))
optimizer = ps.single.GlobalBestPSO(n_particles=10,dimensions=5,options=options,bounds=bounds)
# Execution of the optimizer and storage of the likelihood function at each iteration
iters = 20
likelihood_values = []
for i in range(iters):
    cost,pos = optimizer.optimize(likelihood,iters=1)
    likelihood_values.append(cost)
# Plotting the results
plt.plot(range(iters), likelihood_values,'-')  # Calculated data with lines
plt.xlabel('Iteration number')  # Label for the horizontal axis
plt.ylabel('Likelihood')  # Label for the vertical axis
plt.show()
# Print the optimal parameters
print("The optimal parameters found with maximum likelihood are:")
print(f"p: {pos[0]}, alpha1: {pos[1]}, alpha2: {pos[2]}, beta1: {pos[3]}, beta2: {pos[4]}")
# Calculate and print the value of the function f(x) with optimized values
fx_opt = f(pos)
print(f"The value of the function f(x) calculated with these optimized values is: {fx_opt}")
# Calculate and print the value of the likelihood function with optimized values
likelihood_opt = likelihood(np.array([pos]))
print(f"The value of the likelihood function calculated with these optimized values is: {likelihood_opt}")
```

**Fig. 5.** Modified code of the maximum likelihood optimization program using PSO generated by Bing AI Chat

Results obtained in this case appear in Figures 6 and 7.

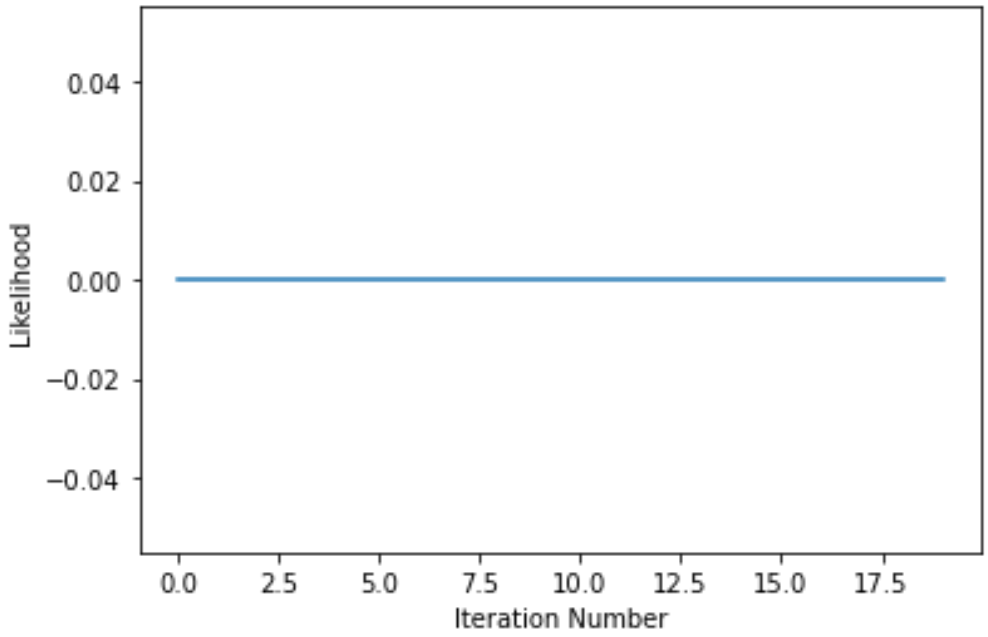


**Fig. 6.** Iteration number Graph vs optimized likelihood function value of. Source: PSO program and maximum likelihood in Python from Bing AI chat. In Jupiter notebook. Anaconda

Optimal parameters found with maximum likelihood are: p: 0.06229598442521622, alpha1: 431.53226191262684, alpha2: -587.9153262587531, beta1: -163.58414373459, beta2: 173.92428544406835 The value of the function f(x) calculated with these optimized values is: [1. 1. 1. 1. 1. 1. 1. 1. 1. 1. 1. 1. 1. 1. 1. 1. 1. 1. 1. 1. 1. 1. 1. 1. 1. 1. 1. 1. 1. 1. 1.] The value of the likelihood function calculated with these optimized values is: [-0.]

**Fig. 7.** Results reported by modified PSO program and maximum likelihood in Python from Bing AI chat. In Jupiter notebook. Anaconda

From Figure 7, parameters obtained by PSO algorithm are: p=0.062296, α1= 431.5323, β1= -163.5841, α2= -587.9154, β2=173.9243, with a number of iterations equal to 20.
To check measured and calculated data, AX program [8] was used as support to obtain double Gumbel function parameters; this program performs an automatic adjustment and for this it uses an optimization by least squares; parameters reported by AX were: p= 0.895 α1= 0.082958 β1= 44.3403 α2 =0.072066 β2=103.7846 standard fit [8] of 3.18.
On the other hand, double Gumbel function parameters obtained with PSO and maximum likelihood from AI program were manually entered into AX. Standard fit error in this case is 129.282, but in this case with AX it is not possible to calculate the x data values to make results comparison.
By increasing iterations number at program to 100 and changing search parameters interval to bounds = (np.array([0.7,0.05,0.05,30,80]), np.array([1,0.1,0.1,50,120])), the results of Figures 8 and 9 are obtained.

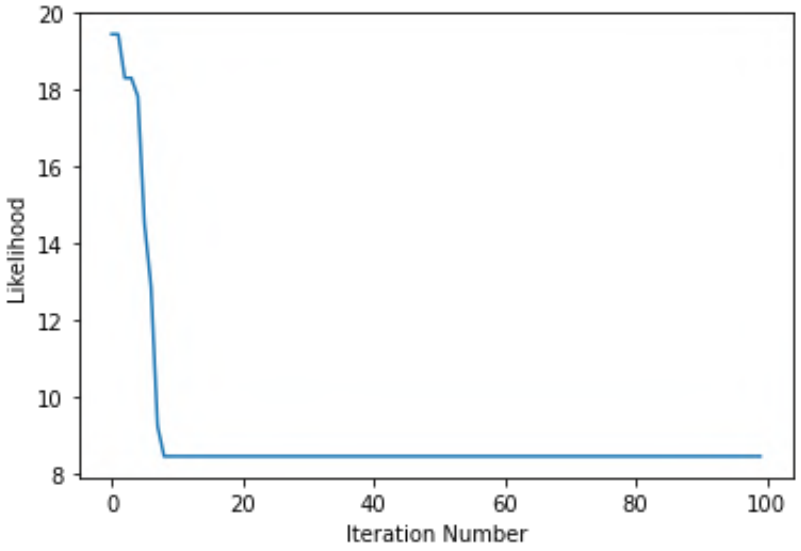


**Fig. 8.** Graph of iteration number vs value of optimized likelihood function. Source: PSO program and maximum likelihood in Python from Bing AI chat. In Jupiter notebook. Anaconda

Optimal parameters found with maximum likelihood are: p: 0.9044526127596921, alpha1: 0.06894210209217676, alpha2: 0.0692385601018597, beta1: 30.760016258389406, beta2: 97.08696390089152 The value of the function f(x) calculated with these optimized values is: [0.76604752 0.53297039 0.88339593 0.58832433 0.93903588 0.45489691 0.79165459 0.72337798 0.82301594 0.96090501 0.58129238 0.57234923 0.97846066 0.53684426 0.32676531 0.32676531 0.42871629 0.72448911 0.84610593 0.53297039 0.31530353 0.79165459 0.53297039 0.62183152 0.79165459 0.82301594 0.82301594 0.82301594 0.69361062 0.62183152 0.8782631 0.82301594] The value of the likelihood function calculated with these optimized values is: [13.61567589]

**Fig. 9.** Results reported by modified pso program and maximum likelihood in Python from Bing AI chat. In Jupiter notebook. Anaconda

From Figure 9, parameters obtained by pso algorithm are: p=0.9045, α1= 0.0689, β1= 30.7600, α2= 0.0692, β2=97.0870, with a number of iterations equal to 40. Upon manually inserting these parameters into AX, a standard fitting error of 13.858 is obtained.
Figure 10 compares results obtained with pso AI maximum likelihood and AX program.

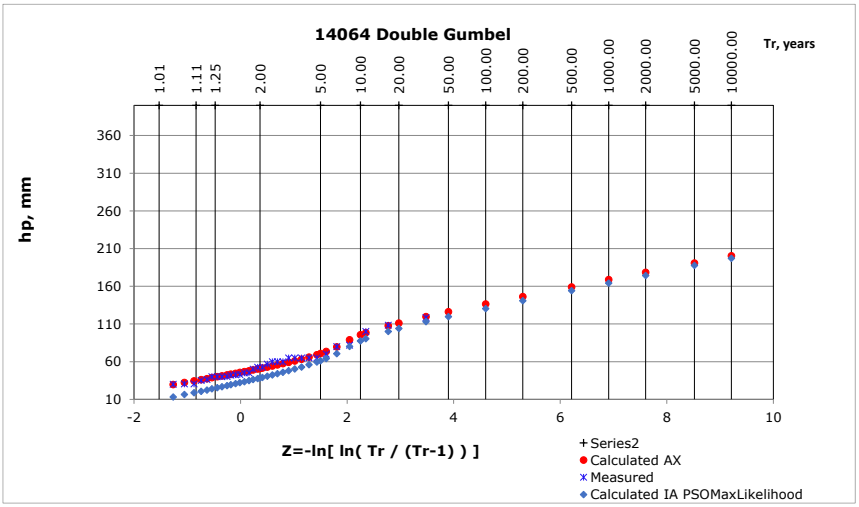


**Fig. 10.** Probabilistic extrapolation comparison using IA PSO Max Likelihood and AX program

Figure 10 illustrates how as AI is oriented, an improved optimization program was obtained that uses a combined evolutionary computing technique and Maximum Likelihood method as support in frequency analysis of a maximum annual rainfall series data to estimate Double Gumbel function parameters to adjust data.

## 4. Conclusions

Double Gumbel function optimization through PSO and maximum likelihood for data analysis is a promising strategy that combines classic techniques with advances in field of machine learning. By using PSI, we can explore search space more efficiently and find optimal solutions in a shorter time. In addition, by applying the maximum likelihood approach, we can obtain more accurate estimates double Gumbel function parameters

By leveraging the power of AI, we can further enhance this process and obtain more accurate and reliable results. The use of supervised machine learning algorithms allows us to train models that can predict the optimal parameters of the double Gumbel function from previously observed data, which accelerates the optimization process and improves efficiency.

This approach leverages classic techniques strengths such as PSO and maximum likelihood, and combines them with the advances in the field of machine learning. By using supervised machine learning algorithms, we can train models that can predict optimal parameters, thereby accelerating the optimization process and improving efficiency. Overall, this strategy holds great promise for enhancing data analysis and achieving more accurate results.

### References

[1] González-Villarreal, Fernando. *Contribution to the analysis of frequencies of extreme values of maximum flows in a river. / Contribución al análisis de frecuencias de valores extremos de los gastos máximos en un río*. Blue Series / Serie Azul, Engineering Institute / Instituto de Ingeniería, UNAM, 1970.

[2] Fuentes Mariles, Óscar A., M. L. Arganis Juárez, R. Domínguez Mora, G. E. Fuentes Mariles, and K. Rodríguez Vázquez. "Maximization of the Likelihood Function of Probability Distributions Using Genetic Algorithms." / "Maximización de la función de Verosimilitud de Distribuciones de Probabilidad usando Algoritmos Genéticos." *Ingeniería Del Agua* 19, no. 1 (January 2015): 17–29.

[3] Rossi, Fabio, Mauro Fiorentino, and Pasquale Versace. "Two-Component Extreme Value Distribution for Flood Frequency Analysis." *Water Resources Research* 20, no. 7 (July 1984): 847-856.

[4] Eberhart, Russel C., and J. Kennedy. "A New Optimizer Using Particle Swarm Theory." Paper presented at the Sixth International Symposium on Micro Machine and Human Science MHS'95, Nagoya, Japan, October 4-6, 1995.

[5] Bing. "Chat Bing AI." 2023. [Available online]

[6] Anaconda. "Jupyter Notebook in Anaconda" / "Jupiter notebook en Anaconda." 2023. [Available online]

[7] Domínguez Mora, Ramón, E. Carrizosa Elizondo, and M.L. Arganis Juárez. *Study to regionalize the expenses generated by maximum floods, as a basis for the preparation of danger maps for river floods in all the basins of the Mexican Republic. Volume II. Regional statistical analysis of maximum annual rainfall. / Estudio para regionalizar los gastos generados por avenidas máximas, como base para la elaboración de mapas de peligro por inundaciones fluviales en todas las cuencas de la república Mexicana. Tomo II. Análisis estadístico regional de las precipitaciones máximas anuales.* IISCONV 103 2016 Project, UNAM, INSTITUTE OF ENGINEERING / Proyecto IISCONV 103 2016, UNAM, INSTITUTO DE INGENIERÍA. Mexico, March 2017.

[8] Jiménez-Espinoza, M. "Ax Program. Hydrometeorological Hazards Area."/ "Programa Ax. Área De Riesgos Hidrometeorológicos." National Disaster Prevention Center / Centro Nacional de Prevención de Desastres. Mexico, 1996.

# Photovoltaic Panels' Downcycling Method that Pushes the Transition to a Circular Economy

Student **Miruna-Andreea TOKAR**[1], Student **Iuliu-Ioan LAZĂR**[1],
Assist. Prof. PhD. Eng. **Dănuț TOKAR**[1,*]

[1] University Politehnica Timisoara, Romania

* danut.tokar@upt.ro

***Abstract:*** *In the current context regarding energy sources' problems, it is estimated that a high percentage of waste will be produced from photovoltaic panels, that will put pressure on the environment. Thus, the study focuses on downcycling them by incorporating them into mortars by six new recipes (R1, R2, R3, R4, R5 and R6) that replace the sand by integrating photovoltaic panels' dust (PVd) and pieces of photovoltaic panels (PVp) (1/3 to 100% of the total amount). All samples were subjected to tensile bending, compression and an economic analysis and were compared with the control sample (R0). As a result of the experimental research, a change in the apparent density of the proposed samples was found, and a general improvement in all areas of testing. The obtained results show that used photovoltaic panels can constitute raw material for the creation of new construction materials.*

***Keywords:*** *Environmental protection, mortars, new materials, PV downcycling*

## 1. Introduction

The electrical context is based on the recent problems regarding the way we produce electricity. Photovoltaic panels seem to be the future regarding green energy production [1]. However, the lies with the waste generated after a period of 25-30 years of usage and the fact that current recycling methods are expensive and inefficient. This issue must be fixed through the use of new legislation and regulations regarding the recycling of photovoltaic panels for each country. It is known that photovoltaic panels, besides having precious metals (silver, aluminium, copper, steel, etc.), contain toxic materials such as lead [1], [2], [3], [4]. In the European Union the legislation forces the recycling of photovoltaic panels (PV), however, in most part only the materials in bulk are collected, such as the aluminium frames and glass, which represent 80% of the total mass of the siliceous panel. The remaining mass is usually incinerated even if it contains certain elements such as silver, copper, and silicon which together represent the two terms of economic value of the materials of a photovoltaic panel [2]. Similar measures are taken in Japan, India, and Australia that intervene through plans of recycling. The top countries, in 2022, regarding cumulative capacity of installed photovoltaic panels are China (414.5GW), the European Union (209.3GW), the USA (141.6GW), Japan (84.9GW), India (79.1GW), Germany (67.2GW), followed, at large differences, of Australia, Spain, Italy, Korea and Brazil [5]. In this paper we will discuss downcycling methods that are not only good for the environment but also bring an economic benefit. Given all of the above, this paper approaches new options of recycling, by integrating photovoltaic panel cells into construction materials. Similar recipes were proposed beforehand, and the result were positive [6]. This article proposes 4 new recipes from which 3 samples of each were created. All were tested for bending tensile strength, compressive strength, and thermal insulation.

## 2. Methods

In order to obtain the raw materials for this study we had to process the photovoltaic panels using equipment such as: ball mill and diamond disc cutting machine.
The basic materials used in all recipes are cement (CEM II A-LL 42.5R), sand (0.5/1-Sort 3), release agent (Master Finish RL 450) and water. For the proposed research, retired monocrystalline and polycrystalline photovoltaic panels were used. The used photovoltaic panels were cut into pieces using a diamond disc cutting machine.

The cut pieces of the panel were crushed with the help of an experimental grade ball mill, resulting in crushed glass and pieces of photovoltaic cells together with plastic material (supporting material for photovoltaic cells and for sealing) and residues from auxiliary material (adhesive, other unknown elements). The final products are shown in Fig.1.

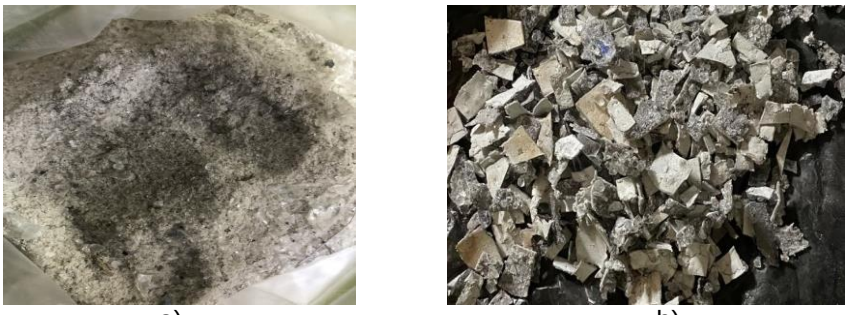

a) b)

**Fig. 1.** The final materials obtained: a) PV dust (PVd), b) PV pieces (glass+plastic)-PVp

## 3. Procedures

After obtaining the materials necessary to study six recipes were made: R1trough R4 without additives, R5 (R0 + superplasticizer SikaPlast (SP)-331, 1% of cement mass) and R6 (R3+ superplasticizer SikaPlast (SP)-331, 1% of cement mass). The mixture R0 (control sample) was realized and tested in conformity with SR EN 196-1: 2016 [7]. Testing was done on four of the six samples (R0 through R4). They were tested after 4 months. The results of the new recipes were compared with R0's results.

The steps of this project are:

- determining the recipes for the control sample R0 (Table 1) and the series of probes R1 through R6 (Table 2).

**Table 1:** Recipe for sample (R0)

| Recipies for the mixtures | Cement CEM II A-LL 42,5R [kg] | Sand 0,5/1-Sort 3 [kg] | PVd [kg] | PVp [kg] | | SPv | Water for mixtures [m³] |
|---|---|---|---|---|---|---|---|
| | | | | glass | plastic | | |
| R0 | 0.45 | 1.35 | - | - | - | - | 0.25 |

**Table 2:** Recipes for (R1-R6)

| Recipies for the mixtures | Cement CEM II A-LL 42,5R [kg] | Sand 0,5/1-Sort 3 [kg] | PVd [kg] | PVp [kg] | | SP | Water for mixtures [m³] |
|---|---|---|---|---|---|---|---|
| | | | | glass | plastic | | |
| R1 | 0.45 | 0.45 | 0 | 0.90 | 0 | - | $22 \cdot 10^{-5}$ |
| R2 | 0.15 | 0.90 | 0 | 0 | 0.45 | - | $21 \cdot 10^{-5}$ |
| R3 | 0.45 | 0.45 | 0.52 | 0.27 | 0.10 | - | $25 \cdot 10^{-5}$ |
| R4 | 0.45 | - | 1.35 | 0 | 0 | - | $28 \cdot 10^{-5}$ |
| R5 | 0.45 | 1.35 | 0 | 0 | 0 | SP 331 | $22 \cdot 10^{-5}$ |
| R6 | 0.45 | 0.45 | 0.52 | 0.27 | 0.10 | SP 331 | $22 \cdot 10^{-5}$ |

- Weighing of the materials (Fig. 2) with the electronic scale KERN that has a precision of 0.0001 g.

**Fig. 2.** The weight of used materials

- The mixture which was initially made manually and then with the help of a mixer for mortar Auto-Mortar Mixer;
- Pouring the samples (Fig. 3) mold that was previously oiled with MasterFinish RL 450, followed by the compacting of the mixture through the usage of mechanical shocks (manual);

**Fig. 3.** Pouring and compacting the mixture

The mould used has the standard dimensions of: b × h × L [m]. The dimensions and weight of the samples are presented in Table 3 and Fig. 4.

**Table 3:** Dimensions and weight of the samples taken out of their mold

| Sample | Dimensions and weight | | | |
|---|---|---|---|---|
| | m[kg] | b[m] | h[m] | L[m] |
| R0 - 4 months | 0.53 | 0.04 | 0.04 | 0.16 |
| R1 - 4 months | 0.55 | 0.04 | 0.04 | 0.16 |
| R2 - 4 months | 0.54 | 0.04 | 0.04 | 0.16 |
| R3 - 4 months | 0.50 | 0.04 | 0.04 | 0.16 |
| R4 - 4 months | 0.49 | 0.04 | 0.04 | 0.16 |
| R5 - 7 days | 2.69 | 0.15 | 0.058 | 0.15 |
| R6 - 7days | 3.01- | 0.15 | 0.068 | 0.15 |

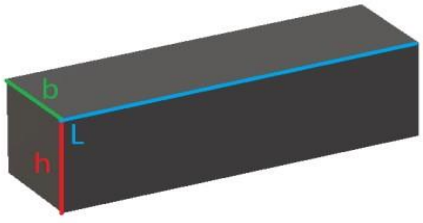


**Fig. 4.** The dimension of the samples without the mold

- Testing the samples (Fig. 5) with a hydraulic press, using a speed of charge of (50±10) N/sec for the bending test and (2400±200) N/sec for the compression test.

a b

**Fig. 5.** Mechanical tests: a) tensile bending test, b) compression test

**Table 4:** The pressing forces p [N], at which the break was initiated for recipes 0 through 4

| Sample | R0 | R1 | R2 | R3 | R4 |
|---|---|---|---|---|---|
| $P_t$ [N] | 2200 | 1800 | 1600 | 1480 | 2300 |
| $P_{c01}$ [N] | 33800 | 42500 | 24500 | 22500 | 32700 |
| $P_{c02}$ [N] | 31500 | 35500 | 23500 | 22000 | 35700 |
| $P_{cavg}$ [N] | 32650 | 39000 | 24000 | 22250 | 34200 |

For analysing the results, it has been used:

- The equation of the resistance at traction $F_t$ [N/m$^2$]:

$$F_t = \frac{3}{2} \cdot \frac{P \cdot d}{b \cdot h^2} \quad (1)$$

where:
P -the potential force of the machine [N];
d- distance [m];
b- width of the sample [m];
h-height of the sample [m].

- The equation of the resistance at compression $F_c$ [N/m$^2$]:

$$F_c = \frac{F}{A} \quad (2)$$

where:
F-the potential force of the machine [N];
A-the area of the section (A=b×h) [m$^2$];
b- width of the sample [m];
h-height of the sample [m].

## 4. Data and analysis

The attempt to recycle and use photovoltaic panels and repurposing them into construction materials materialized in this research through the creation of 6 new mortar recipes.

### 4.1 Testing

Their structure is a combination of the mortar recipe (according to SR EN 196-1: 2016) [7] and the three materials obtained from PV (dust, glass and plastic pieces). Thus, sample R1 (25% Sand + 50 % Glass), R2 (50% Sand, 25% Plastic pieces), R3 (25% Sand, 29% Dust, 15% glass, 6%Plastic pieces), R4 (0% Sand, 100% Dust) and two recipes (R5 and R6) which are the equivalent of R0 and R3 with added additives.

The physical and mechanical characteristics of the samples R0 trough R4 that have been analyzed after 7 days under the influence of mentioned loads, are presented in Fig. 6-8.

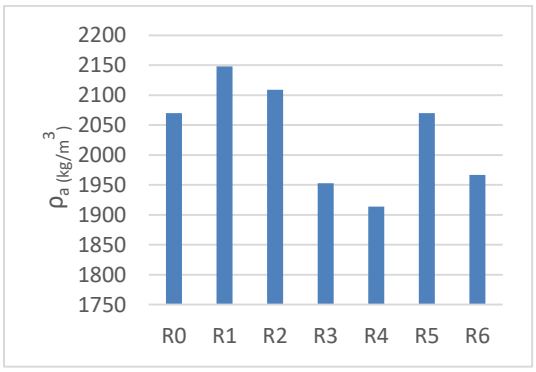


**Fig. 6.** Pouring and compacting the mixture

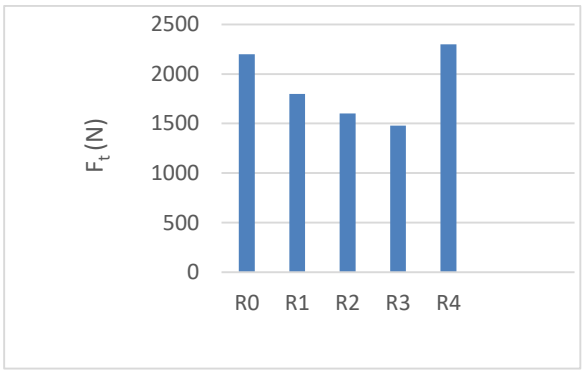


**Fig. 7.** The resistance at traction

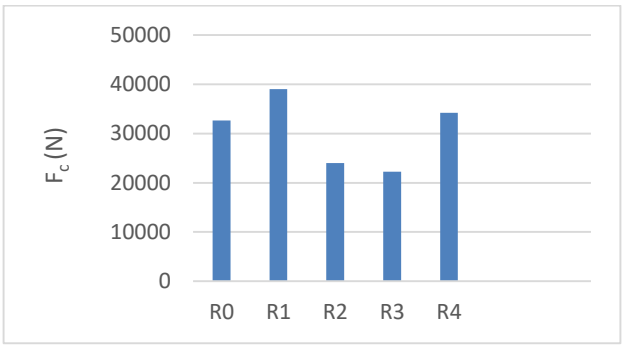


**Fig. 8.** The resistance at compression

It can be noted that R3, R4 and R6 have a lower density than R0 while R5 has a similar density. Sample 4 was found superior in both tensile and compression tests while R1 was found superior in the compression test.
Although in some areas the proposed recipes performed less than the control sample, they were still in parameters regarding functionality the main benefit being their small density.
Therefore, a possibility of recycling by reusing the degraded photovoltaic panels is the creation of new materials such as new mortars which could be included in the field of constructions.

### 4.2 Economical stand point

An economic analysis shows that all recipes but R2 help decrease the budget for mortars without compromising on quality as shown in Table 5.

**Table 5:** Cost savings for a sample of 1.8 kilograms

| Recipes | Cement | Sand | Water | Dust | Glass | Plastic | Total RON | Savings % |
|---|---|---|---|---|---|---|---|---|
| ron/ton | 910 | 40 | 14 | 22.7 | 19.98 | 18.2 | | |
| R0 | 0.6 | 0.08 | 0.005 | 0.00 | 0.00 | 0.00 | 0.68 | 0.0 |
| R1 | 0.6 | 0.03 | 0.005 | 0.00 | 0.03 | 0.00 | 0.66 | 3.9 |
| R2 | 0.6 | 0.05 | 0.004 | 0.00 | 0.00 | 0.01 | 0.67 | -1.8 |
| R3 | 0.6 | 0.03 | 0.005 | 0.02 | 0.00 | 0.01 | 0.66 | 1.5 |
| R4 | 0.6 | 0.00 | 0.006 | 0.05 | 0.00 | 0.00 | 0.65 | 1.3 |
| R5 | Similar to R0 | | | | | | | |
| R6 | Similar to R3 | | | | | | | |

## 5. Conclusions

Nowadays, PV waste starts to become a global problem, especially in countries that invested in photovoltaic systems. However, given results presented earlier show that these can be used as a resource in the field of construction. The study has shown and proved experimentally that the six different recipes performed generally better than the standard sample R0 in a combination of all three areas of testing. R4 performed better than R0 in all three areas of testing. In addition, R3, R5, and R6 also had smaller densities than R0 while R1 performed better than the standard material in the compression test. Moreover, this new method of downcycling is beneficially from an economical point of view due to the fact that all but R2 have a lower production cost.
In light of all of the above, our study shows that the downcycling method of introducing PV waste intro construction materials can not only benefit the environment but also bring economic value.

## 6. Further research questions

As future research directions, we propose to create new recipes (in different mixtures) to obtain construction materials that use these wastes and the results to be a basis for research in the field. At the same time, we propose to test these materials in real operating conditions. Parallel to the mechanical tests we propose to test the current and future samples for thermal insulation.

**Acknowledgement**

T.A.M thanks VOLT for the materials given to conduct this study.

**References**

[1] Mahmoudi, Sajjad, Nazmul Huda, and Masud Behnia. "Photovoltaic waste assessment: Forecasting and screening of emerging waste in Australia." *Resources, Conservation and Recycling* 146 (July 2019): 192-205.
[2] Peplow, Mark. "Solar panels face recycling challenge." *ACS Central Science* 8, no.3 (March 2022): 299-302.
[3] Lewis, Michelle. "Where do solar panels go when they die?", *Electrek*, August 24, 2020. Accessed October 5, 2023. https://electrek.co/2020/08/24/where-do-solar-panels-go-when-they-die/.
[4] Heath, Garvin A., Timothy J. Silverman, Michael Kempe, Michael Deceglie, Dwarakanath Ravikumar, Timothy Remo, Hao Cui, Parikhit Sinha, Cara Libby, Stephanie Shaw, Keiichi Komoto, Karsten Wambach, Evelyn Butler, Teresa Barnes, and Andreas Wade. "Research and development priorities for silicon photovoltaic module recycling to support a circular economy." *Nature Energy* 5 (July 2020): 502-510.
[5] Masson, Gaetan. *Snapshot of Global PV Markets 2022-Task 1 Strategic PV Analysis and Outreach PVPS*, Publisher IEA PVPSV, 2023.
[6] Tokar, Miruna, and Andrea Altomonte. "Study on recycling photovoltaic panels: Their integration into construction materials." Paper presented at the 32nd Conference with International Participation on Building Facilities and Environmental Comfort ICCA 2023, Timisoara, Romania, May 4-5, 2023.
[7] ***. "SR EN 196-1: 2016 - Methods of testing cement. Part 1: Determination of strength." Romanian Standards Association, 2016.

# Pedagogical Valences of the MIT App Inventor® Platform in Creating Applications for Soil Monitoring and Protection

PhD Eng. IT expert **Bogdan-Vasile CIORUȚA**[1,3,*], Stud. **Ioana-Elisabeta SABOU (CIORUȚA)**[2], Assoc. Prof. Dr. Eng. **Mirela-Ana COMAN**[3,4], Eng. IT expert **Alexandru Leonard POP**[1]

[1] Technical University of Cluj-Napoca - North University Centre of Baia Mare, Office of Informatics, 62A Victor Babeș Str., 430083, Baia Mare, Romania

[2] Technical University of Cluj-Napoca - North University Centre of Baia Mare, Faculty of Letters, Department of Specialty with Psychopedagogical Profile, 76 Victoriei Str., 430083, Baia Mare, Romania

[3] University of Agricultural Sciences and Veterinary Medicine from Cluj-Napoca, 3-5 Calea Mănăștur, 4000372, Cluj-Napoca, Romania

[4] Technical University of Cluj-Napoca - North University Centre of Baia Mare, Faculty of Engineering, 62A Victor Babeș Str., 430083, Baia Mare, Romania

* bogdan.cioruta@staff.utcluj.ro

***Abstract:*** *In today's information consumption society, key competencies are considered to represent a multifunctional, transferable package of knowledge, skills, and attitudes, which all individuals need for personal fulfillment and development, social inclusion, and finding a job. In addition, they must have developed by the end of the compulsory education cycle, to act as a foundation for lifelong learning. In this context, through the present work, we aimed to identify, analyze, and describe the pedagogical valences of the MIT App Inventor® platform in the configuration, creation, and development of dedicated applications, especially for the monitoring and protection of soil resources.*

***Keywords:*** *MIT App Inventor®, applied pedagogy, soil protection, dedicated mobile applications*

## 1. Introduction

Modern trends in the social and professional development of individuals are defined not only by the information society but increasingly by a knowledge-based society (Society 5.0), which is affected by the rapid changes in the digital world 0 and which focuses on human productivity in advanced technological services 0. To understand their content and their implementation strategy, it is necessary to fully understand the increasingly visible contradictions, with the current society of information consumption 0.

The current society of information consumption requires the rigorous selection of materials and documentation tools, from the immense amount of academic information generated in the last decades 0, in which case the skills of searching, sorting, and filtering information are more than a necessity. Moreover, in the same context, it is considered that digital literacy and the associated key competencies represent a multifunctional, transferable package of knowledge, skills, and attitudes that all individuals need for personal fulfillment, social inclusion, and finding a job 0. These skills must have been developed by the end of the compulsory education cycle and must act as a foundation for lifelong learning.

Moreover, to facilitate the acquisition of such key skills, in the process of selecting digital tools, teachers are the ones who must follow the pedagogical valences of the platforms (e.g., *the degree of interaction*, *communication, and collaboration*; *the implications for the development of skills specific to the 21st century*; *malleability and adaptability to various multidisciplinary work scenarios,* etc). To achieve this main task, methods of analysis and synthesis, prediction, comparison, and abstraction are usually used 0. A rigorous selection of work tools brings the most diverse benefits, namely a much more comfortable learning environment, where the exchange of best practices and assistance can be much more accessible.

Educational applications, tools, or platforms are an excellent way to complement traditional classroom learning, providing both resources and digital content for pupils and students, as well as virtual spaces for carrying out the most diverse educational activities.

These applications, tools, and platforms often include features such as interactive content, quizzes and games, virtual tutoring (e.g. personalized learning paths), and combinations thereof, which can provide/reveal valuable information about both learner preferences, motivation, and engagement, as well as about their adaptation and resistance to the new 0.
All of the above can be used to help pupils and students learn, develop skills, and build attitudes - from math and science (eg, concerning STEM) to the arts and social sciences. In addition, many of these applications, tools, and platforms include reporting and (benchmark) analysis functions, which allow teachers to monitor student/student progress and measure the effectiveness of educational interventions. In addition, they must allow for association with the highlighted knowledge, skills, and attitudes, which in turn must have been developed by the end of the compulsory education cycle, acting as a foundation for lifelong learning. In this context, through the present work, we aimed to identify, analyze, and describe the pedagogical valences of the MIT App Inventor® platform in the configuration, creation, and development of dedicated applications, especially for the monitoring and protection of soil resources.

## 2. Material and methods

About the use of current mobile devices (e.g., phones, laptops, tablets, smartwatches, etc.) we note the existence of a special information link with the environment. Also, users of these categories of devices have access to an almost infinite offer of multimedia educational content; in this sense, we refer to databases and information obtained through sensors and/or associated applications. Regarding the establishment of the framework for configuration, design, and creation of mobile applications dedicated to soil protection, as a working method, we tried several scenarios, namely innovative puzzle-type programming environments (**Fig. 1**), which are based on the drag-and-drop programming technique (e.g., *Android Studio*®, *apprat.io*®, *AppsGeyser*®, *AppyBuilder*®, *Basic4Android*®, *Kodular*®, *MIT App Inventor*®, *Thunkable*® etc).


**Fig. 1.** Configuration, design, and development environments used to create mobile applications

After comparing the facilities offered and the ease of application implementation, we opted for the version provided by the MIT App Inventor® platform, under development at Google®, designed and used as a teaching-learning tool in a variety of real contexts.
A substantial contribution to the choice made was also the use of the platform in question (i.e. MIT App Inventor®), successfully "in learning programs, summer schools, workshops for teachers, and in programs dedicated to the faculty" 0. Thus, over the years, there have been several attempts to simplify the software development process and allow users to learn to develop their mobile applications through MIT App Inventor® 0-0. As such, to date, 6.8 million people in more than 190 countries have used MIT App Inventor® to create more than 24 million apps to provide solutions to real problems in their communities.
In the context of the above, we will try from a pedagogical perspective to identify, analyze, and describe the pedagogical valences of MIT App Inventor® in the configuration, creation, and development of dedicated applications, especially for the monitoring and protection of soil resources, by referring to other specialist articles and relevant user reports/observations.

## 3. Results and discussion. Using the MIT App Inventor® platform as a pedagogical tool

### 3.1 Functional features and characteristics

Over the years, as I was able to notice by leisurely consulting the specialized literature, there have been several attempts to simplify the software development process and allow everyone interested to develop their applications through the MIT App Inventor® platform, respectively HAMILTON, 2011; JORDAN and GREYLING, 2011; TYLER, 2011; WOLBER, 2011; WOLBER et al., 2011; ABELSON et al., 2012; GRAY et al., 2012; KRISHNENDU, 2012; MACKLLAR, 2012; POKRESS and DOMINGUEZ, 2012; POKRESS et al., 2012; MITCHELL, 2014-2016; PARTDIKURI, 2014; ZHANG, 2014; TURBAK et al., 2014; AMERKASHI, 2015; KRISHNENDU, 2015; SHERMAN, 2015; WALTER and SHERMAN, 2015; WOLBER et al., 2015; COLTER, 2016; TSAI, 2016; XIE and ABELSON, 2016; GERBELLI and GERBELLI, 2017; GUTHALS, 2017; VOŠTINÁR, 2017; XINOGALOS et al., 2017; XINYUE, 2017; MARTINEZ and MARTÍNEZ-IJAJÍ, 2018; PANSELINAS et al., 2018; TANG, 2018; CHO, 2019; CLARKE, 2019; PATTON et al., 2019; RUIZ-RUBE et al., 2019; TSVENTOZAR, 2019; LOGAN, 2020; yes CRUZ et al., 2022; LANG, 2022; CIORUȚA et al., 2022 etc. (Fig. 2).

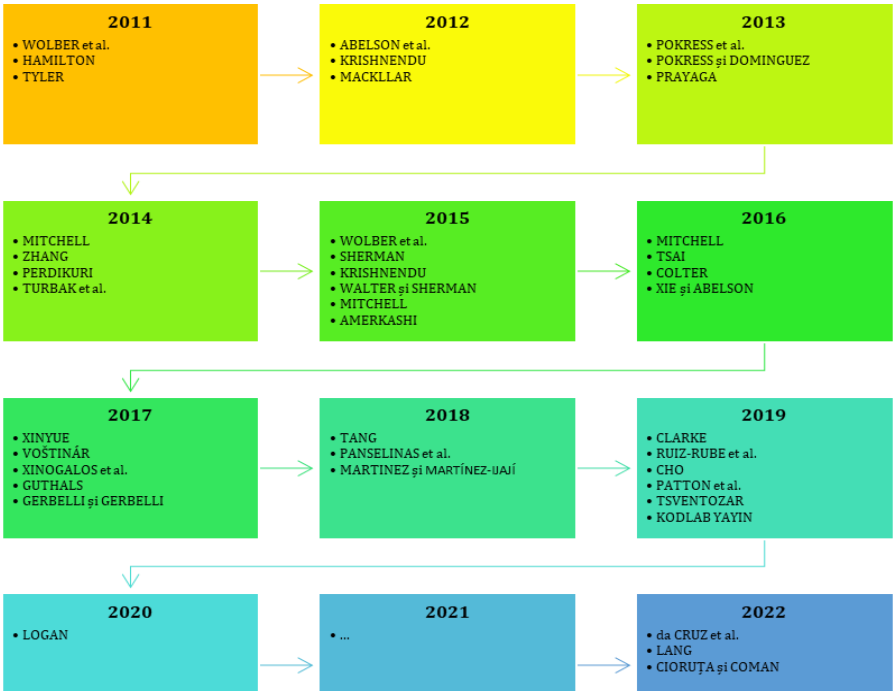


**Fig. 2.** An insight into the authors who researched the MIT App Inventor® app closely

MIT App Inventor® is a tool that can bring software development to the masses, rather than being in the hands of a small number of professionals 0. It has been defined in the specialized consulted literature as:

- "(...) a new drag-and-drop visual programming tool for building mobile applications on the Android platform" 0;
- "(...) an informal online learning environment with over 5 million users and 15.9 million projects/apps created" and "an environment that uses a visual language based on blocks to enable people to create mobile applications for Android devices" 0;
- "(...) an open-source programming tool based on blocks that allow users with no previous programming experience to create apps specifically for mobile devices" 0.

For the above, we define the App Inventor® tool as "a new drag-and-drop visual programming environment or an informal web-based platform that allows users - non-programmers or beginners - to create applications for mobile devices". It follows step by step, several milestones highlighted by computer-assisted instruction, and presents attributes that are worth pursuing from the perspective of applied pedagogy and educational alternatives.

### 2.2 Pedagogical implications and valences in creating new mobile applications

In direct relation to the current state of knowledge regarding the configuration, creation, testing, and use of mobile applications dedicated to soil protection, it is certified that the use of modern technologies represents a very topical challenge for specialists in many fields of activity, implicitly for those who are in charge of monitoring environmental factors, economic evaluation of ecosystem services, ecological security, soil protection, etc.

In the same context, alignment with international standards specific to soil protection requires the use of GIS/GIS, monitoring of specific quality parameters, data processing with specialized programs, creation of mega-databases that can be updated in real-time, etc. Moreover, nowadays, mobile applications dedicated to soil protection occupy a well-defined place in all fields of activity: production and service provision, management and monitoring, research, and public involvement in decision-making. These have become mandatory and necessary tools in soil science, which track specific and relevant indicators for soil protection.

Among the modern technologies that ensure alignment with the above standards, MIT App Inventor®, as a configuration and development environment for various categories of mobile applications, accesses device functions (e.g., *camera for capturing images and sound recording*, *GPS module for logging location, altitude, and orientation*, etc.), stimulates creativity, encourages innovation, (re)defines application design, but also develops and supports research skills. It enables users to create and share fully functional Android applications, providing an innovative way to solve increasingly complex environmental problems.

The creation of various mobile applications is done with the *MIT App Inventor® Designer* - where the graphic components for the desired application are selected and the block editor (*MIT App Inventor® Blocks Editor*) - where the code blocks are assembled like pieces of a puzzle, and where you specify how the tools used in creating the interface should behave.

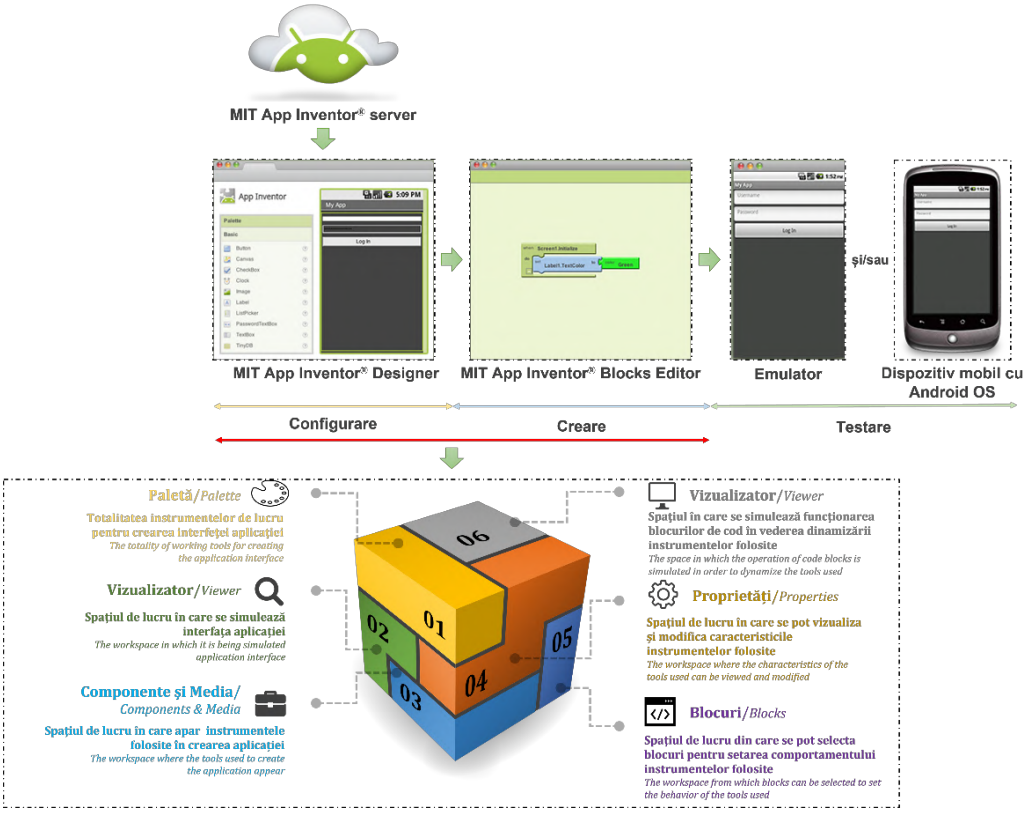


**Fig. 3.** How to configure, build, and test a mobile app in MIT App Inventor®

The application appears on the phone, step by step so that the work done can be tested while the construction continues. Users who do not own a device with an Android operating system can create the applications using the *Android emulator* (software that runs on the computer screen, behaving similarly to a mobile device).

From the interaction of the users with the application menu and with the functionalities it proposes (Fig. 4), various aspects can be determined, such as *the degree of structuring and organization of the educational material*, *the degree of interaction*, *the degree of communication and collaboration*, *the implications in the development of the 21st-century specific-skills* (e.g., digital skills, language skills, entrepreneurial and innovation skills), *malleability and adaptability to various multidisciplinary work scenarios*, etc. All these characteristics were recorded in Table 1, where, along with the App Inventor® platform, other development environments with similar characteristics were considered, tested, and analyzed.

| | App Inventor | DroidDraw | Rhomobile | PhoneGap | Appcelerator |
|---|---|---|---|---|---|
| | | | Mobile Platform Compatibility | | |
| Android | Yes | Yes | Yes | Yes | Yes |
| iPhone/iPad | No | No | Yes | Yes | Yes |
| Windows Mobile 6 | No | No | Yes | Maybe | No |
| Windows Phone 7 | No | No | Maybe | Maybe | No |
| Palm | No | No | No | Yes | No |
| BlackBerry (RIM) | No | No | Yes | Yes | Planned |
| Symbian | No | No | Yes | Yes | No |
| | | | Development Environment OS Support | | |
| Windows | Yes | Yes | Yes (no iPhone) | Yes (no iPhone) | Yes (no iPhone) |
| Mac | Yes | Yes | Yes | Yes | Yes |
| Linux | Yes | Yes | Yes (no iPhone) | Yes (no iPhone) | Yes (no iPhone) |

**Fig. 4.** Interaction of mobile application development environments with device operating systems

**Table 1:** Characterization of mobile app development environments with their pedagogical values

| Pedagogical aspect followed / Platform | The degree of structuring and organization of the material | The degree of interaction | The degree of communication and collaboration | Implications in the development of digital skills | Adaptability to multidisciplinary work scenarios |
|---|---|---|---|---|---|
| *Appcelerator®* | ++ | ++ | ++ | ++ | ++ |
| *Android Studio®* | +++ | ++ | +++ | **++++** | **++++** |
| *apprat.io®* | ++ | + | ++ | ++ | ++ |
| *AppsGeyser®* | ++ | + | ++ | ++ | ++ |
| *AppyBuilder®* | ++ | + | ++ | ++ | ++ |
| *Basic4Android®* | ++ | ++ | +++ | +++ | ++ |
| *DroidDraw®* | ++ | ++ | ++ | ++ | +++ |
| *Kodular®* | **++++** | **+++** | **++++** | ++ | +++ |
| *MIT App Inventor®* | **++++** | **+++** | +++ | **+++++** | **++++** |
| *PhoneGap®* | ++ | + | + | ++ | ++ |
| *Rhomobile®* | ++ | + | ++ | ++ | ++ |
| *Thunkable®* | **++++** | **+++** | **++++** | ++ | +++ |

From the analysis of the results obtained, as a result of the interactions with the students, favorable characteristics of using the App Inventor® application for various teaching-learning-evaluation scenarios are noted. The degree of structuring and organization of the work material, practically the menu of functionalities itself, includes several components that familiarize the user with IT concepts, while also allowing knowledge by association of the Kodular® and/or Thunkable® platform. The degree of interaction and the degree of communication and collaboration are also on the same principles as in the case of the two previously mentioned platforms.
Regarding the implications of the MIT App Inventor® platform in the development of digital skills, as well as its adaptability to support various multidisciplinary work scenarios, these elements can only be appreciated and validated by direct reference to the creation of mobile applications for various

fields of interest, from themed games and applications for courier services to applications for the monitoring and protection of soil resources.
For the latter scenario, the MIT App Inventor® platform provides a unique and impressive palette of elements for designing and automating mobile device components (e.g., *interface configuration elements*, *graphics, and animation elements*, *elements for data science and processing*, *elements for sensor management and data storage* etc), in which case it leads detachedly about the last two characteristics considered.

## 4. Conclusions

Ensuring access to the key skills needed by today's society, including digital ones, should find its natural place in teaching-learning-assessment approaches, and be equally within the reach of each learner. Responsible for this initiative is the teaching staff who should manage the training climate (by finding the right work options, as well as the favorable tools for the efficient performance of the tasks).
In the sense of the mentioned, teachers must be able to characterize the applications used, including the application development environments, in full agreement with the current needs of the students they train. The pedagogical values of the applications, referring to *the degree of structuring and organization of the educational material*, *the degree of interaction*, *the degree of communication and collaboration*, *the implications in the digital skills development*, *the malleability and adaptability to various multidisciplinary work scenarios,* etc, teachers must ensure that it offers a multifunctional and representative package of knowledge, skills, and attitudes that all individuals need for personal fulfillment, social inclusion and finding a job.
In the case of the MIT App Inventor® platform, which has validated and recognized affinities in the configuration, creation, and development of dedicated applications, especially for the monitoring and protection of soil resources, the specific pedagogical valences of digital systems used in training appear, the evaluated characteristics having values far above of other similar applications. This result does nothing but certify that the MIT App Inventor® application has pedagogical valences with various classroom work scenarios and that, equally, it can be a useful teaching tool in supporting the configuration, creation, testing, and use of mobile applications in various fields.

**Acknowledgments**

We would like to thank the students who configured, created, tested, and used several dedicated mobile applications in the computer-assisted instruction classes. Through their activity, they helped us to understand better their preferences, motivation, and involvement, as well as how to adapt to the new.

**References**

[1] Simelane, B., and H. Smuts. "Selecting a Knowledge Management Methodology in Society 5.0." Paper presented at the 3rd Society 5.0 Conference, Pretoria, South Africa, June 5-7, 2023. *Proceedings of Society 5.0 Conference 2023* 93 (2023): 164-173.
[2] Dominic, N., N. R. Pratama, K. Cornelius, S. H. Senewe, and B. Pardamean. "Society with Trust: A Scientometrics Review of Zero-Knowledge Proof Advanced Applications in Preserving Digital Privacy for Society 5.0." Paper presented at the 7th International Conference on Innovative Technologies in Intelligent Systems & Industrial Applications CITISIA 2022, online, November 16-18, 2022. *Lecture Notes in Electrical Engineering* 1029 (2023): 69–78.
[3] Usanova, L., and I. Usanov. "Contradictions of a Knowledge Society: Educational Transformations and Challenges." *Philosophical Horizons* 47 (2023): 51-60.
[4] Ranjan, Prabhat, and Bhupendra Kumar Singh. "Sustainability Threats to the Information Society: Gap of Sustainability Knowledge and Practice." Sahdev, Supriya Lamba, Chitra Krishnan, Ahdi Hassan (eds.). *Promoting Sustainable Management Through Technological Innovation*. Hershey, Pennsylvania, IGI Global, 2023.
[5] Dobryakova, Maria, Isak Froumin, Gemma Moss, Norbert Seel, Kirill Barannikov, and Igor Remorenko. "A Framework of Key Competences and New Literacies." Dobryakova, M., I. Froumin, K. Barannikov, G. Moss, I. Remorenko, and J. Hautamäki (eds). *Key Competences and New Literacies*. Cham, UNIPA Springer Series, Springer, 2023.

[6] Cherusheva, G., B. Nowak, A. Maksymenko, M. Kabysh, and M. Vakerych. "Higher pedagogical education in the European Union: Innovative technologies." *Eduweb. Revista de Tecnología de Información y Comunicación en Educación* 17, no. 2 (April - June 2023): 257-266.
[7] Asare, S., A. Amponsah, M. Agyemang, and V. Akwaah. "Utilizing educational apps and online platforms for home economics learning: An investigation of student's attitudes and perceptions." *World Journal of Advanced Research and Reviews* 19, no. 3 (September 2023): 411-419.
[8] Gray, J., H. Abelson, D. Wolber, and M. Friend. "Teaching CS principles with MIT App Inventor." Paper presented at the 50th Annual Southeast Regional Conference ACM-SE '12, Tuscaloosa, Alabama, USA, March 29-31, 2012.
[9] Jordan, Lucas, and Pieter Greyling. "App Inventor”, pp. 361–386. *Practical Android Projects*. Berkeley, California, Apress, 2011.
[10] Hamilton, Eric. *Tech Empowerment: Android App Inventor*. Raleigh, North Carolina, Lulu Press, Inc., 2011.
[11] Krishnendu, Roy. "App inventor for Android: Report from a summer camp." Paper presented the 43rd ACM Technical Symposium on Computer Science Education SIGCSE '12, Raleigh, North Carolina, USA, February 29 - March 3, 2012.
[12] Krishnendu, Roy. "Position statement: App inventor instructional resources for creating tangible apps." Paper presented at 2015 IEEE Blocks and Beyond Workshop (Blocks and Beyond), Atlanta, Georgia, USA, October 22, 2015.
[13] Lang, Karen, and Selim Tezel. *Become an App Inventor: The Official Guide from MIT App Inventor*. MITeen Press, 2022.
[14] Wolber, D., H. Abelson, E. Spertus, and L. Looney. *App Inventor. Create Your Own Android Apps*. 1st edition. Sebastopol, O'Reilly Media, Inc., 2011.
[15] Deng, Xinyue. *Group Collaboration with App Inventor*. M.Sc. Thesis. Massachusetts Institute of Technology, 2017.
[16] Cho, Kevin Kyung Bum. *A 3-Dimensional Editor for App Inventor*. M.Sc. Thesis. Massachusetts Institute of Technology, 2019.

# Sustainability of Nuclear Energy as a Source of the Future

Student **Florin-Alexandru LUNGA**[1], Student **Bogdan-Darian TOADER**[1],
Assist. Prof. PhD. Eng. **Dănuț TOKAR**[1,*]

[1] University Politehnica Timișoara, Romania

* danut.tokar@upt.ro

***Abstract:*** *Nuclear power is one of the most profitable, reliable, and low-carbon energies, so it can be seen as a source of the future. The article makes a comparative study between renewable technologies (photovoltaic, wind and nuclear) addressing both classical high-power (LR) and small-scale systems (SMRs) located in electrical energy consumption centres. The study highlights the advantages of nuclear energy in terms of land use, agricultural production, impact on wildlife and finally the possibility of cogeneration. In addition to these advantages, SMRs can provide charging stations for electric vehicles, which are also a solution of the near future.*

***Keywords:*** *RES, nuclear, thermal island, low carbon emissions, low footprint*

## 1. Introduction

Nuclear energy is relatively one of the most cost-effective and reliable energies compared to other sources. Apart from the initial cost of construction, the cost of generating electrical energy is cheaper and more sustainable than other forms of energy such as oil, coal and gas. One of the additional benefits of nuclear power is that it involves minimal risk of cost inflation compared to traditional energy sources that fluctuate regularly over periods. [1]
Nuclear fission generates much more energy than fossil fuels such as coal, oil or gas. The process produces nearly 8,000 times more energy than regular fossil fuels, resulting in fewer materials used and causing less waste [1].
Nuclear energy is the lowest carbon source of energy with a lower carbon footprint than other sources such as fossil fuels [1, 2].
A typical 1,000 MW nuclear plant has an average need of 34 ha to operate, while for the same installed power wind systems occupy 24 ha and solar systems 92 ha, according to the Nuclear Energy Institute (NEI) [3].

## 2. Comparative study between renewable energy sources (photovoltaic, wind and nuclear)

Analysing the share of electrical energy consumption in Romania (Fig. 1) as a result of efficiency measures, there is a slight decrease in electrical energy consumption in the residential sector, services and industry, as well as a slight increase in agriculture and transport [4].

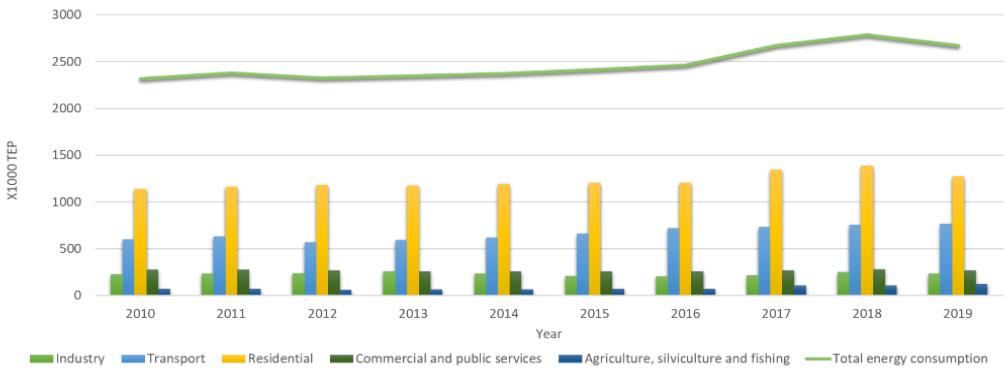


**Fig. 1.** Share of electrical energy consumption in Romania by sectors of activity [4]

On the other hand, the directive of the European Court of Auditors provides for the installation of 1,000,000 charging stations for electric vehicles by 2025 [5], which will put immense pressure on the Energy System (ES) of the European Union, forcing Member States to rethink their own ES.
Analysing the share of energy sources participating in electrical energy production in Romania, 33.35% are fossil fuels, 66.62% renewable energy sources (RES) (Fig. 2) [6].

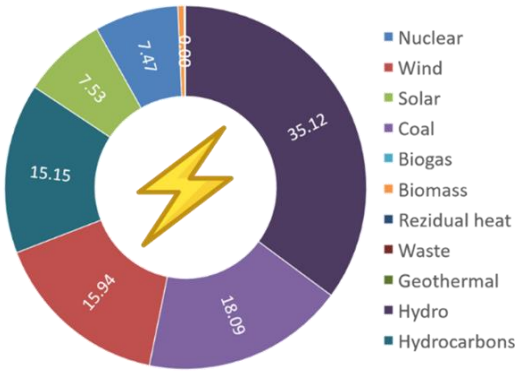


**Fig. 2.** Electrical energy production in Romania [6]

Romania's proposed targets for reducing greenhouse gas emissions consider three scenarios (Fig. 3) [7].

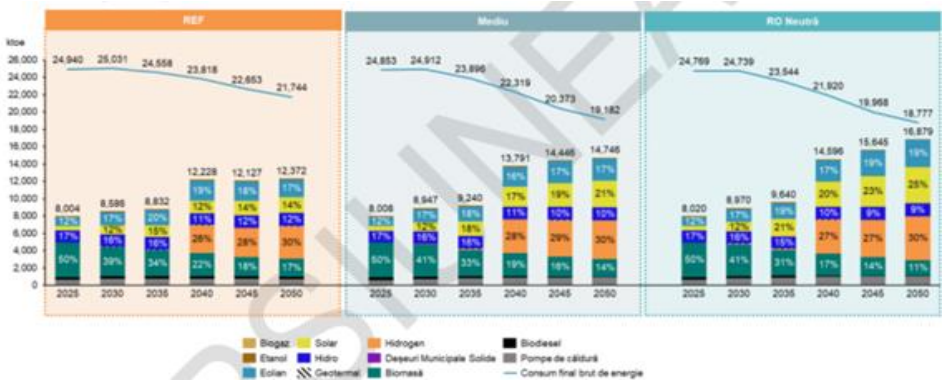


**Fig. 3.** Romania's targets for the share of RES in gross final energy consumption [7]

The baseline scenario for moving away from fossil fuels by 2050 calls for increasing solar and wind capacity to around 20% of the energy mix, with 27% hydrogen deployment by 2040, with a target of 30% by 2050.
These commitments involve occupying large areas of agricultural land (Fig. 4, 5, 6) [7].

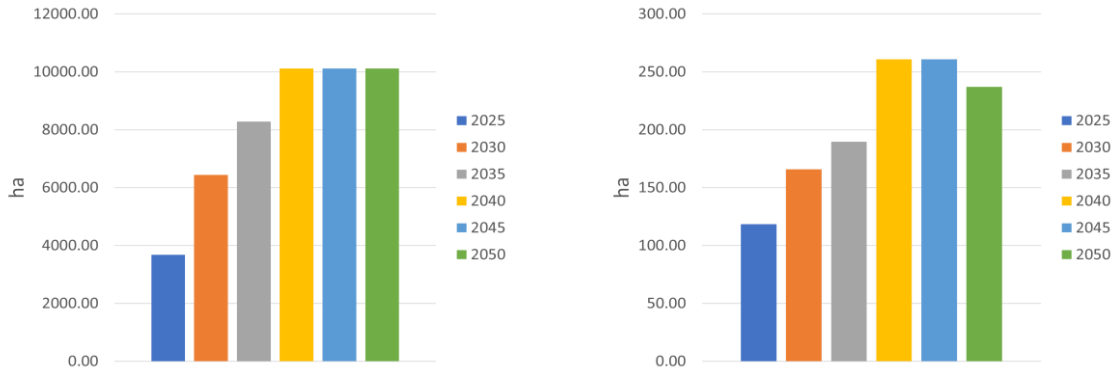


a) b)

**Fig. 4.** Land areas occupied by RES in the Baseline scenario. a) Solar, b) Wind [7]

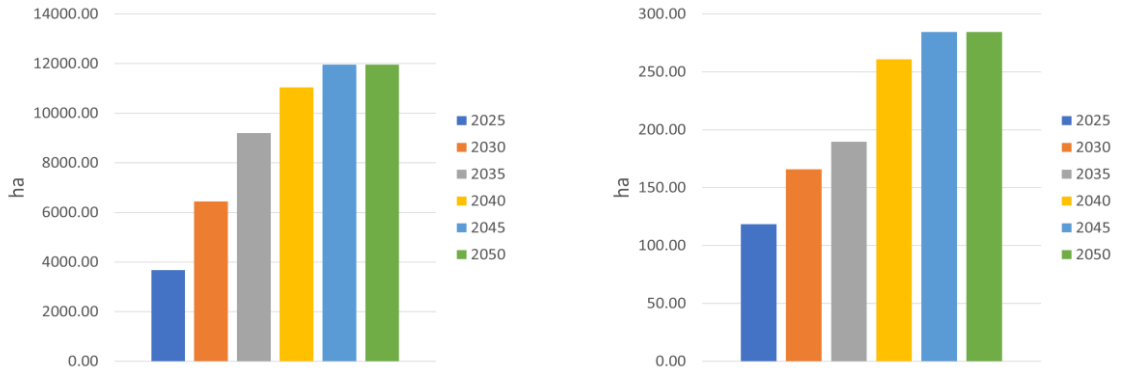


a) b)

**Fig. 5.** Land areas occupied by RES in the Medium scenario. a) Solar, b) Wind [7]

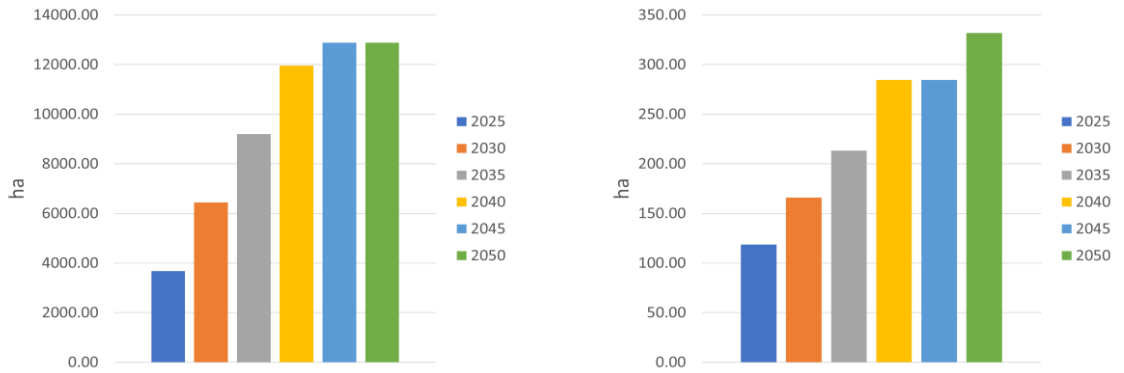


a) b)

**Fig. 6.** Land areas occupied by RES in the RO Neutral scenario. a) Solar, b) Wind [7]

On the other hand, the fluctuating nature of solar and wind energy forces us to consider a possible alternative to them (Fig. 7) [8].
According to data recorded in 2022, nuclear energy is found to be a source capable of ensuring the stable operation of the National Energy System (NES) (Fig. 7).

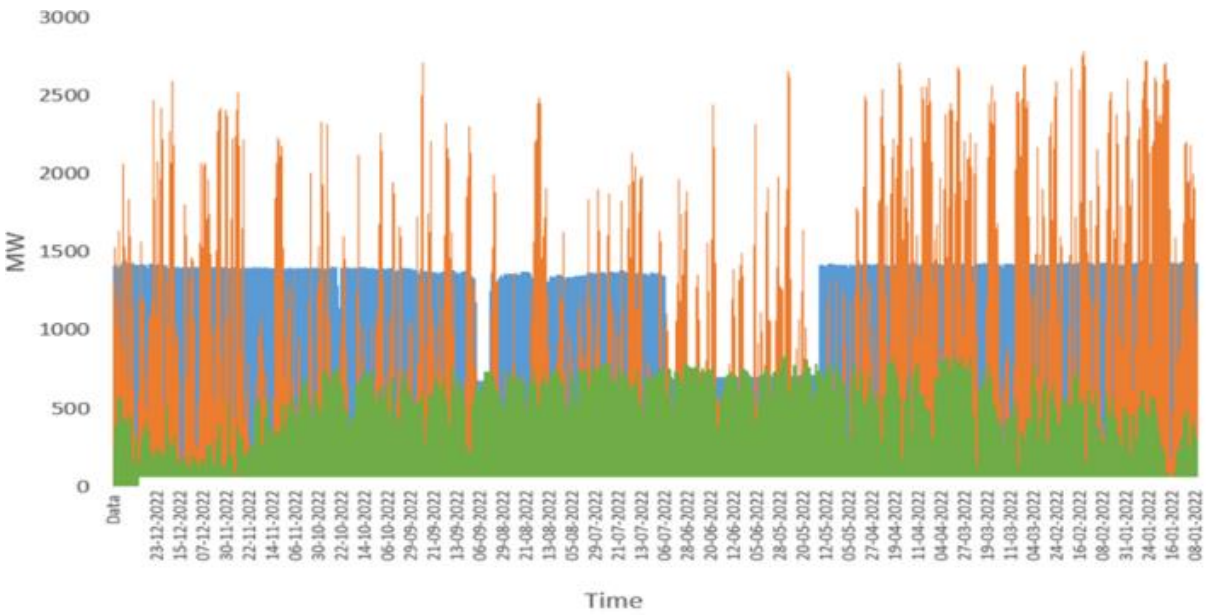


**Fig. 7.** Renewable energy sources (Wind, Photovoltaics, Nuclear) [8]

In the current context of the policies of some European states regarding the reconsideration of RES, the Swedish Parliament returns to the 2010 decision (by which it closed 4,000 MW of nuclear capacity) approving "Changing the target from 100% green energy to 100% energy without fossil fuels". Increasing energy production from 163 TWh to 300 TWh by 2040 is not possible without commissioning new nuclear power capacities (Fig. 8) [9, 10, 11].

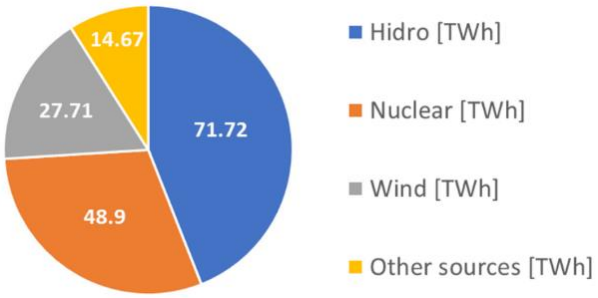


**Fig. 8.** Sweden's energy production in 2021 [9, 10, 11]

Analysing the variable character of RES, photovoltaic and wind (Fig. 7), the land areas occupied in Romania (Table 1) can assess the negative impact that these constructions have on the environment.

**Table 1:** Installed power and occupied area of RES

| Capacity Type production | Installed power [MW] | Occupied area [ha] |
|---|---|---|
| Nuclear | 1413 | 47.62 |
| Wind | 3014.91 | 71.45 |
| Solar | 1425.13 | 1311.12 |

It is known that during migration birds do not notice the rotational movement of the blades, producing a real carnage, and supporting photovoltaic panels requires special constructions [12].
Another aspect that should not be neglected is the thermal island effect due both to the high temperature under photovoltaic panels and to the fact that solar radiation is largely reflected from their surface (Fig. 9) [12].

**Fig. 9.** Resistance structures of photovoltaic panels [12]

Ensuring energy needs and achieving the targets assumed by the strategy can be achieved using nuclear energy.
The principle of electrical energy generation (Fig. 10) in NPP nuclear power plants is like that in TPP thermal power plants. The large amount of electrical energy and heat produced by NPP, no

greenhouse gas emissions, low footprint and low operating cost, recommends these systems in the energy mix.

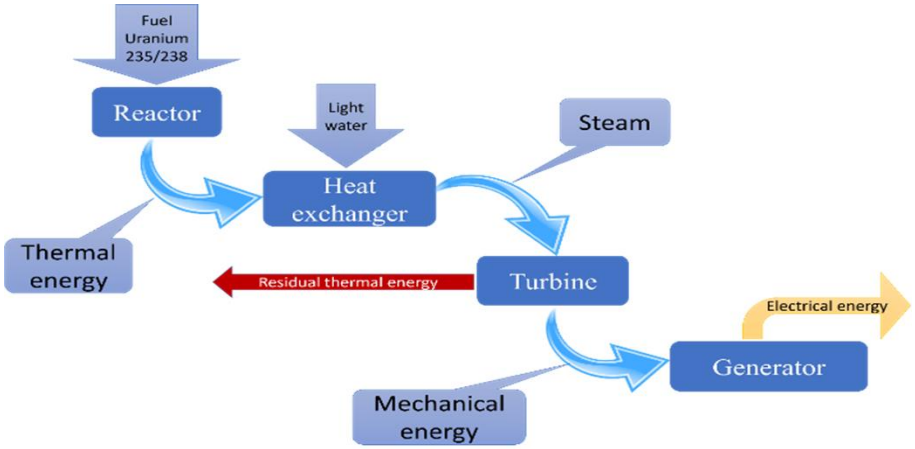


**Fig. 10.** Block diagram of NPP

There are 32 countries in the world that have NPP, and in France, Slovakia, Ukraine and Belgium this source is the basic source for electrical energy production [13]. The installed power in Romania is very small compared to other states, representing 0.59% (Table 2) of the installed power in the world [13].

**Table 2:** Technical characteristics of Cernavodă NPP [13]

| Thermal power | Electrical power | Number of fuel channels | Feed water temperature |
|---|---|---|---|
| MWt | MWe | - | °C |
| 2062 | 706.5 | 380 | 187.2 |

Even though there have been a few major accidents (Fukushima in Japan in 2011, Chernobyl in Ukraine in 1986, and Three Mile Island in the US in 1979), nuclear technology is increasingly mature.
Despite the known advantages, NPP has the disadvantage of disposable radioactive waste and the imposition of safety and vulnerability restrictions to terrorist attacks.
By analysing the targets in the strategy and the estimated production per hectare for different agricultural crops, the quantity not realized due to land occupation by dispatchable photovoltaic and wind systems was calculated (Fig. 11, 12, 13, 14, 15, 16) [7].

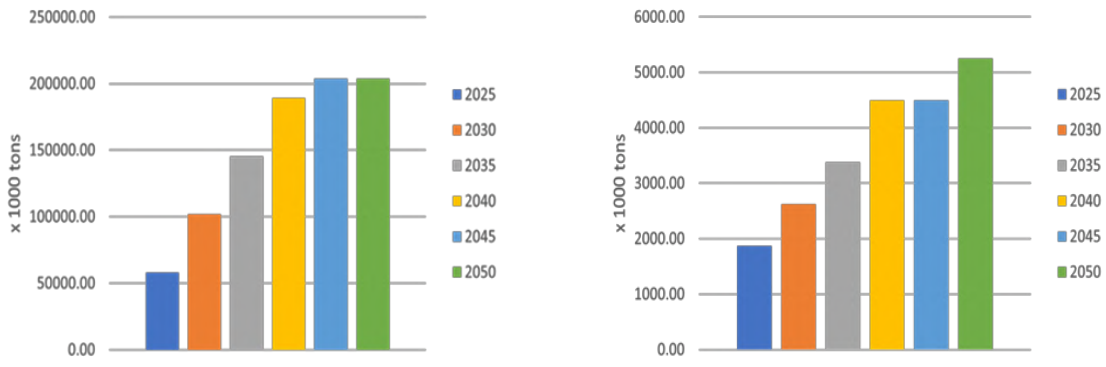


a) b)

**Fig. 11.** Quantities of agricultural products (potatoes) not realized as a result of land occupation by RES systems in the Baseline scenario. a) Solar, b) Wind [7]

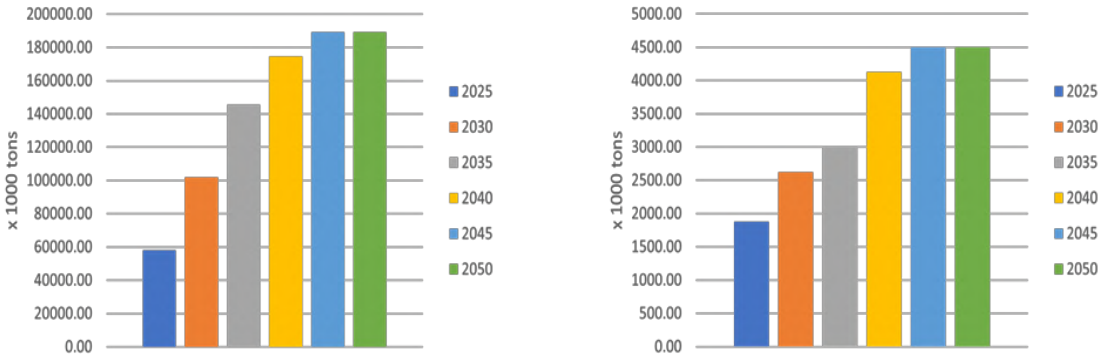


a) b)

**Fig. 12.** Quantities of agricultural products (potatoes) not realized as a result of land occupation by RES systems in the Medium scenario. a) Solar, b) Wind [7]

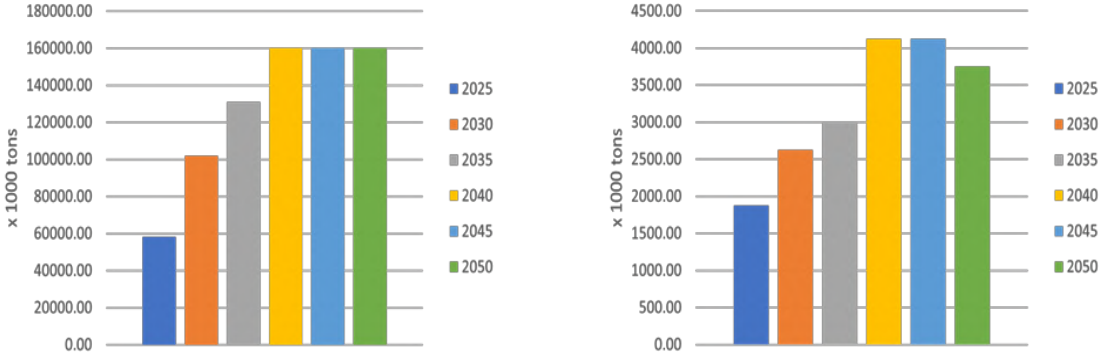


a) b)

**Fig. 13.** Quantities of agricultural products (potatoes) not realized as a result of land occupation by RES systems in the RO Neutral scenario. a) Solar, b) Wind [7]

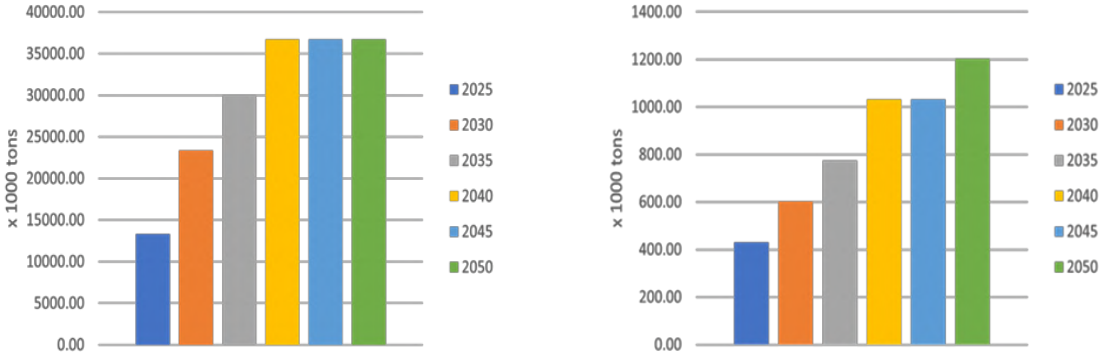


a) b)

**Fig. 14.** Quantities of agricultural products (cereals) not realized as a result of land occupation by RES systems in the Baseline scenario. a) Solar, b) Wind [7]

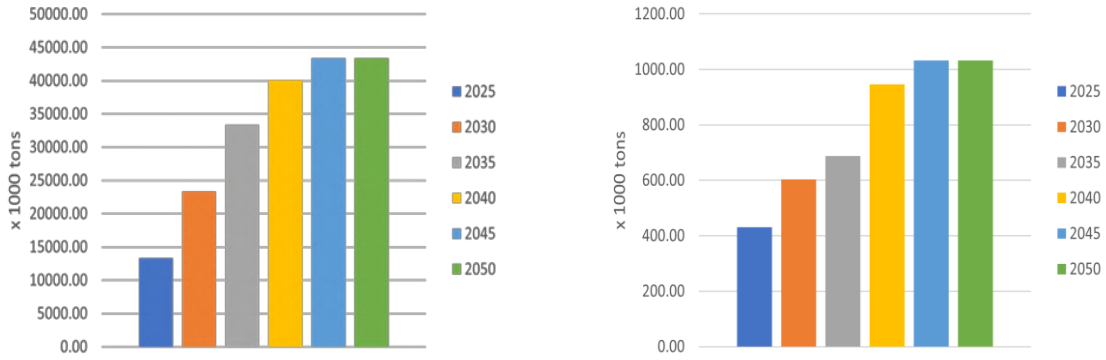


a) b)

**Fig. 15.** Quantities of agricultural products (cereals) not realized as a result of land occupation by RES systems in the Medium scenario. a) Solar, b) Wind [7]

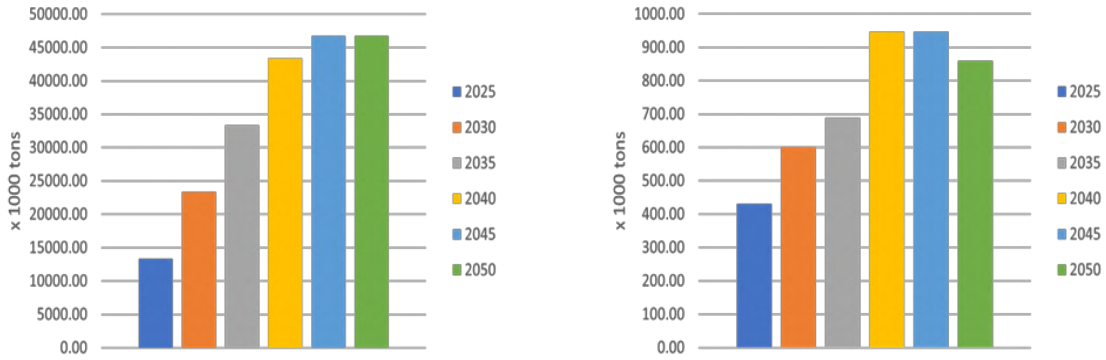


a) b)

**Fig. 16.** Quantities of agricultural products (cereals) not realized as a result of land occupation by RES systems in the RO Neutral scenario. a) Solar, b) Wind [7]

An emerging energy technology is small modular nuclear reactors (SMRs) suitable for areas with limited capacities and dispersed populations.
Small and medium-sized reactors, as defined by the International Atomic Energy Agency (IAEA), have installed capacities of up to 300 MWe compared to classical NPPs which have installed capacities bigger than 700 MWe.
SMRs differ from NPPs both by size and modularity in terms of design, installation, low fuel requirements [14] and storage of radioactive waste, the possibility of underground installation and finally the way of recovering waste thermal energy (cogeneration).
SMRs can be said to be a solution to eradicating energy poverty [12], as the technology is known and used in transport, medical, district heating and desalination [14].
SMRs can be appreciated as a solution for developing economies [12].

## 3. Conclusions

The growing need for electrical energy, but especially the achievement of the targets assumed by European countries, is not possible without the development of stable sources capable of generating large amounts of energy.
The "unloading" of transmission networks and the decentralization of electrical energy generation sources without increasing $CO_2$ emissions, the provision of thermal energy from reactor cooling water (technological residue) recommends SMRs as an alternative source to fossil fuels.
Even if the benefits obtained are firm, the need to ensure an emergency planning zone (EPZ) determines the implementation of specific preparation procedures and implicitly leads to increased production costs.

Although operational safety is enhanced by underground installation of this equipment in areas with low population density, public opinion is still sceptical about these systems.
The comparative study between RES (f, w, n) presents a possible solution in the future for increasing electrical energy production capacities to a low degree of land occupancy and with low $CO_2$ emissions, proposes even the notion of "prosumer" of electrical energy and heat.

**References**

[1] Igini, Martina. "The Advantages and Disadvantages of Nuclear Energy." *Global Commons*, January 28, 2023. Accessed June 30, 2023. https://earth.org/the-advantages-and-disadvantages-of-nuclear-energy/.
[2] Dassonville, Clara, and Thies Siemen. *Nuclear Energy: The Pros and Cons*. Brussels, Friedrich-Ebert-Stiftung Competence Centre for Climate and Social Justice FES Just Climate Publishing, 2023.
[3] Nuclear Energy Institute (NEI). "Nuclear energy is essential for a clean, reliable, modern grid that can support our growing electricity needs." *Infrastructure*. Accessed June 30, 2023. https://www.nei.org/advantages/infrastructure.
[4] National Institute of Statistics. "Final energy consumption in Romania (2010-2019)" / "Consumul final de energie în România (2010-2019)", *National Institute of Statistics*, June 5, 2020. Accessed June 30, 2023. https://insse.ro/cms/ro/content/statistica-energiei.
[5] European Court of Auditors. "Infrastructure for charging electric vehicles: more charging stations but uneven deployment makes travel across the EU complicated", *Special Report 05/2021: Infrastructure for charging electric cars is too sparse in the EU*, March 19, 2021. Accessed June 30, 2023. https://op.europa.eu/webpub/eca/special-reports/electrical-recharging-5-2021/en/.
[6] ANRE. "Installed power in electricity production capacities (in MW)" / "Puterea instalată în capacitățile de producție energie electrică (în MW)", *National Energy Regulatory Authority/ Autoritatea Naţională de Reglementare în domeniul Energiei (ANRE)*, June 30, 2023. Accessed June 30, 2023. https://anre.ro/puteri-instalate/.
[7] Government of Romania. "Romania's Long-Term Strategy for Reducing Greenhouse Gas Emissions, Version 1.0", *Long term strategy of Romania*, May 5, 2023. Accessed June 30, 2023. http://www.mmediu.ro/app/webroot/uploads/files/LTS%20-%20Versiunea%201.0%20-%20Eng%20-%2005.05.2023.pdf.
[8] Transelectrica. "Graph of National Power System (NPS) production, consumption and balance" / "Grafic producția, consumul și soldul Sistemului Energetic Național (SEN)", *Transelectrica*, December 31, 2022. Accessed June 30, 2023. https://www.transelectrica.ro/widget/web/tel/sen-grafic/-/SENGrafic_WAR_SENGraficportlet.
[9] Petrescu, Roxana. "Sweden reopens nuclear chapter to cover significant increase in energy demand by 2040. Relinquishes 100% green and goes 100% fossil-free" / "Suedia redeschide capitolul nuclear pentru a acoperi creşterea semnificativă a cererii de energie la nivelul anului 2040. Renunţă la 100% verde şi trece la 100% fără fosili", *Finance Newspaper*, June 28, 2023. Accessed June 30, 2023. https://www.zf.ro/companii/suedia-redeschide-capitolul-nuclear-pentru-a-acoperi-Growth-21973765.
[10] World Nuclear News. "Changes to Swedish law proposed to enable nuclear new build", *World Nuclear News*, January 12, 2023. Accessed June 30, 2023. https://world-nuclear-news.org/Articles/Changes-to-Swedish-law-proposed-to-enable-nuclear.
[11] Johnson, Simon. "Swedish parliament passes new energy target, easing way for new nuclear power", *Reuters*, June 20, 2023. Accessed June 30, 2023. https://www.reuters.com/sustainability/climate-energy/swedish-parliament-passes-new-energy-target-easing-way-new-nuclear-power-2023-06-20/.
[12] Baciu, Simion, Eugen Bârsan, Mircea Hordilă, Cristian Ivășcanu, Ionuț Nicoraş, Adriana Tokar, and Dănuț Tokar. "Environmental comfort versus energy poverty." *Student Scientific Bulletin, Partnership developed for Student Counseling and Practice in order to increase their employability – Conpractis* 1 (2015): 168-172.
[13] International Atomic Energy Agency (IAEA). "Nuclear Share of Electricity Generation in 2022", *World Statistics*, June 8, 2023. Accessed June 30, 2023. https://pris.iaea.org/pris/worldstatistics/nuclearshareofelectricitygeneration.aspx.
[14] International Atomic Energy Agency (IAEA). *Advances in Small Modular Reactor Technology Developments*. Vienna, IAEA Department of Nuclear Energy, 2018.

# Mechanical Frontal Seals Used in Centrifugal Pumps - From Theory to Experiment

Assoc. Prof. PhD eng. **Sanda BUDEA**[1,*]

[1] National University of Science and Technologies Politehnica of Bucharest, Romania, Energy Engineering Faculty; Department of Hydraulics, Hydraulic Machinery and Environmental Engineering

* sanda.budea@upb.ro

***Abstract:*** *The paper includes a theoretical approach to the frontal mechanical seals with rubber bellows, used in the conveyance of fluids in centrifugal pumps, in terms of friction coefficients, balancing and possible fluid losses. The study also presents an experimental study for a mechanical seal with rubber bellows and a shaft diameter of 35 mm, operating at different speeds at the pump shaft and different pressures of the transported fluid. At higher pressure the seal is balanced and at lower pressures is discharged.*

***Keywords:*** *Balanced seal, mechanical seal, friction coefficients, fluid pressure*

## 1. Introduction

Seals are landmarks of centrifugal pumps that have the role to prevent the flow of the fluid transported from inside the hydraulic machine to the outside. They are mounted on the drive shaft, between the housing towards the bearings, preventing fluid leaks to the outside.
Seals can be: - soft seal, cord-type, allowing a slight dripping of the fluid and used only for transporting water,
- mechanical seal, which can ensure seals up to pressures of 450 bars and peripheral rotation speeds of maximum 60 m/s.
A category very often used in centrifugal pumps are mechanical seals with rubber bellows, which are analyzed in this study. The advantages of frontal mechanical seals, according to the Eagle Burgmann catalog [1] are:
- protection of the shaft along the entire length of the seal
- protection of the sealing face by the special design of the bellows
- they have a high capacity to take over axial displacements
- high flexibility through the wide range of materials.

The most frequently used unbalanced frontal mechanical seals are the MG1 and the RMG12 version for hot water centrifugal pumps. In the experimental part I will use this sealing model with rubber bellows - fig. 1 [1], which can be mounted on shafts with diameters d1=10...100 mm, works at pressures of 16 bar, temperatures t = -20 °C … +140 °C, peripheral speed of 10 m/s and accepts an axial displacement of ±2.0 mm.
Materials used: for the mobile ring of the seal - carbon graphite antimony impregnated, or carbon graphite resin impregnated, or silicon carbide; for the fixed ring – silicon carbide, tungsten carbide. Bellows is made of elastomers as: NBR, EPDM, FKM, HNBR, and the mechanical components are from CrNiMo steel or Hastelloy, mentioned by [1].
The reference standard for this type of seal is EN 12756. The catalog states that the front seals MG1 can also be used as a multiple seal in tandem or in a back-to-back arrangement, depending on the conditions in the installations.
The applications of these FMS seals are manifold: water supply, water and wastewater pumps, circulating pumps, submersible pumps, chemical standard pumps, oil industry, paper industry, food technology etc.,

**Fig. 1.** Mechanical seal model MG1 [1]

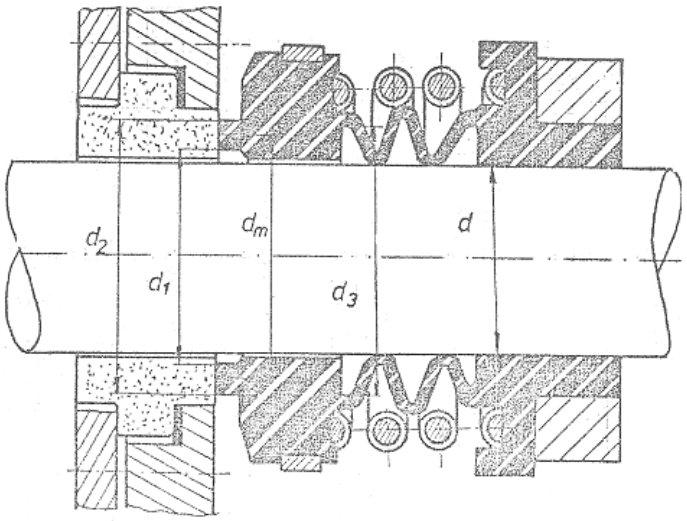


**Fig. 2.** Frontal mechanical seal with rubber bellows [2]

## 2. Theoretical approach

In the analysis of the correct functioning of a frontal mechanical seal, it is important to determine the coefficient of friction between the sealing rings and the flow rate of possible leaks, these depending on the shaft speed and the pressure of the transported fluid.
In fig. 3 you can see the distribution of pressures on the rings of an FMS and the way to achieve the balance of forces.
It was noted: $p_f$ – fluid pressure,

$d_1$, $d_2$, $d_3$ – characteristic diameters,
$p_{at}$ – atmospheric pressure,
$F_p$, $F_{p'}$ – pressure forces on the rings of seal
$F_r$ – force from the spring,
$F_f$ – friction force.

### 2.1 Equations

To calculate the coefficient of friction $\mu$ of a frontal mechanical seal, important in the tribological analysis of the phenomenon of Friction - Lubrication - Wear [3-6], it starts from the balance of forces:

$$F_r + F_p = F_f + F_p^{'} \tag{1}$$

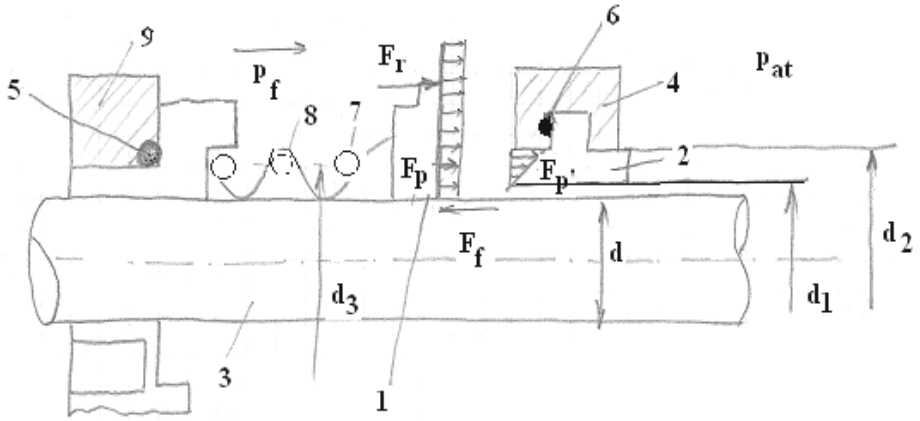


**Fig. 3.** Pressure distribution on the front mechanical seal rings 1- mobile ring, 2- fixed ring in the housing, 3- shaft, 4 - housing, 5, 6 - O-rings, 7 - spring, 8 - rubber bellows [2]

- axial force exerted on the contact between the two rings by the force of the spring $F_r = K_r f_o$ = the multiplication of the spring constant and its mounting arrow, the force due to the pressure of the fluid to be sealed, which is opposed by the force due to the pressure of the fluid, assumed in linear variation, flowing through the gap between the two rings, equal to

$$F_p^{'} = \frac{\pi}{4}\left(d_2^2 - d_1^2\right)\cdot\frac{p_f}{2} \qquad F_p = \frac{\pi}{4}\left(d_2^2 - d_3^2\right)\cdot p_f \qquad F_f = \mu N \qquad F_r = 150\,N \tag{2}$$

$$\mu N = F_r - \frac{p_f}{2}(d_2^2 - d_1^2)\frac{\pi}{4} + p_f(d_2^2 - d_3^2)\frac{\pi}{4} \tag{3}$$

This relative to the contact surface between the two rings gives us the pressure in the fluid film, called sliding pressure $p_g$, compared with the fluid pressure $p_f$.

$$p_g = \frac{N}{\frac{\pi}{4}(d_2^2 - d_1^2)} \geq\leq p_f \tag{4}$$

and allows us to determine if the seal is loaded, balanced, or unloaded, thus:
$p_g = p_f$ the seal is balanced otherwise the seal is unbalanced i.e.
$p_g < p_f$ the seal is loaded,
$p_g > p_f$ the seal is unloaded.
$d_1$ – the starting diameter of the seal, $d_2$ – the ended diameter of the seal, $d_3$ –the spring diameter (bellows).
To determine the friction losses of the sealing rings, from the power absorbed by the direct current electric motor, the losses in the motor rotor windings are subtracted $P_i$, current losses through ventilation, hysteresis are reduced, due to magnetizations $P_0'$, mechanical losses are reduced $P_M$, resulting the power dissipated by friction in the sealing rings $P_{fr}$.

$$P_a = U_A I_A, \quad P_i = f(I_A), \quad P_0' = f(E_o),$$
$$E_o = U_A - r_A I_A, \quad P_M = f(n) = \frac{1}{70}n \tag{5}$$

The friction moment is:

$$M_{fr} = 9550\,\frac{P_{fr}}{n} = F_f \cdot \frac{d_m}{2} = F_f\,\frac{d_1 + d_2}{2},$$

resulting

$$F_f = \frac{M_{fr}}{d_m} \tag{6}$$

we will be able to calculate the coefficient of friction between the two sealing rings using equation:

$$\mu = \frac{2M_{fr}}{d_m} \cdot \frac{1}{N}. \tag{7}$$

with reaction force *N* from equation (3).

### 2.2 Lubrication conditions

Regarding the losses from the mechanical seal, depending on its values, the friction can be:

- Fluid friction - $\mu$ = 0.005
- Mixed friction - $\mu$ =0.005-0.03
- friction at the operating limit $\mu$ =0.15-0.8
- dry friction - $\mu$ > 0.8.

## 3. Experimental study

The experimental stand of the mechanical seal with the shaft diameter $d_1$ of 35 mm, from figure 4, consists of shaft, frontal mechanical seal FMS, casing, bearings, coupling with the electric drive.

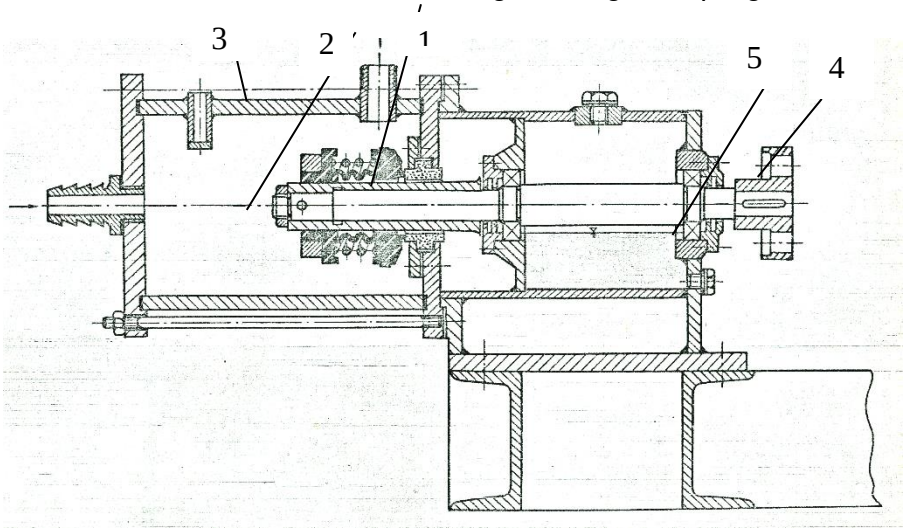


**Fig. 4.** The test bench of a front seal with a shaft diameter of 35 mm 1-seal, 2-shaft, 3-seal chamber, 4-coupling, 5-oil bearing [2]

Figure 2 shows the mechanical seal in detail, with the fixed ring in the housing, the movable ring on the shaft, the spring, the rubber bellows, the rotating shaft and the housing. Figure 3 shows the distribution of pressures on the frontal mechanical sealing rings and the way to achieve the balance of forces.

*The measuring equipment used in these experiments.*

Bourdon type manometers are used to measure the pressure to be sealed, having a precision class of 0.6.

The extremely low flow of liquid lost between the sealing rings is measured by the volumetric method, with the help of a graduated cylinder and a timer. For electrical quantities we use ammeter, voltmeter, and tachometer for speed.

To determine the electrical losses mentioned in equation (5), the calibration diagrams of the 1kW / 3000 rpm alternating current motor, illustrated in fig. 5.

*Working Procedure*

The start of the stand will not be done dry, but first the liquid will be introduced between the two sealing rings at a certain pressure and then the speed will be gradually increased and the axial force between the rings or the sealing pressure will be increased.

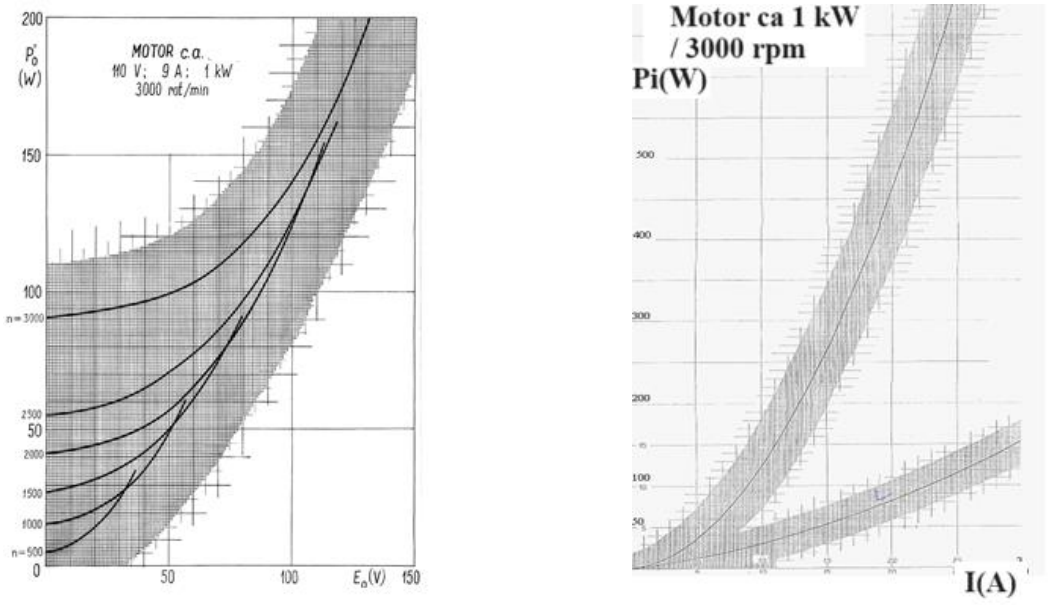


**Fig. 5.** The curve of electrical losses in copper $P_I$ (W), curve $P_o'$ ($n$, $E_o$) for mechanical losses in bearing, for ventilation and hysteresis [2]

Load the seal with fluid pressures of 0.5 bar, 1 bar, 1.5 bar; 2 bar, 2.5 bar; for each pressure the speed is varied, performing measurements at speeds n = 500, 1000, 1500 and 2000 rpm. Some of the experimental data obtained for different sealing pressures at various operating speeds of the sealing will be shown in table no. 1.

**Table 1:** Experimental results

| | $p_f$ | $n$ | $q$ | $I_A$ | $U_A$ | $P_a$ | $Pi$ | $Eo$ (V) | $Po$ (W) | $P_M$ (W) | $Pfr$ (W) | $Mfr$ daN cm | $Ff$ daN | $\mu$ (-) | $p_g$ bar | Obs |
|---|---|---|---|---|---|---|---|---|---|---|---|---|---|---|---|---|
| | bar | rpm | $cm^3/s$ | (A) | (V) | (W) | (W) | | | | | | | | | |
| 1 | 0.5 | 500 | 0.6 | 1.44 | 24 | 34.56 | 10 | 19.6 | 12 | 7.14 | 5.42 | 1.035 | 0.265 | 0.018 | 0.35 | loded |
| 2 | 0.5 | 1000 | 0.53 | 1.96 | 32 | 62.72 | 11.2 | 29.6 | 28 | 14.29 | 9.23 | 0.882 | 0.226 | 0.015 | 0.3 | loded |
| 3 | 0.5 | 1500 | 0.51 | 2.45 | 39 | 95.55 | 11.6 | 36.6 | 30 | 21.43 | 32.52 | 2.071 | 0.531 | 0.035 | 0.34 | loded |
| 4 | 0.5 | 2000 | 0.47 | 2.5 | 60 | 150 | 11.7 | 56 | 57 | 28.57 | 52.73 | 2.518 | 0.646 | 0.043 | 0.31 | loded |
| 5 | 0.5 | 2500 | 0.43 | 2.92 | 83 | 242.36 | 15.4 | 80 | 80 | 35.71 | 111.25 | 4.250 | 1.090 | 0.073 | 0.47 | loded |
| 6 | 1 | 500 | 1.04 | 2.4 | 20.5 | 49.2 | 11.1 | 18.22 | 13 | 7.14 | 17.96 | 3.430 | 0.879 | 0.059 | 0.29 | loded |
| 7 | 1 | 1000 | 1.1 | 2 | 41 | 82 | 8.8 | 39 | 35 | 14.29 | 23.91 | 2.284 | 0.586 | 0.039 | 0.24 | loded |
| 8 | 1 | 1500 | 1.15 | 2.1 | 60 | 126 | 11.6 | 58 | 60 | 21.43 | 32.97 | 2.099 | 0.538 | 0.036 | 0.31 | loded |
| 9 | 1 | 2000 | 1.07 | 2.5 | 80 | 200 | 15 | 80 | 77 | 28.57 | 79.43 | 3.793 | 0.972 | 0.065 | 0.45 | loded |
| 10 | 1 | 2500 | 1.02 | 3 | 92 | 276 | 15.3 | 85 | 89 | 35.71 | 135.99 | 5.195 | 1.332 | 0.089 | 0.47 | loded |
| 11 | 1.5 | 500 | 1.13 | 2 | 21 | 42 | 8.8 | 19.5 | 15 | 7.14 | 11.06 | 2.112 | 0.542 | 0.036 | 1.24 | loded |
| 12 | 1.5 | 1000 | 1.1 | 2.1 | 30 | 63 | 8.1 | 28 | 27 | 14.29 | 13.61 | 1.300 | 0.333 | 0.022 | 1.29 | loded |
| 13 | 1.5 | 1500 | 1.07 | 2.3 | 51 | 117.3 | 11.6 | 39 | 34 | 21.43 | 50.27 | 3.201 | 0.821 | 0.055 | 1.45 | loded |
| 14 | 1.5 | 2000 | 1.05 | 2.5 | 80 | 200 | 15.2 | 67 | 57 | 28.57 | 99.23 | 4.738 | 1.215 | 0.081 | 1.52 | balanced |
| 15 | 1.5 | 2500 | 1.04 | 2.85 | 94 | 267.9 | 15.4 | 77 | 84 | 35.71 | 132.79 | 5.072 | 1.301 | 0.087 | 1.55 | balanced |
| 16 | 2 | 500 | 1.33 | 2.1 | 22 | 46.2 | 8.8 | 20 | 15 | 7.14 | 15.26 | 2.914 | 0.747 | 0.050 | 1.89 | loaded |
| 17 | 2 | 1000 | 1.33 | 2 | 31 | 62 | 8.1 | 29 | 28 | 14.29 | 11.61 | 1.109 | 0.284 | 0.019 | 1.8 | loaded |
| 18 | 2 | 1500 | 1.37 | 2 | 40 | 80 | 8.3 | 38 | 34 | 21.43 | 16.27 | 1.036 | 0.266 | 0.018 | 2 | balanced |
| 19 | 2 | 2000 | 1.4 | 2.4 | 61 | 146.4 | 11 | 58 | 56 | 28.57 | 50.83 | 2.427 | 0.622 | 0.041 | 2.1 | balanced |
| 20 | 2 | 2500 | 1.44 | 2.7 | 80 | 216 | 13 | 77 | 84 | 35.71 | 83.29 | 3.182 | 0.816 | 0.054 | 2.2 | unloaded |

## 4. Analysis of the experimental results

From the analysis of the experimental results, the author found that the pressure between the two rings of the FMS, called sliding pressure, increases as the pressure of the transported fluid also increases.

The mechanical losses only depended on the driving speed, which was predictable. The power dissipated by friction rests constant with the pressure of the transported fluid and increases significantly with the drive speed of the centrifugal pump.

The coefficient of friction between the two rings of the EMF varies both with the pressure of the circulating fluid and with the speed of the shaft of the centrifugal pump. At speeds lower than 1500 rpm, the coefficient of friction between the rings is decreasing, because at speeds above 1500 rpm it becomes increasing, as in fig. 6. In all cases the friction is fluid or mixed.
The flow of leaks that can occur in the frontal mechanical seal increases both with the pressure of the transported fluid and with the speed of the shaft of the hydraulic machine. Comparable results regarding seal leakage can be found in [7].
Regarding the ratio between the fluid pressure and the sliding pressure, the analyzed seal FMS is balanced in few cases, like in Table 1, and in many cases it is loaded.
Based on the experimental results, we plotted the variation graphs of the friction coefficient depending on the speed $\mu = \mu(n)$ resulting curves for each seal fluid pressure. Such a variation of the friction coefficient as a function of speed has the typical form in fig. 6.

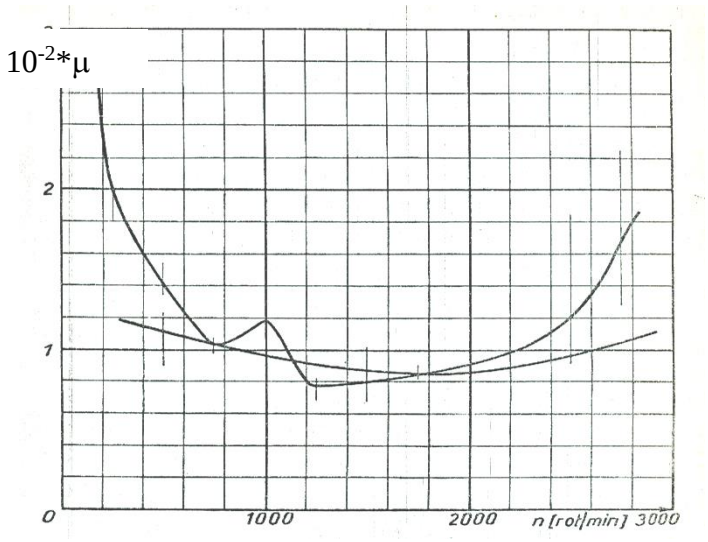


**Fig. 6.** The variation of the friction coefficient depending on the shaft speed

## 5. Conclusions

The coefficient of friction between the two rings of the frontal mechanical seal FMS varies both with the pressure of the circulating fluid and with the speed of the shaft of the centrifugal pump. At speeds lower than 1500 rpm, the coefficient of friction between the rings is decreasing, because at speeds above 1500 rpm it becomes increasing. The variation of the friction coefficient depending on the speed is explained by the fact that at low speeds the low friction speed between the two rings does not allow sufficient heating of the graphite ring [8]. It is a poor thermal conductor, leading to its additional superficial expansion compared to its colder depth. This would cause the formation of thermal plumes, creating hydrodynamic lift and therefore the appearance of fluid friction.
On the other hand, at higher speeds, the hydrodynamic frictions caused by the rotation of the mobile ring in the liquid begin to dominate, the so-called ventilation losses, which would require a more hydrodynamic shape of the exterior of the rotating seal while respecting an optimal radial distance from the outer wall of the sealing housing.
The experienced seal being of the maximum pressure 16 bar and the testing being carried out at low pressures, only at the fluid pressure of 2.5 bar, the sliding pressures are equalized with the pressure of the transported fluid, the seal being balanced, at lower pressures the FMS is discharged.

**Acknowledgments**

Thanks to my mentor, the late Prof. M.D. Cazacu, and also to the representative of the Burgmann company for their support.

**References**

[1] EagleBurgmann. “Catalog MG1. Mechanical seals | Mechanical seals for pumps | Elastomer bellows seals.” Accessed December 8, 2023. https://www.eagleburgmann.com/en/products.
[2] Budea, Sanda. *Hydraulic measurements and test of hydraulic machines like pumps, fans and blowers / Masurari hidraulice si incercarea unor masini hidraulice din categoria pompe, ventilatoare si suflante.* Bucharest, Printech Publishing House, 2010.
[3] Cazacu, Mircea Dimitrie, and Sanda Budea. *3D fluid flowing of viscous fluids through machines and equipment / Curgeri tridimensionale ale lichidelor vâscoase prin mașini și echipamente.* Bucharest, Printech Publishing House, 2012.
[4] Exarhu, Mihai. *Hydraulic, pneumatic and environmental measurements / Măsurători hidraulice, pneumatice și de mediu.* Bucharest, SC Andor Tipo Publishing House, 2007.
[5] Florea, Julieta, and Valeriu Panaitescu. *Fluid Mechanics / Mecanica Fluidelor.* Bucharest, Didactic and Pedagogical Publishing House, 1979.
[6] Tavoularis, Stavros. *Measurement in Fluid Mechanics*. Cambridge University Press, 2005.
[7] Luo, Yin, Yakun Fan, Yuejiang Han, Weqi Zhang, and Emmanuel Acheaw. “Research on the Dynamic Characteristics of Mechanical Seal under Different Extrusion Fault Degrees.” *Processes* 8, no. 9 (2020):1057.
[8] Xiao, Nian, and M. M. Khonsari. “A Review of Mechanical Seals Heat Transfer Augmentation Techniques.” *Recent Patents on Mechanical Engineering* 6, no. 2 (2013): 87-96.

# Comparative Study between the Operation of Refrigeration Installations with Refrigerants R134A and R471A for a Refrigerated Warehouse. Case Study

Eng. **Adrian MIHAI**[1], Assoc. Prof. PhD. Eng. **Adriana TOKAR**[2,*], Assoc. Prof. PhD. Eng. **Mihai CINCA**[2], R. A. PhD. student Eng. **Daniel MUNTEAN**[2]

[1] SildorProd S.R.L.

[2] University Politehnica Timisoara

* adriana.tokar@upt.ro

***Abstract:*** *In the context of the acceleration of the transition process from refrigerants with high global warming potential (GWP over 1500 units) to refrigerants with low global warming potential, within the limit of 150 units according to the F-GAS regulation, the refrigeration industry has difficulties in the development of refrigerants that meet safety standards (class A1L – non-toxic and non-flammable), environmental standards (GWP-under 150 units), efficiency standards (COP) and long-term viability. The study shows that slowly but surely, refrigerants are starting to appear that meet all these regulations and that can be integrated into commercial installations of small and medium power up to 50kW. Based on the versatility of the refrigeration plant components, starting with the compressor, the condenser, the evaporator, continuing with the refrigeration automation and ending with the command-and-control automation, the article wants to show that, very soon, we can choose technical solutions that comply with the current requirements.*

***Keywords:*** *R134, refrigerants, R471A, GWP, COP*

## 1. Introduction

Refrigeration installations represent a set of components brought together in subsystems such as refrigerating units, heat exchanger and command and control automation [1].
All refrigeration installations have the role of ensuring, primarily, the temperature in a space or fluid that in turn cools a technological process [1, 2].
The availability of good quality perishable food products, throughout the year, is dependent on ensuring optimal temperature and humidity parameters in cold storage. The cooling of raw materials and food products through the refrigeration plant is among the first stages of their processing processes. Due to the fact that, in the food industry, refrigeration installations represent one of the largest consumers of electricity in companies in the food industry, the choice of the refrigerant must take into account both its thermodynamic properties and its impact on the environment [3, 4].
So, the challenge of our days is conception the refrigeration system in accordance with the energy efficiency and environmental protection norms.

## 2. Method of approach

In the conception phase of the technical solution for cooling finished products stored at ºC temperature, and taking into account the efficiency of installation costs and annual operating costs, the following refrigeration systems were considered for analysed the refrigerated warehouse:

- cooling with direct expansion system with mixed refrigerant R134A, GWP=1430, with possibility of retrofitting R513A, GWP= 631 [5];
- cooling with direct expansion system with refrigerant R471A, mixture of 78.7% R1234ze(E), 17% R1336mzz and 4.3% ignition inhibitor HFC227ea, GWP=148 [5].

The subject of the comparative analysis was carried out for a refrigerated warehouse with the destination of cooling the finished product, located in the western part of Romania highlighted on the climatic zoning map I of Romania (-12°C) (Fig. 1) [6] with the aim of making it more efficient

investment costs related to operating costs respecting environmental protection norms, following the following steps:

- determining the thermal requirement according to the application requirement;
- selection of equipment according to thermal requirements;
- determining the installation costs for the refrigeration system;
- estimation of maintenance costs;
- estimating the costs of retrofitting the installation;
- life cycle cost analysis for refrigeration systems, including installation costs, annual maintenance, energy required to operate the system.

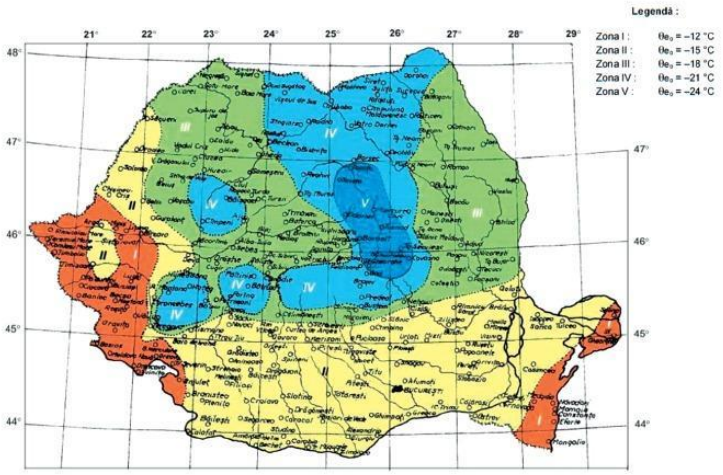


**Fig. 1.** Climatic zoning map of Romania and the Republic of Moldova [6]

### 2.1. Description of the refrigerated warehouse analyzed

The feasibility analysis of the solution was suitable for an existing cold store with C1 15-minute fire-resistant flammability envelopes, consisting of heat-insulated metal panels with basalt mineral wool G=15 cm, reaction to fire class B-s2d0 EI-30. The wall of the cold store doubles the covering on the inside perimeter with metal panels thermally insulated with polyurethane with a thickness of 10 cm (Fig. 2) [4].

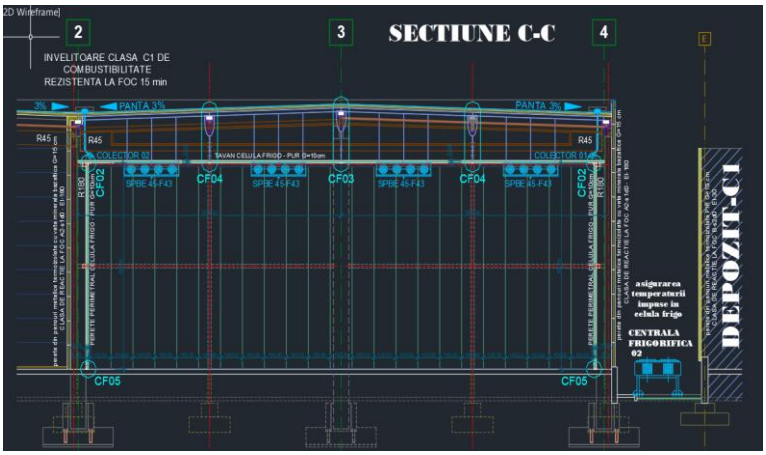


**Fig. 2.** Refrigerated warehouse envelope plan section

The surface of the warehouse analyzed is S = 533.60 m$^2$ and a height H = 8.5 m. The 20 cm thick concrete floor is for a bearing capacity of 50 kN/m$^2$.
The thermal requirement for the cold store was simulated using the Cold Store Cooling Load Calculation software [7], and the input/output data are presented in Fig. 3 [7].

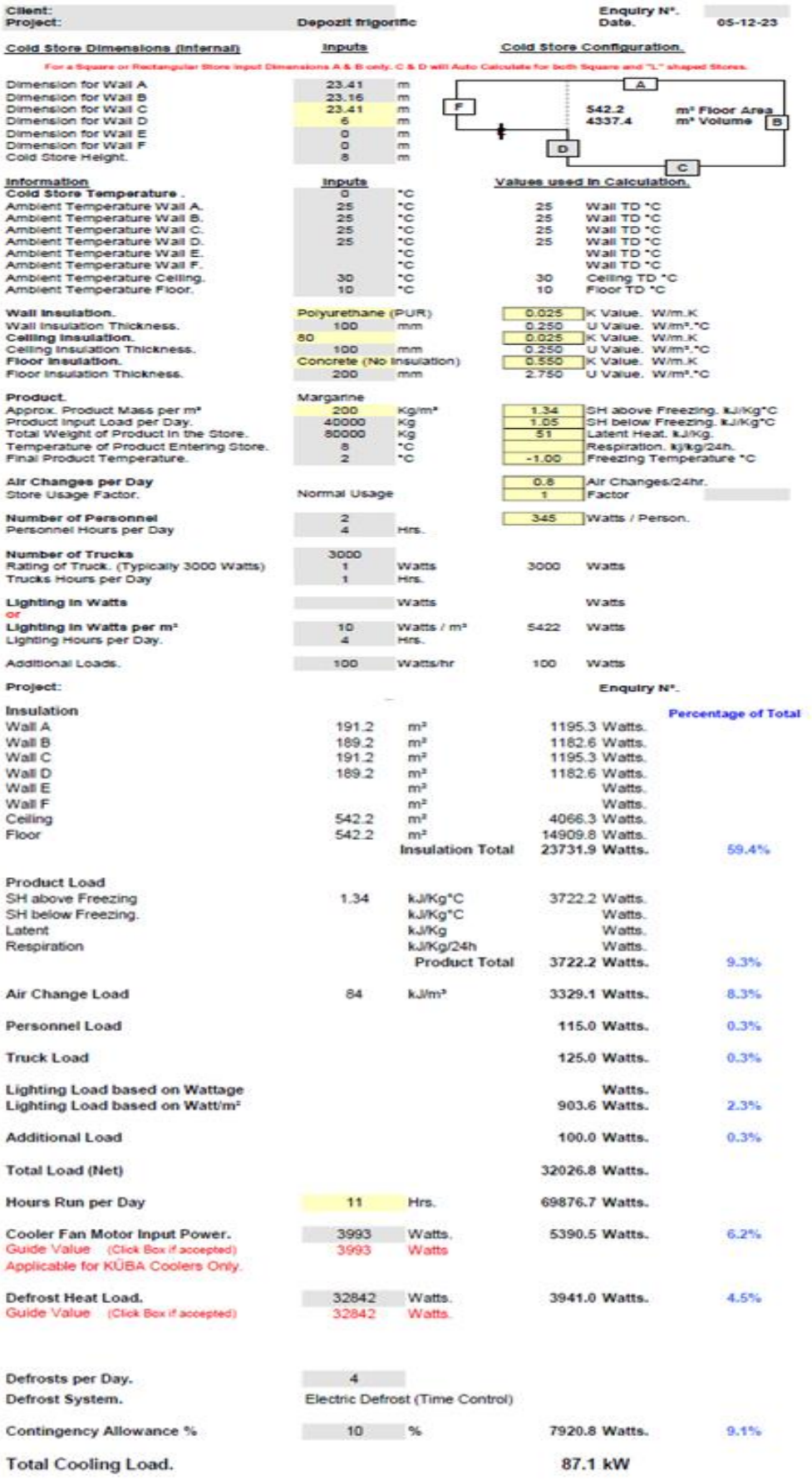

| | | | | | |
|---|---|---|---|---|---|
| Client: | | | | Enquiry N°. | |
| Project: | Depozit frigorific | | | Date. | 05-12-23 |
| **Cold Store Dimensions (Internal)** | **Inputs** | | **Cold Store Configuration.** | | |
| For a Square or Rectangular Store input Dimensions A & B only. C & D will Auto Calculate for both Square and "L" shaped Stores. | | | | | |
| Dimension for Wall A | 23.41 | m | | | |
| Dimension for Wall B | 23.16 | m | | | |
| Dimension for Wall C | 23.41 | m | | | |
| Dimension for Wall D | 6 | m | | | |
| Dimension for Wall E | 0 | m | | | |
| Dimension for Wall F | 0 | m | | | |
| Cold Store Height. | 8 | m | | | |
| | | | 542.2 | m² Floor Area | |
| | | | 4337.4 | m³ Volume | |
| **Information** | **Inputs** | | **Values used in Calculation.** | | |
| **Cold Store Temperature .** | 0 | °C | | | |
| Ambient Temperature Wall A. | 25 | °C | 25 | Wall TD °C | |
| Ambient Temperature Wall B. | 25 | °C | 25 | Wall TD °C | |
| Ambient Temperature Wall C. | 25 | °C | 25 | Wall TD °C | |
| Ambient Temperature Wall D. | 25 | °C | 25 | Wall TD °C | |
| Ambient Temperature Wall E. | | °C | | Wall TD °C | |
| Ambient Temperature Wall F. | | °C | | Wall TD °C | |
| Ambient Temperature Ceiling. | 30 | °C | 30 | Ceiling TD °C | |
| Ambient Temperature Floor. | 10 | °C | 10 | Floor TD °C | |
| **Wall Insulation.** | Polyurethane (PUR) | | 0.025 | K Value. W/m.K | |
| Wall Insulation Thickness. | 100 | mm | 0.250 | U Value. W/m².°C | |
| **Ceiling Insulation.** | 80 | | 0.025 | K Value. W/m.K | |
| Ceiling Insulation Thickness. | 100 | mm | 0.250 | U Value. W/m².°C | |
| **Floor Insulation.** | Concrete (No Insulation) | | 0.550 | K Value. W/m.K | |
| Floor Insulation Thickness. | 200 | mm | 2.750 | U Value. W/m².°C | |
| **Product.** | Margarine | | | | |
| Approx. Product Mass per m³ | 200 | Kg/m³ | 1.34 | SH above Freezing. kJ/Kg°C | |
| Product Input Load per Day. | 40000 | Kg | 1.05 | SH below Freezing. kJ/Kg°C | |
| Total Weight of Product in the Store. | 80000 | Kg | 51 | Latent Heat. kJ/Kg. | |
| Temperature of Product Entering Store. | 8 | °C | | Respiration. kj/kg/24h. | |
| Final Product Temperature. | 2 | °C | -1.00 | Freezing Temperature °C | |
| **Air Changes per Day** | | | 0.8 | Air Changes/24hr. | |
| Store Usage Factor. | Normal Usage | | 1 | Factor | |
| **Number of Personnel** | 2 | | 345 | Watts / Person. | |
| Personnel Hours per Day | 4 | Hrs. | | | |
| **Number of Trucks** | 3000 | | | | |
| Rating of Truck. (Typically 3000 Watts) | 1 | Watts | 3000 | Watts | |
| Trucks Hours per Day | 1 | Hrs. | | | |
| **Lighting in Watts** | | Watts | | Watts | |
| or | | | | | |
| **Lighting in Watts per m²** | 10 | Watts / m² | 5422 | Watts | |
| Lighting Hours per Day. | 4 | Hrs. | | | |
| Additional Loads. | 100 | Watts/hr | 100 | Watts | |

| | | | | | |
|---|---|---|---|---|---|
| **Project:** | | | | **Enquiry N°.** | |
| **Insulation** | | | | | **Percentage of Total** |
| Wall A | 191.2 | m² | 1195.3 | Watts. | |
| Wall B | 189.2 | m² | 1182.6 | Watts. | |
| Wall C | 191.2 | m² | 1195.3 | Watts. | |
| Wall D | 189.2 | m² | 1182.6 | Watts. | |
| Wall E | | m² | | Watts. | |
| Wall F | | m² | | Watts. | |
| Ceiling | 542.2 | m² | 4066.3 | Watts. | |
| Floor | 542.2 | m² | 14909.8 | Watts. | |
| | | **Insulation Total** | **23731.9** | **Watts.** | 59.4% |
| **Product Load** | | | | | |
| SH above Freezing | 1.34 | kJ/Kg°C | 3722.2 | Watts. | |
| SH below Freezing. | | kJ/Kg°C | | Watts. | |
| Latent | | kJ/Kg | | Watts. | |
| Respiration | | kJ/Kg/24h | | Watts. | |
| | | **Product Total** | **3722.2** | **Watts.** | 9.3% |
| **Air Change Load** | 84 | kJ/m³ | 3329.1 | Watts. | 8.3% |
| **Personnel Load** | | | 115.0 | Watts. | 0.3% |
| **Truck Load** | | | 125.0 | Watts. | 0.3% |
| **Lighting Load based on Wattage** | | | | Watts. | |
| **Lighting Load based on Watt/m²** | | | 903.6 | Watts. | 2.3% |
| **Additional Load** | | | 100.0 | Watts. | 0.3% |
| **Total Load (Net)** | | | 32026.8 | Watts. | |
| **Hours Run per Day** | 11 | Hrs. | 69876.7 | Watts. | |
| **Cooler Fan Motor Input Power.** | 3993 | Watts. | 5390.5 | Watts. | 6.2% |
| Guide Value (Click Box if accepted) | 3993 | Watts | | | |
| Applicable for KÜBA Coolers Only. | | | | | |
| **Defrost Heat Load.** | 32842 | Watts. | 3941.0 | Watts. | 4.5% |
| Guide Value (Click Box if accepted) | 32842 | Watts. | | | |
| **Defrosts per Day.** | 4 | | | | |
| **Defrost System.** | Electric Defrost (Time Control) | | | | |
| **Contingency Allowance %** | 10 | % | 7920.8 | Watts. | 9.1% |
| **Total Cooling Load.** | | | **87.1 kW** | | |

**Fig. 3.** Simulation of the thermal requirement according to the application requirement [7]

The air flow was determined to ensure the number of air hourly exchanges necessary for the proper cooling of the product (Table 1).

**Table 1:** Number of hourly air exchanges / refrigerated warehouse

| Room type | Deposit volume [$m^3$] | Air flow rate circulated by vaporizers [$m^3/h$] | Number of air hourly exchanges |
|---|---|---|---|
| Refrigerated warehouse with cooling load | 4536.9 | 65520 | 14 |

## 2.2 Refrigeration systems analyzed

The technical solutions analyzed consist in the choice of a refrigeration installation with direct expansion that works with refrigerant R134A or a refrigeration installation with direct expansion that works with refrigerant R471A related to energy consumption and environment protection.

- *R134 A system*

First installation consists of a refrigerating plant composed of a compact, cased and fully self-contained refrigerating and electronic assembly with 3 pieces of Frascold compressors model V35-103Y (the simulation of input/output data is shown in Fig. 4 [8]), Modine remote condenser with vertical air jet equipped with 5 fans, model EGK715DN4D02V (Fig. 5) [9] and 4 Modine evaporators model CTE502A8ED (Fig. 6) [9] fully equipped with thermostatic valve, separation ball valves and solenoid valve on each of them.

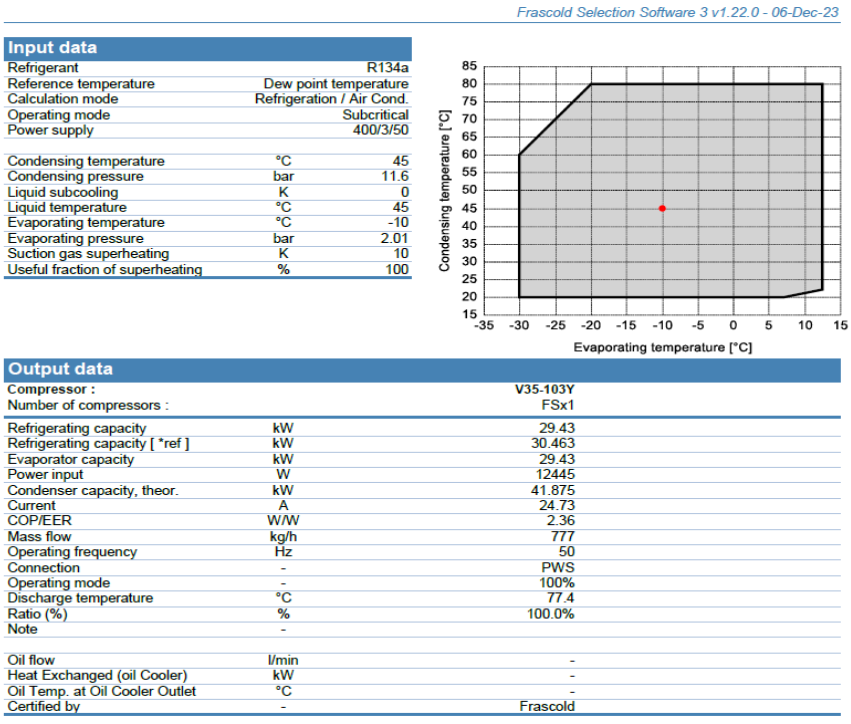

*Frascold Selection Software 3 v1.22.0 - 06-Dec-23*

**Input data**

| | | |
|---|---|---|
| Refrigerant | | R134a |
| Reference temperature | | Dew point temperature |
| Calculation mode | | Refrigeration / Air Cond. |
| Operating mode | | Subcritical |
| Power supply | | 400/3/50 |
| Condensing temperature | °C | 45 |
| Condensing pressure | bar | 11.6 |
| Liquid subcooling | K | 0 |
| Liquid temperature | °C | 45 |
| Evaporating temperature | °C | -10 |
| Evaporating pressure | bar | 2.01 |
| Suction gas superheating | K | 10 |
| Useful fraction of superheating | % | 100 |



**Output data**

| | | |
|---|---|---|
| Compressor : | | V35-103Y |
| Number of compressors : | | FSx1 |
| Refrigerating capacity | kW | 29.43 |
| Refrigerating capacity [ °ref ] | kW | 30.463 |
| Evaporator capacity | kW | 29.43 |
| Power input | W | 12445 |
| Condenser capacity, theor. | kW | 41.875 |
| Current | A | 24.73 |
| COP/EER | W/W | 2.36 |
| Mass flow | kg/h | 777 |
| Operating frequency | Hz | 50 |
| Connection | - | PWS |
| Operating mode | - | 100% |
| Discharge temperature | °C | 77.4 |
| Ratio (%) | % | 100.0% |
| Note | - | |
| Oil flow | l/min | - |
| Heat Exchanged (oil Cooler) | kW | - |
| Oil Temp. at Oil Cooler Outlet | °C | - |
| Certified by | - | Frascold |

**Fig. 4.** Simulation of input/output data for V35-103Y compressors with R134A [8]

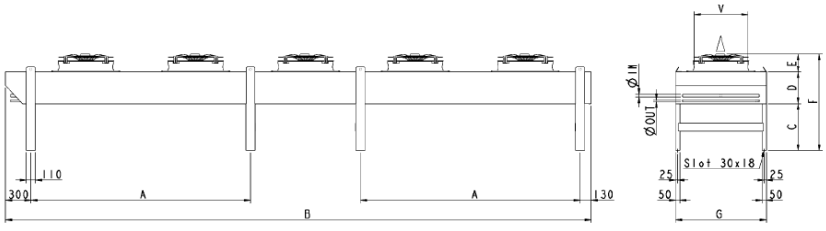


**Fig. 5.** Condenser Modine EGK715DN4B01V [9]

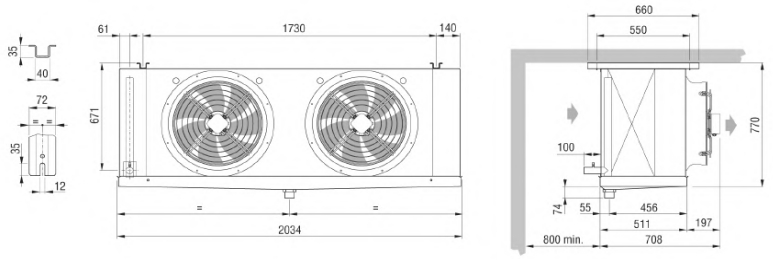


**Fig. 6.** Evaporators Modine CTE502A8ED [9]

- *R471A system*

The second installation consists of a refrigerating plant composed of a compact, cased and fully self-contained refrigerating assembly with 5 pieces of Frascold compressors model V35-103Y, remote (the simulation of input/output data is shown in Fig. 7) [8] Modine condenser with vertical air jet equipped with 4 fans, model EGK814DN4A02V (Fig. 8) [9] and 4 pieces of Modine evaporators model CTE503A8ED (Fig. 9) [9] fully equipped with thermostatic valve, separation ball valves and solenoid valve on each of them.

*Frascold Selection Software 3 v1.22.0 - 06-Dec-23*

| Input data | | |
|---|---|---|
| Refrigerant | | R471a |
| Reference temperature | | Dew point temperature |
| Calculation mode | | Refrigeration / Air Cond. |
| Operating mode | | Subcritical |
| Power supply | | 400/3/50 |
| Condensing temperature | °C | 45 |
| Condensing pressure | bar | 11.6 |
| Liquid subcooling | K | 0 |
| Liquid temperature | °C | 45 |
| Evaporating temperature | °C | -10 |
| Evaporating pressure | bar | 2.01 |
| Suction gas superheating | K | 10 |
| Useful fraction of superheating | % | 100 |

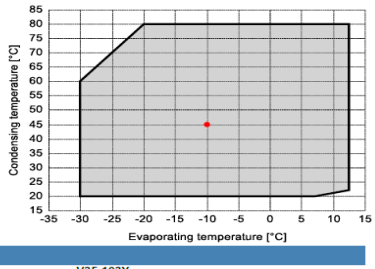


| Output data | | |
|---|---|---|
| Compressor : | | V35-103Y |
| Number of compressors : | | FSx1 |
| Refrigerating capacity | kW | 17.89 |
| Evaporator capacity | kW | 17.89 |
| Power input | W | 8275 |
| Condenser capacity, theor. | kW | 26.21 |
| Current | A | 22.15 |
| COP/EER | W/W | 2.16 |
| Mass flow | kg/h | 777 |
| Operating frequency | Hz | 50 |
| Connection | - | PWS |
| Operating mode | - | 100% |
| Discharge temperature | °C | 72.56 |
| Ratio (%) | % | 100.0% |
| Note | - | |
| Oil flow | l/min | - |
| Heat Exchanged (oil Cooler) | kW | - |
| Oil Temp. at Oil Cooler Outlet | °C | - |
| Certified by | - | Frascold |

**Fig. 7.** Simulation of input/output data for V35-103Y compressors with R471A [8]

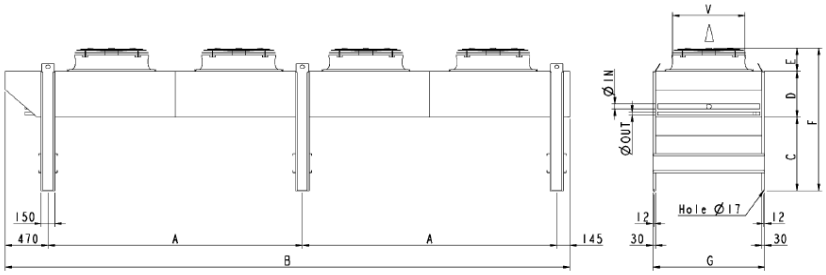


**Fig. 8.** Condenser Modine EGK715DN4B01V [9]

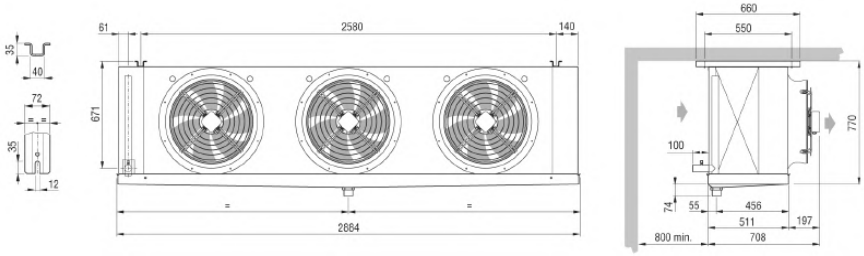


**Fig. 9.** Evaporators Modine CTE502A8ED [9]

## 3. Result

In order to choose a system that meets the environmental protection requirements, the refrigerating installation that works with R471A meets this condition. Comparing the cost efficiency of the refrigeration systems analyzed in Table 2, the factors that were taken into account are presented: installation costs, maintenance costs, costs related to the estimated annual electricity consumption, as well as the cost of the retrofit according to the regulations, assuming that the refrigeration system it works according to the data resulting from the thermal demand.

**Table 2:** The costs of refrigeration systems analyzed

| Refrigeration system | Installation costs [Euro] | Annual maintenance costs [Euro] | Annual electricity cost [Euro] | Retrofit costs [Euro] | Total annual costs [Euro] |
|---|---|---|---|---|---|
| R134A | 97776 | 2000 | 14080 | 77107 | 16080 |
| R471A | 149426 | 2000 | 10220 | - | 12972 |

For the calculation of the annual cost of the energy required to power the refrigeration equipment, an approximate price of 0.16 EUR/kWh was considered.
The lifetime of the installation, having provided annual service, is between 15 and 20 years (Table 3).

**Table 3:** Energy savings according to the life cycle for a period of up to 20 years

| Lifetime [years] | Energy savings / year I.F. R471A vs.R134A [Euro ] | Total recovered [Euro] | Investment value recovered only from energy savings [%] |
|---|---|---|---|
| 10 | 3860 | 38600 | 25.8% |
| 15 | | 57900 | 38.7% |
| 20 | | 77200 | 51.7% |

## 4. Discussions

Analyzing the initial costs of the investment, it can be seen that a refrigerant solution with a GWP greater than 150 units is cheaper than an installation with GWP under the limit of 150 units. But this must also be correlated with a possible improvement of the installation by retrofitting the refrigerant if the situation requires it according to the regulations to be implemented and then the advantage is clearly in favor of the installation with R471A.

## 5. Conclusions

The theoretical results of the case study showed that for such applications with large volume deposits, the correct choice of the technical solution from the point of view of energy efficiency is very important in the medium and long term.
Of particular importance is the fact that the installation with R471A refrigerant can be used in the long term, without the need for substantial changes in the installation or retrofit, giving it reliability and durability.
This solution no longer requires subsequent retrofit interventions, protecting the investor from other subsequent expenses.
The technical solution with refrigerant R471A can be considered as an optimal solution from the energy point of view, but especially optimal from the point of view of environmental protection, regarding installations with refrigerating power up to 100kw.

**References**

[1] Niculiță, Petru. *Refrigeration technique and technology in agro-food fields* / *Tehnica și tehnologia frigului în domenii agroalimentare*. Bucharest, Didactic and Pedagogical Publishing House, 1998.
[2] Necula, Horia. *Refrigeration installations / Instalații frigorifice*. Bucharest, Universe of Energy Publishing House, 2005.
[3] Hristov, Hristo. ”Energy and environmental efficiency of industrial refrigeration installations.” *Acta Technica Corviniensis – Bulletin of Engineering* 11, no. 3 (July – September 2018): 43-46.
[4] Mihai, Adrian, Adriana Tokar, Mihai Cinca, and Daniel Muntean. “Energy Efficient Refrigeration Solutions.” *Hidraulica Magazine*, no. 3 (September 2023): 44-49.
[5] International Institute of Refrigeration (IIR). "Commercial refrigeration: marketing of R471A, a new alternative to R404A." Accessed November 22, 2023. https://iifiir.org/en/news/commercial-refrigeration-marketing-of-r471a-a-new-alternative-to-r404a.
[6] Ministry of Regional Development and Public Administration – MDRAP. Order no. 386/2016 for the modification and completion of the Technical Regulation "Regulation on the thermotechnical calculation of the construction elements of buildings", indicator no. C 107-2005, approved by the Order of the Minister of Transport, Construction and Tourism no. 2.055/2005 - Appendix 1 / Ordinul nr. 386/2016 pentru modificarea şi completarea Reglementării tehnice "Normativ privind calculul termotehnic al elementelor de construcţie ale clădirilor", indicativ C 107-2005, aprobată prin Ordinul ministrului transporturilor, construcţiilor şi turismului nr. 2.055/2005 – Anexa 1. *The Official Gazette of Romania*, Part I, no. 306 (April 2016).
[7] Stapley, Ron. Software - Cold Store Cooling Load Calculation, 2000.
[8] Frascold S.p.a. ”Selection Software 3 v1.18.” Accessed December 06, 2023. https://www.frascold.it/it
[9] Modine Manufacturing Company. ”Scelte. Selection Software.” Accessed December 06, 2023. https://www.modinecoolers.com/coolers-software/.

# Water Pollution with Plastic - Scenarios Aimed at International Promotion through Pedagogy and Thematic Philately

Eng. IT expert **Alexandru Leonard POP**[1], Eng. IT expert **Bogdan-Vasile CIORUȚA**[1-3,*], Stud. **Ioana-Elisabeta SABOU (CIORUȚA)**[2], Assoc. Prof. Dr. Eng. **Mirela-Ana COMAN**[3,4]

[1] Technical University of Cluj-Napoca - North University Centre of Baia Mare, Office of Informatics, 62A Victor Babeș Str., 430083, Baia Mare, Romania

[2] Technical University of Cluj-Napoca - North University Centre of Baia Mare, Faculty of Letters, Department of Specialty with Psychopedagogical Profile, 76 Victoriei Str., 430083, Baia Mare, Romania

[3] University of Agricultural Sciences and Veterinary Medicine from Cluj-Napoca, 3-5 Calea Mănăștur, 4000372, Cluj-Napoca, Romania

[4] Technical University of Cluj-Napoca - North University Centre of Baia Mare, Faculty of Engineering, 62A Victor Babeș Str., 430083, Baia Mare, Romania

* bogdan.cioruta@staff.utcluj.ro

***Abstract:*** *Water pollution with plastic waste continues to be one of the biggest environmental problems of the modern world. Its impact is not only significantly negative but also materialized long-term repercussions, affecting the dynamics of marine life and the development of tourist activities. Beyond the various scenarios regarding the long-term sustainability of some measures and solutions, an impressive effort must be made to reduce and prevent other situations of a similar nature. In this sense, we sought to identify if there are solutions aimed at promoting work scenarios in the case of water pollution with plastic waste. What we noticed, are several philatelic effects (postage stamps, first-day covers/FDCs, envelopes and blocks, illustrated postcards, maximum postcards) that have appeared in the last 7-10 years, internationally, most being intended to emphasize and impose the (re)adaptation of scenarios to fight against pollution. Consequently, it matters not only what we propose to do, but also what each of us can do; or in this case, promoting the problems faced by the environment, and their associated solutions, are a niche that deserves more attention.*

***Keywords:*** *Water pollution, plastics, thematic philately, international promotion*

## 1. Introduction

Water pollution with plastic waste continues to be, according to the latest report issued by the Ellen MacArthur Foundation 0 and circular economy specialists, one of the biggest environmental problems of the modern world. It is found globally from deserts to farms, tropical landfills, and arctic snow, as well as from mountaintops to the deep ocean, where it has become a major threat to aquatic environments 0.

Reports of plastic debris in the marine environment began many years ago, with plastic pollution continuing to build up over the past 50 years. Estimates of global emissions of plastic waste to rivers, lakes, seas, and oceans range from 9 to 23 million t/year 0, with a similar amount emitted. Furthermore, plastic in seas and oceans can kill marine animals (turtles, dolphins, and whales) by suffocating or blocking their digestive system. Plastic can also pollute beaches and affect tourism, an important source of income for many countries. Therefore, we agree that its impact is not only significantly negative but also with tangible repercussions over time, affecting the dynamics of marine life and tourist activities.

Water pollution with plastic waste is mainly caused by human activities, such as dumping waste in oceans or on river banks, the use of single-use plastic products, and the accidental loss of plastic from ships or oil rigs. Waste treatment methods such as incineration or improper storage also contribute to all of this. There are many proposed solutions to tackle the problem of water pollution with plastic waste. One of these is represented by reducing the use of single-use plastics, by promoting sustainable alternatives, such as biodegradable or reusable products.

At the same time, there must be better waste management, to reduce its dumping in the oceans and on the banks of rivers. Equally important is the involvement of all actors, from consumers and

industry to governments and international organizations, to promote concrete actions to prevent and reduce water pollution with plastic.
As such, aligning with this approach, through this paper, we will try to explore the impact of plastic water pollution, the causes of this problem, and the proposed solutions to address this global problem. Thus, we noticed that in recent years, many countries around the world have issued postage stamps related to plastic water pollution. These postage stamps were designed to draw attention to this global issue and promote awareness and action. Some stamps issued featured images of marine animals that have been affected by plastic pollution, such as turtles and whales, and others featured images of plastic-filled oceans or strong messages to promote the reduction of single-use plastic use.

## 2. Material and methods

The initiative to identify materials with a philatelic character started from an article published in a specialized blog in the field, namely "Jurnalul Philatelic"/Philatelic Journal 0. Starting from this, to identify the pieces in question, we turned to a series of sites, with philatelic specifics, on the list of which we can find Colnect®, Delcampe®, Okazii®, eBay®, WOPA+®, etc.
The indexing, analysis, and description of the identified pieces were carried out step by step, starting from the data provided by the Colnect® and Delcampe® sites, to which were added the data published by the postal administrations. Following the identification of the philatelic pieces in the topic addressed, due to the large number of results, we applied the following selection criteria, which can equally be criteria with a pedagogical effect:

- *thematic relevance*: the philatelic materials should properly address issues related to plastic water pollution, providing information or awareness about this global problem;
- *design quality*: the visual aspect of the philatelic issue must be attractive and highlight the visual impact of plastic pollution on the aquatic environment;
- *Innovation, novelty, and originality of the exhibition*: the philatelic materials that bring innovative elements or original approaches to the theme will be considered to highlight the creativity and impact of the message;
- *educational content*: the philatelic materials should provide educational information on the effects of plastic pollution on aquatic ecosystems and potential solutions for this problem;
- *connection with other current events*: if the philatelic issue correlates with current events or awareness campaigns regarding plastic pollution, it can be evaluated positively;
- *representation of diversity*: the philatelic materials should reflect the diversity of species affected by pollution and convey a comprehensive message regarding the need to protect the environment;
- *the effectiveness of the message transmitted*: the philatelic materials must clearly and effectively communicate the message regarding the negative impact of plastic pollution on waters;
- *availability of information*: the philatelic materials should be accompanied by additional information or descriptions that provide context and details about the problem of plastic pollution and efforts to combat it;
- *quality of philatelic material*: the use of quality materials for philatelic issues (eg sustainable paper or other recyclable materials), can be an additional selection factor.

These criteria have decisively contributed to the selection and promotion of the identified philatelic issues, which successfully address the problem of plastic water pollution, equally drawing attention to scenarios with possible negative impacts.

## 3. Results and discussions

Plastic, ubiquitous in everyday life, constitutes a significant part of our living environment. This versatile and durable material has become an essential component of modern society, being used in a variety of products, from packaging and household utensils to components of electronic devices and medical equipments. However, the excessive presence of plastic in our environment can cause significant problems.

Plastic waste poses a threat to terrestrial and aquatic ecosystems, affecting biodiversity and water quality. Plastic can persist in the environment for long periods, contributing to long-term pollution. Plastic fragmentation is a growing problem with the potential to affect human health and ecosystems. Awareness of the negative impact of plastic on the environment has increased in recent years, leading to sustained efforts to reduce the use of single-use plastic, promote recycling, and develop more sustainable alternatives. Education and individual and collective action are essential to reduce plastic pollution and protect the environment for future generations.

### 3.1 Pollution: plastic in the oceans, 31.08.2012, Republic of Burundi

Commemorative philatelic issue "Pollution: Plastic in the Oceans" (indexed by Mi BI#2590..93KB, Sn #BI-1115..18, Bel #BI-BL321) 0, consisting of four multi-colored comb lace stamps 13½, printed by offset lithography and arranged in the miniature school in Fig. 1, with the nominal value of 8,140 FBu (Burundian francs), very well captures this current environmental problem. Along with them appears the note whose stamp has a nominal value of 7,500 FBu.

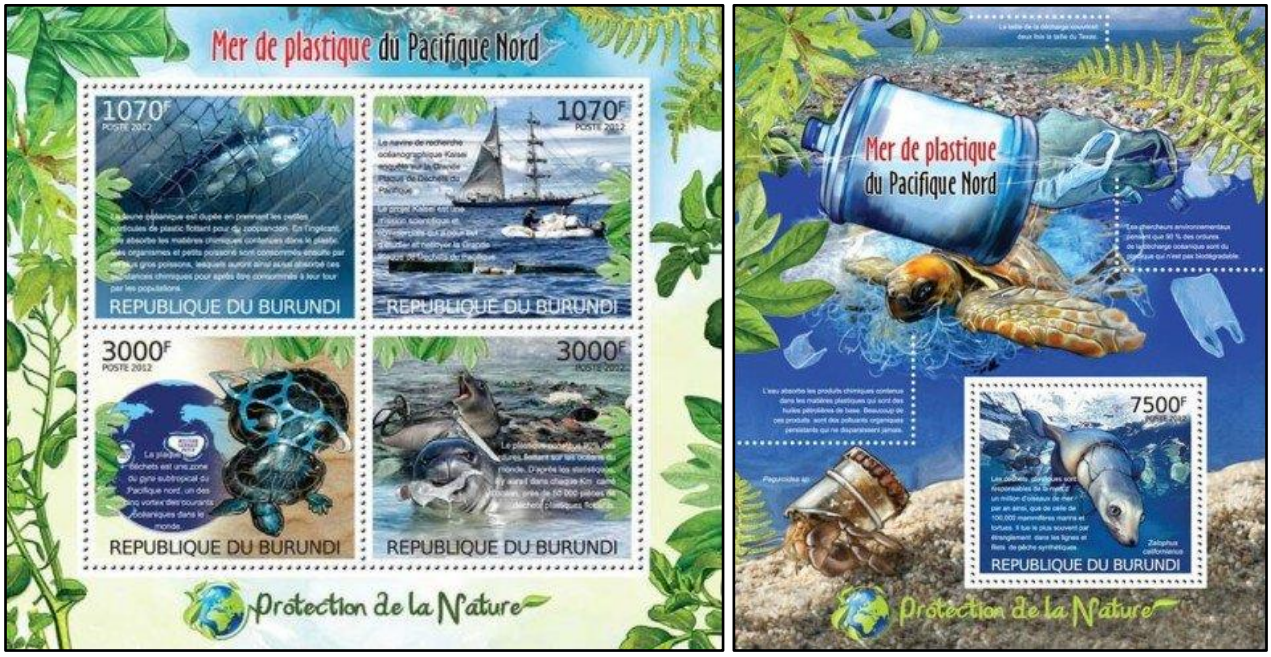


**Fig. 1.** Minisheet and sheet of the philatelic issue "Pollution: plastic in the oceans", 31.08.2012, Republic of Burundi 0

The first two stamps, with a face value of 1,070 francs each, highlight the circuit of plastic in the food chain and the importance of the Kaisei project in its effort to clean up the Pacific 0. The project in question aims to remedy situations where ocean fauna falls into the trap of ingesting small plastic particles, often mistaking them for zooplankton. By consuming these particles, aquatic organisms absorb the chemicals contained in the plastic and are then consumed by larger specimens, which accumulate these chemicals. Eventually, the accumulated chemicals become part of the human food chain.

Oceanographic research vessel Kaisei focuses on the study of the Great Pacific Debris Field (MCDP). Launched in 2009, the Kaisei project is a complex mission with dual scientific and commercial goals, aiming at the research and cleanup of MCDP 0. The ship is actively involved in the research and analysis of this vast area of the ocean where significant amounts of plastic waste accumulate. The crew and equipment on the ship are ready to contribute to efforts to clean the oceans of plastic pollution.

The Kaisei project explores and implements innovative technologies for efficient waste management. In addition to research and cleanup activities, the Kaisei Ship has a crucial role in informing and educating the public about the impact of plastic waste on the marine environment. Kaisei's project works in close collaboration with other organizations, institutions, and researchers globally to address the complex issue of marine litter.

The next two stamps in the block, with face values of 3,000 francs, illustrate aspects of the impact of plastic on marine life - effectively remaining captive. Plaques of plastic debris tend to form in the subtropical areas of the North Pacific, where one of the world's five ocean currents eddies originates. Plastic constitutes 90% of the total floating waste in the world's oceans.
According to statistical data from 2012, it is estimated that for every square kilometer of ocean, there are approx. 50,000 pieces of floating plastic waste. They are responsible for the death of over a million birds each year, as well as approx. 100,000 deaths among marine mammals and turtles (eg, by strangulation in the mesh of synthetic fishing nets). This is also highlighted on the stamp of the 7,500-franc note, which shows a young California sea lion (*Zalophus californianus*) captive in an ocean fishing net 0.

### 3.2 World Environment Day - Fight Plastic Pollution 05.06.2018, India

The "World Environment Day" commemorative philatelic issue, appearing under the motto "Fight plastic pollution" (Fig. 2), was put into circulation on 06.05.2018 in the form of a block (142 x 105 mm) of four multicolored stamps. Modeled by graphic artist Suresh Kumar, the four stamps (Mi #IN-3394..97, Yt #IN-3083..86, Sg #3502..05) 0, have a face value of 5 rupees, dimensions of 39 x 29 mm, and the lace of 13¼ x 13¾ units.


**Fig. 2.** Official FDC of the philatelic issue "World Environment Day – Fight against plastic pollution", franked with all four postage stamps and canceled with a special stamp, 05.06.2018, New Delhi (India) 0


**Fig. 3.** Special envelope made under the slogan "Fight against plastic pollution", stamped with one of the postage stamps of the philatelic issue "World Environment Day - Fight against Plastic Pollution" and canceled with the special stamp of the Philatelic Exhibition "Bilasapex 2019", 02.01.2019, Bilaspur (India) 0

The image of the stamps brings to our attention the presence of plastic waste in our everyday life, these being captured alongside runners on the beach (on the green stamp), by those who hike in the forest (on the blue stamp), by couples practicing yoga by the rivers (on yellow stamp) and even families with children playing on the beach (on the purple stamp) (as presented in Fig. 3).

### 3.3 MERCOSUR 2019: Environment protection, 05.06.2019, Uruguay

A new commemorative issue entitled "MERCOSUR 2019: Environmental Protection" (Mi #UY-3659, Yt #UY-2948, WADP-WNS #UY-025.19) 0 saw the light of day at the administrations of Uruguay on 05.06.2019.


**Fig. 4.** Official FDC of the philatelic issue "MERCOSUR 2019: Environmental Protection", postmarked and canceled with a special stamp, 05.06.2019, Uruguay 0

The campaign against plastic pollution is also the theme of this issue (see Fig. 4), which is captured through the multicolored postage stamp, in format 42 x 30 mm with comb lace 12½, a turtle fighting for its survival with a plastic bag. The design of the piece with the nominal value of $65 (Uruguayan peso) belongs to the graphic artist Alvaro Rodriguez, it was printed by offset lithography at Sanfer SRL in a limited edition of only 15,003 copies.

### 3.4 Campaign against plastic pollution, 29.09.2020, Marocco

The commemorative philatelic issue "Campaign against plastic pollution", with the theme of environmental protection, appeared on 29.09.2020, consisting of four multi-colored postage stamps, in 41 x 30 mm format, with syncopated lacing13¼. The printing of postage stamps with the face value of 3.75 د.م (Moroccan dirham) was done by offset lithography, and indexed in catalogs Mi #MA-2043..46, Sn #MA-1289a-d, Yt #MA-1887 ..90 and WAD #MA008..11.20 (see Fig. 5) 0.

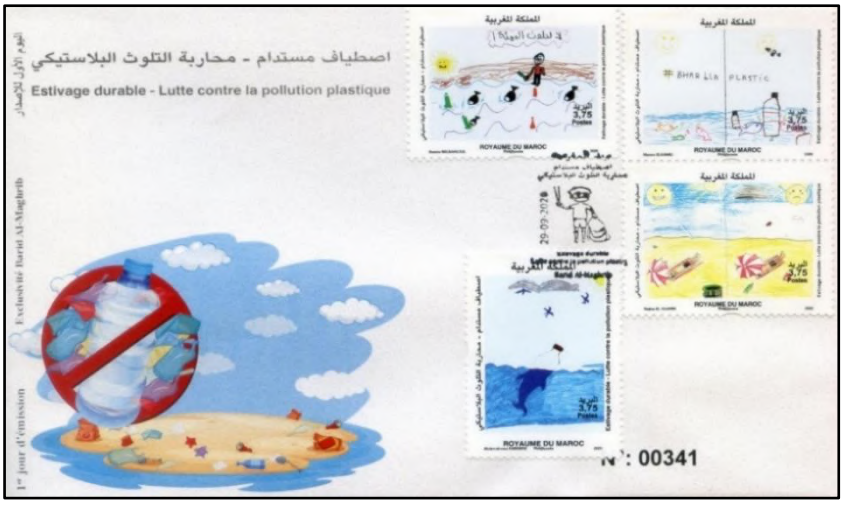


**Fig. 5.** Official FDC of the philatelic issue "Campaign against Plastic Pollution", franked with all four postage stamps and canceled with a special stamp, 29.09.2020, Morocco 0

Plastics floating on the surface of the waters may seem bright in their playful movement, but when these little explorers discover that those objects are waste that can injure and poison sea creatures, the initial amazement turns to deep sadness and disgust. Through their eyes, marine life suffocated under the weight of plastic waste becomes a disturbing story that motivates them to get involved. By nature, they feel the need to protect the world and as a result become messengers of innocence and responsibility, reminding us to protect resources for future generations.

### 3.5 Campaign against Plastic Pollution in the Oceans, 20.02.2023, Cook Islands

The commemorative philatelic issue "Campaign against plastic pollution in the oceans", having as its theme the protection of marine life, appeared on 20.02.2023, also consisting of four multicolored postage stamps, with lace 13½ x 13¼ 0. The $1 (NZD) face value postage stamps were printed by offset lithography, indexed to Yt #CK-1892..95.
The postage stamps franking the FDC in Fig. 6 0-0, show a whale, a crab, a dolphin, and a turtle in the company of several categories of plastic waste. It was not by chance that these animals were chosen to illustrate the stamps of this philatelic issue. Some marine species, such as whales and dolphins, may mistake plastic fragments for their natural food, such as squid or fish. This can lead to accidental ingestion of plastic waste, which can have serious consequences for their digestive system, general health, and even their survival. Plastic waste such as plastic bags and fragments can become death traps for whales, dolphins, and other species; animals can become trapped or drown with these objects, leading to mortality and significantly affecting population dynamics.


**Fig. 6.** Official FDC of the philatelic issue "Campaign against plastic pollution in the oceans", 20.02.2023, Cook Islands 0-0

Plastic pollution can affect the natural habitat of marine species such as coral reefs, mangroves, and others. This indirect impact can lead to loss of food, and shelter, and changes in their ecosystems, affecting the entire food web. Plastic waste can carry toxic chemicals and pathogens that can affect the health of marine species. In addition, plastic fragments can act as vectors, spreading pollution throughout the food chain and into different marine habitats.
Plastic can also affect the reproductive processes of marine species. Chemicals released by plastic or absorbed by marine animals can interfere with their hormone systems and affect the normal development of eggs and chicks. To protect these vulnerable species, efforts to reduce plastic pollution, promote recycling, and adopt sustainable practices are essential. Public awareness and active involvement in protecting the marine environment are crucial to ensuring the health and survival of these species.

### 3.6 Campaign against Plastic Pollution in the Seas, 20.04.2023, Croatia

Another philatelic issue dedicated to the theme of environmental protection is the one entitled "Campaign against plastic pollution in the seas" (Yt #HR1485, WADP-WNS #HR0.19.23, #HR1439), consisting of a single multicolored postage stamp, in the 42.75 format *35.5 mm with lace 14, appeared on 20.04.2023 (for more details see Fig. 7) 0. The design belongs to Enea Knežević, being printed by offset lithography with the support of Agencija Za Komercijalnu Djelatnost, with a face value of €1.14 (Euro) in a print run of 30,000 copies.

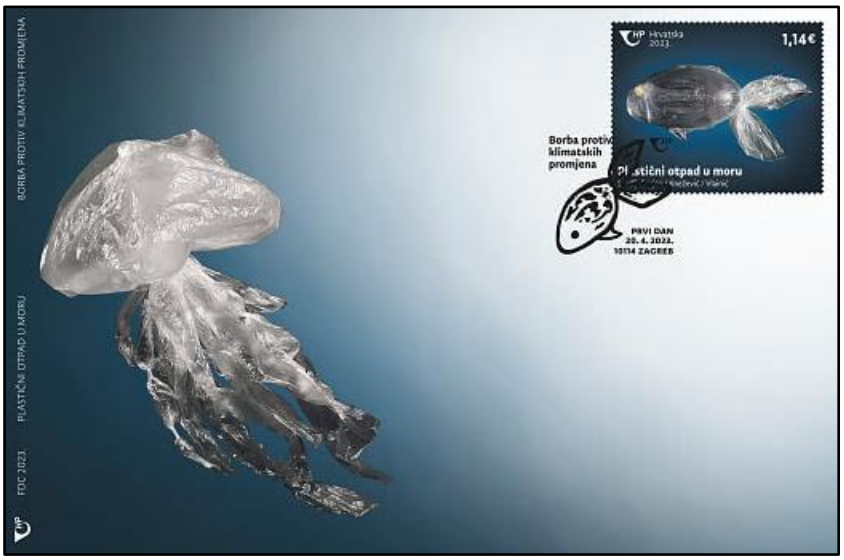


**Fig. 7.** Official FDC of the philatelic issue "Campaign against plastic pollution in the seas", 20.04.2023, Croatia 0-0

The serious and alarming threat of plastic suffocation of marine life stems from the excessive amount of plastic waste in the oceans and seas, directly and indirectly affecting marine life in multiple ways. Solving this problem requires concerted global efforts to reduce plastic production and use, promote recycling, and actively participate in cleanup and marine pollution prevention actions. Awareness and action also taken by postal administrations that circulate philatelic issues on the theme of plastic pollution of the seas and oceans are essential to protect the marine environment and ensure a future for these vulnerable species.

### 3.7 World Environment Day, 31.07.2023, Mali

The campaign against plastic pollution in the world's seas and oceans is also the theme of the 100-franc stamp from the "World Environment Day 2023" issue put into circulation by the Postal Administration of Mali on July 31, 2023 (for more details see Fig. 8) 0. The stamp wants to emphasize that turtles are heavily affected by plastic pollution and the impact on these vulnerable creatures is significant. Especially those that feed near the surface of the water, they may mistake plastic fragments for their natural food, such as jellyfish or other small marine organisms. Accidental ingestion of plastic can lead to obstruction of the digestive tract, which in turn can cause injury, illness, and even death.
Plastic waste, such as abandoned fishing nets or lost fishing gear, can become traps for turtles. They can very easily become entangled in these objects, leading to distress and the inability to feed or move normally.
Plastic pollution also affects turtles' natural habitat (e.g., nesting beaches). The presence of litter can disrupt nesting and egg-hatching processes, and plastic fragments can create obstacles that prevent chicks from accessing water. Plastic often contains toxic chemicals that can be released into the water. This can have negative effects on health and reproduction, affecting the entire life cycle of marine life. Plastic pollution is contributing to the decline of turtle populations, which are already suffering from other threats (eg, habitat loss due to climate change).


**Fig. 8.** Official FDCs of the "World Environment Day" philatelic issue, stamped with a philatelic sheet and associated block, 31.07.2023, Mali 0,0

## 4. Conclusions

Plastic water pollution is a significant global problem with negative impacts on the environment and marine life. This situation is mainly generated by human activities and can be addressed by reducing the use of single-use plastic, more efficient waste management, and the involvement of all actors. Action must be taken now to protect our planet and ensure a sustainable future for future generations.

Pedagogy through various educational alternatives, in which thematic philately can be used as a working tool (in teaching-learning-evaluation), can be a new way of promotion among young people. Besides, thematic philately also remains in the current research context an effective way to convey messages with a deep emotional impact, thus contributing to the promotion of awareness even at the international level. Both benchmarks, pedagogy, and thematic philately, can encourage today's society to act promptly and effectively to save marine habitats and species, assuring future generations the chance to enjoy them. In addition, they can accelerate and sustain the motivation of decision-makers, both in managing plastic waste situations and in saving and conserving marine species and habitats.

**References**

[1] Ellen MacArthur Foundation. "Designing out plastic pollution", October 13, 2023. Accessed October 16, 2023. www.ellenmacarthurfoundation.org/topics/plastics/overview.
[2] Valavanidis, A. "Oceans and Forests are Lungs of Planet Earth. Anthropogenic pollution of oceans and marine ecosystems is a worrying global problem", September 2023. Accessed October 16, 2023. http://chem-tox-ecotox.org/wp-content/uploads/2023/09/OCEANS-ECOSYSTEM-HEALTH-POLLUTION-2023.pdf.
[3] Pop, A.L. "Plastic Pollution in Water: Impact, Causes and Solutions." / "Poluarea apelor cu plastic: Impact, Cauze și Soluții." *Jurnalul Filatelic*, November 6, 2023. Accessed November 10, 2023. jurnalulfilatelic.blogspot.com/2023/11/poluarea-apelor-cu-plastic-impact-cauze.html.
[4] ***. "Pollution: Plastic in the Oceans" / "Poluarea: plastic în oceane", Colnect®, August 31, 2012. Accessed November 10, 2023. https://colnect.com/ro/stamps/list/country/35-Burundi/series/279485-Pollution_Plastic_in_the_Oceans.
[5] Whaley, G., and K. Perry. "Project Kaisei: Entrepreneurship to Potentially Save the Pacific Ocean from Environmental Disaster." *Journal of Critical Incidents* 5 (2012): 135-139.
[6] Gronewold, K. "Environmental Effects of Garbage Island." Paper presented at the Undergraduate Research Symposium, Mankato, MN, USA, April 21, 2014.
[7] ***. "World Environment Day 2018 Souvenir Sheet" / "Ziua Mondială a Mediului - Combate poluarea cu plastic", Colnect®, June 5, 2018. Accessed November 10, 2023. colnect.com/ro/stamps/list/country/433-India/series/400026-World_Environment_Day_%E2%80%98Beat_Plastic_Pollution%E2%80%99.
[8] ***. "World Environment Day, FDC , set 4v, First Day Cover, New Delhi Cancelled" / "Ziua Mondială a Mediului - Combate poluarea cu plastic", Delcampe®, June 5, 2018. Accessed November 10, 2023. www.delcampe.net/en_GB/collectables/stamps/india/fdc/india-2018-world-environment-day-FDC-set-4v-first-day-cover-new-delhi-cancelled-608433286.html.
[9] ***. "Say No To Plastic's - Fight Against Plastic Pollution for Environment" / "Ziua Mondială a Mediului - Combate poluarea cu plastic", Delcampe®, June 5, 2018. Accessed November 10, 2023. www.delcampe.net/en_GB/collectables/stamps/india/2010-2019/covers-documents/india-2019-say-no-to-plastic-s-fight-against-plastic-pollution-for-environment-raipur-cover-inde-indien-1543873192.html.
[10] ***. "MERCOSUR 2019 : Environmental Protection" / "MERCOSUR 2019: Protecția mediului", Colnect®, June 5, 2019. Accessed November 10, 2023. https://colnect.com/ro/stamps/stamp/870509-MERCOSUR_2019_Environmental_Protection-Uruguay.
[11] ***. "Loggerhead Turtle (Caretta caretta) Species threatened with extinction. FDC Uruguay 2019" / "Tortue La Caouanne (Caretta caretta) Espèce menacée d'extinction. FDC Uruguay 2019" / "MERCOSUR 2019: Protecția mediului", Delcampe®, June 5, 2019. Accessed November 10, 2023. www.delcampe.net/en_GB/collectables/stamps/reptiles-amphibians/turtles/uruguay-tortue-la-caouanne-caretta-caretta-espece-menacee-d-extinction-fdc-uruguay-2019-1207522876.html.
[12] ***. "Campaign Against Plastic Pollution" / "Campanie împotriva poluării cu plastic", Colnect®, September 29, 2020. Accessed November 10, 2023. colnect.com/ro/stamps/list/country/145-Maroc/series/392919-Campaign_Against_Plastic_Pollution_2020.
[13] ***. "Campaign Against Plastic Pollution" / "Lutte contre la pollution plastique" / "Campanie împotriva poluării cu plastic", Delcampe®, September 29, 2020. Accessed November 10, 2023. www.delcampe.net/en_GB/collectables/stamps/morocco-1956/maroc-fdc-1er-jour-2020-lutte-contre-la-pollution-plastique-morocco-marruecos-1641721463.html.
[14] ***. "Campaign Against Plastic Pollution in Oceans" / "Campanie împotriva poluării cu plastic în oceane", Colnect®, February 20, 2023. Accessed November 10, 2023. https://colnect.com/ro/stamps/list/country/51-Insulele_Cook/series/429411-Campaign_Against_Plastic_Pollution_in_Oceans_2023.
[15] ***. "Campaign Against Plastic Pollution in Oceans, whale, crabs, dolphin, turtle, 4val in FDC" / "Campanie împotriva poluării cu plastic în oceane", Delcampe®, February 20, 2023. Accessed November 10, 2023. www.delcampe.net/en_GB/collectables/stamps/crustaceans/cook-2023-campaign-against-plastic-pollution-in-oceans-whale-crabs-dolphin-turtle-4val-in-fdc-1800489865.html.
[16] ***. "Campaign Against Plastic Pollution in Oceans, whale, crabs, dolphin, turtle, 4val in FDC" / "Campanie împotriva poluării cu plastic în oceane", Delcampe®, February 20, 2023. Accessed November 10, 2023. www.delcampe.net/en_GB/collectables/stamps/environment-climate-protection/cook-2023-campaign-against-plastic-pollution-in-oceans-whale-crabs-dolphin-turtle-4val-in-fdc-1800489952.html.
[17] ***. "Campaign Against Plastic Pollution in Oceans, whale, crabs, dolphin, turtle, 4val in FDC" / "Campanie împotriva poluării cu plastic în oceane", Delcampe®, February 20, 2023. Accessed November 10, 2023. www.delcampe.net/en_GB/collectables/stamps/reptiles-amphibians/turtles/cook-

2023-campaign-against-plastic-pollution-in-oceans-whale-crabs-dolphin-turtle-4val-in-fdc-1800489898.html.
[18] ***. "Campaign Against Plastic Pollution in the Sea” / "Campanie împotriva poluării cu plastic în mări", Colnect®, April 20, 2023. Accessed November 10, 2023. https://colnect.com/ro/stamps/stamp/1363586-Campaign_Against_Plastic_Pollution_in_the_Sea-Croa%C5%A3ia.
[19] ***. "Fauna Fish Climate Action - Plastic waste in the sea FDC" / "Campanie împotriva poluării cu plastic în mări", Delcampe®, April 20, 2023. Accessed November 10, 2023. www.delcampe.net/en_GB/collectables/stamps/croatia/croatia-kroatien-mnh-2023-delivery-4-weeks-issued-04-19-climate-action-plastic-waste-in-the-sea-fdc-1759567489.html.
[20] ***. "Fauna Fish Climate Action - Plastic waste in the sea FDC" / "Campanie împotriva poluării cu plastic în mări", Delcampe®, April 20, 2023. Accessed November 10, 2023. www.delcampe.net/en_GB/collectables/stamps/croatia/croatia-2023-fauna-fish-climate-action-plastic-waste-in-the-sea-fdc-1758903412.html.
[21] ***. "Fauna Fish Climate Action - Plastic waste in the sea FDC" / "Campanie împotriva poluării cu plastic în mări", Delcampe®, April 20, 2023. Accessed November 10, 2023. www.delcampe.net/en_GB/collectables/stamps/croatia/croatia-2023-fauna-fish-climate-action-plastic-waste-in-the-sea-fdc-1758903148.html.
[22] ***. "World Environment Day 2023" / "Ziua Mondială a Mediului", Colnect®, July 31, 2023.. Accessed November 10, 2023. https://colnect.com/ro/stamps/list/country/132-Mali/series/436531-World_Environment_Day_2023.
[23] ***. "Environment Day - Turtle Monkey Hippopotamus Butterfly Frogs Owls Mushroom Giraffe Elephant"/ "Ziua Mondială a Mediului", Delcampe®, July 31, 2023. Accessed November 10, 2023. www.delcampe.net/en_GB/collectables/stamps/mali-1959/mali-2023-rare-fdc-sheet-environment-day-turtle-monkey-hippopotamus-butterfly-frogs-owls-mushroom-giraffe-elephant-1835324616.html.
[24] ***. "Environment Day - Turtle Monkey Hippopotamus Butterfly Frogs Owls Mushroom Giraffe Elephant"/ "Ziua Mondială a Mediului", Delcampe®, July 31, 2023. Accessed November 10, 2023. www.delcampe.net/en_GB/collectables/stamps/mali-1959/mali-2023-rare-fdc-sheet-environment-day-turtle-monkey-hippopotamus-butterfly-frogs-owls-mushroom-giraffe-elephant-1840247268.html.
[25] ***. "Environment- Beat Plastic Pollution- MS on FDC- Unique PMK- India-2018-BX2-22 " / "Ziua Mondială a Mediului - Combate poluarea cu plastic", Delcampe®, June 5, 2018. Accessed November 10, 2023. www.delcampe.net/en_GB/collectables/stamps/environment-climate-protection/environment-beat-plastic-pollution-ms-on-fdc-unique-pmk-india-2018-bx2-22-1423953743.html.
[26] ***. "World Environment Day Beat Plastic Pollution Nature Health M/s on FDC" / "Ziua Mondială a Mediului - Combate poluarea cu plastic", Delcampe®, June 5, 2018. Accessed November 10, 2023. www.delcampe.net/en_GB/collectables/stamps/environment-climate-protection/india-2018-world-environment-day-beat-plastic-pollution-nature-health-m-s-on-fdc-645446218.html.
[27] ***. "World Environment Day, FDC ,Miniature Sheet First Day Cover, Jabalpur Cancelled" / "Ziua Mondială a Mediului - Combate poluarea cu plastic", Delcampe®, June 5, 2018. Accessed November 10, 2023. www.delcampe.net/en_GB/collectables/stamps/india/fdc/india-2018-world-environment-day-fdc-miniature-sheet-first-day-cover-jabalpur-cancelled-611517271.html.
[28] ***. "Fight against plastic pollution" / "Lutte contre la pollution plastique" / "Campanie împotriva poluării cu plastic", Delcampe®, September 29, 2020. Accessed November 10, 2023. www.delcampe.net/en_GB/collectables/stamps/environment-climate-protection/maroc-enveloppe-de-1er-jour-fdc-de-4-timbres-2020-estivage-durable-lutte-contre-la-pollution-plastique-1236991744.html.
[29] ***. "DC Plastic Pollution n° Y&T coming soon" / "DC Pollution Plastique n° Y&T à venir" / "Campanie împotriva poluării cu plastic", Delcampe®, September 29, 2020. Accessed November 10, 2023. www.delcampe.net/en_GB/collectables/stamps/morocco-1956/2020-maroc-enveloppe-1er-jour-fdc-pollution-plastique-n-y-t-a-venir-1512315034.html.
[30] ***. "MNH - FDC Recycling 2020" / "Campanie împotriva poluării cu plastic", Delcampe®, September 29, 2020. Accessed November 10, 2023. www.delcampe.net/en_GB/collectables/stamps/morocco-1956/marokko-maroc-postfris-mnh-fdc-recycling-2020-1131348961.html.

## Annexes


**Fig. 9.** Various FDCs for Philatelic Issue "World Environment Day - Fight Plastic Pollution", 06/05/2018, New Delhi/Kanpur/Jabalpur (India) 0-0

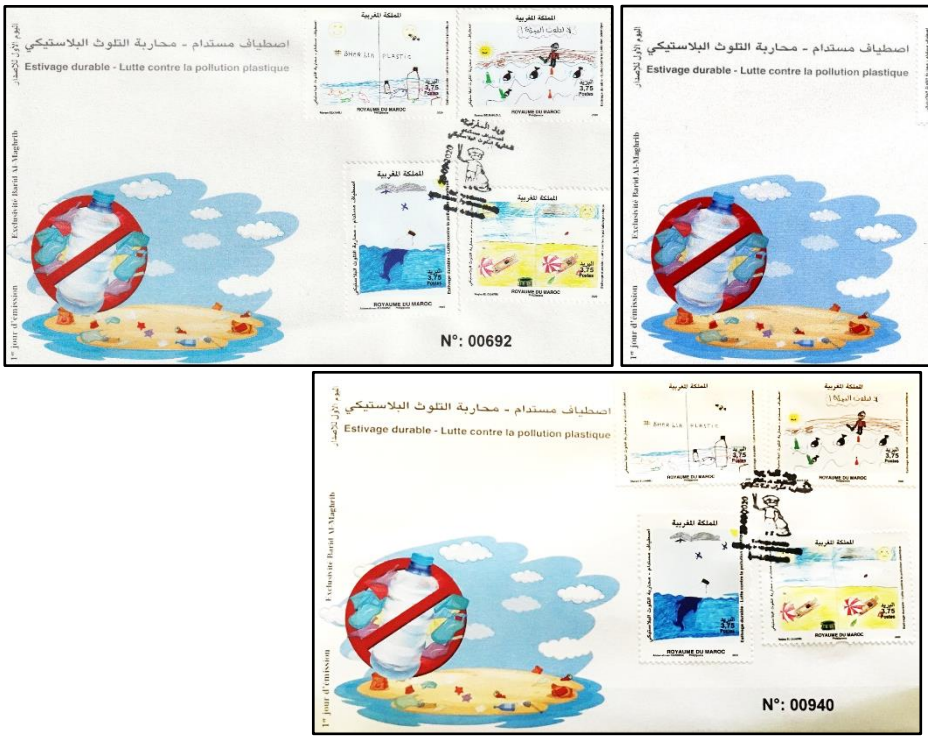


**Fig. 10.** Official FDC of the philatelic issue "Campaign Against Plastic Pollution", franked with all four postage stamps and canceled with a special stamp, 29.09.2020, Morocco 0-0

# FLUIDAS

## NATIONAL PROFESSIONAL ASSOCIATION OF HYDRAULICS AND PNEUMATICS IN ROMANIA


fluidas@fluidas.ro